NATIONAL BUREAU OF STANDARDS
MICROCOPY RESOLUTION TEST CHART

FOR FURTHER TRAN

⑤

TECOM NO. 6-CO-242-ESS-105

SPONSOR: USACEEIA

PUBLICATION NO. USAEPG-FR-1065

FEASIBILITY STUDY

NOISE AND ITS RELATIONSHIP
TO
VEHICLE ELECTROMAGNETIC EMISSIONS

JUNE 1978

U.S. ARMY ELECTRONIC PROVING GROUND
Fort Huachuca, Arizona

78 06 14 017

REPORT DOCUMENTATION PAGE		READ INSTRUCTIONS BEFORE COMPLETING FORM
1. REPORT NUMBER USAEPG-FR-1065	2. GOVT ACCESSION NO.	3. RECIPIENT'S CATALOG NUMBER
4. TITLE *(and Subtitle)* NOISE AND ITS RELATIONSHIP TO VEHICLE ELECTROMAGNETIC EMISSIONS		5. TYPE OF REPORT & PERIOD COVERED Feasibility Study
		6. PERFORMING ORG. REPORT NUMBER
7. AUTHOR(s)		8. CONTRACT OR GRANT NUMBER(s)
9. PERFORMING ORGANIZATION NAME AND ADDRESS U. S. Army Electronic Proving Ground Fort Huachuca, Arizona 85613		10. PROGRAM ELEMENT, PROJECT, TASK AREA & WORK UNIT NUMBERS TECOM Project No. 6-CO-242-ESS-105
11. CONTROLLING OFFICE NAME AND ADDRESS U. S. Army Communications-Electronics Engineering Installation Agency Fort Huachuca, Arizona 85613		12. REPORT DATE June 1978
		13. NUMBER OF PAGES 176
14. MONITORING AGENCY NAME & ADDRESS *(if different from Controlling Office)*		15. SECURITY CLASS. *(of this report)* Unclassified
		15a. DECLASSIFICATION/DOWNGRADING SCHEDULE

16. DISTRIBUTION STATEMENT *(of this Report)*

Distribution unlimited.

17. DISTRIBUTION STATEMENT *(of the abstract entered in Block 20, if different from Report)*

18. SUPPLEMENTARY NOTES

19. KEY WORDS *(Continue on reverse side if necessary and identify by block number)*

Amplitude probability detection	Noise measurement instrumentation
Communication systems degradation	Noise models
Communication System Performance Models	Vehicular noise
Electromagnetic emissions	

20. ABSTRACT *(Continue on reverse side if necessary and identify by block number)*

This report presents the results of a feasibility study of noise and its relationship to vehicle electromagnetic emissions and the resultant effects on communication system performance. Previous efforts in this field are summarized through a series of matrices which identify the advantages, disadvantages, and status of specific noise parameters or models and communication system performance models. The report also identifies areas for future work.

DD FORM 1473 EDITION OF 1 NOV 65 IS OBSOLETE

EXECUTIVE SUMMARY

This report presents the results of a feasibility study of noise and its relationship to vehicle electromagnetic emissions and the resultant effects on communication system performance.

The report summarizes previous efforts in this field through a series of matrices which identify the advantages, disadvantages, and status of specific noise parameters or models and communication system performance models. Additionally, the report identifies areas for future work. It was concluded that--

1. Documented cases exist which show that vehicular and other manmade noise emissions can detrimentally affect communication system performance.

2. At the present time, an overall program to address and resolve the problems associated with vehicular noise emissions and their effect on communication systems does not exist.

3. Certain specific areas which require additional effort are--

a. Analytical models for analog (voice) communication systems, and the noise parameters required to evaluate such systems.

b. A data base for manmade and vehicular noise environments to support the utilization of analytical models.

c. Detailed deployment data on vehicles for test beds which are used for the tactical scenario evaluation of communication system performance.

d. Meaningful standards for automotive ignition noise.

ACCESSION for

NTIS	White Section	☒
DDC	Buff Section	☐
UNANNOUNCED		☐
JUSTIFICATION		

BY
DISTRIBUTION/AVAILABILITY CODES

Dist.	AVAIL. and/or SPECIAL	
A		

i

FOREWORD

Bell Technical Operations Textron, Tucson, Arizona, assisted in the preparation of this report under contract DAEA18-76-C-0002. The consultant services of Dr. A. D. Spaulding of the Office of Telecommunications, U. S. Department of Commerce, and Mr. George Hagn and Mr. Richard Shepherd, both from SRI International, were used to prepare various sections of the report. Contributions were also made by Dr. D. Middleton and Dr. A. Perkins, who represented the sponsor USACEEIA.

TABLE OF CONTENTS

LIST OF ILLUSTRATIONS

Figure

TABLE OF CONTENTS (CONT)

PAGE

LIST OF TABLES

Table

SECTION 1 - INTRODUCTION

1.1 BACKGROUND

a. Numerous research efforts and experiments (refs 2-20, app D) have, to a limited degree, identified the effects of vehicle electromagnetic (EM) emissions on the performance of various types of communication systems and equipments. For example, experiments have shown that one of the severest cases of communications receiver performance degradation exists in the land mobile very high frequency (VHF) and ultrahigh frequency (UHF) bands (refs 18 and 19, app D). This is due in part to the rapid increase in the number of vehicles on the road and the rise in popularity of citizens band radio. Although the degradation from vehicular ignition noise is more prevalent in these bands, experiments have indicated that these deleterious effects may extend into the high frequency (HF) (refs 8 and 9, app D) and super high frequency (SHF) bands (ref 13, app E). Methods to evaluate, quantify, and measure this degradation have not been firmly determined up to this time. These factors have resulted in a growing awareness by the U. S. Army concerning the undesirable or harmful degradation (interference) caused by vehicle noise emissions to the performance of Army and other communications-electronics (C-E) systems and equipments. This degradation problem has both technical and economic consequences as outlined below.

b. The electromagnetic noise from a vehicle can affect on-board C-E systems such as receivers or low-level logic control circuits as well as other systems, operating at HF and above, within range of the vehicle. Groups of vehicles (e.g., convoys) can be more disruptive than isolated vehicles. This potential for vehicle-caused interference gives rise to several noise-related decisions that Army planners must make. For example, whenever the Army purchases new vehicles a decision must be made as to whether MIL-STD-461A (ref 1, app D), or another standard, is to be included in the procurement specification or whether a waiver is to be granted. This decision has an economic and, possibly, a schedule impact at the time of purchase and there can be a negative operational impact later if the specification neglects vehicle ignition noise. The implementation of the recommendation of the Wheels Study (ref 2, app D) to buy more non-military-specification vehicles makes this subject timely. Another example is the decision of a commander at a communication station as to whether he will try to restrict especially noisy vehicles from the vicinity of his antenna field.

c. Despite several recent surveys (refs 3 through 5, app D) and studies (refs 6 through 20, app D), these Army decision makers currently have little technical information on which to base their decisions or assess the ramifications (ref 21, app D). The current Department of Defense (DoD) standards [MIL-STD-461A (ref 1, app D) for tactical vehicles and SAE J551e (ref 22, app D) for administrative vehicles] do not provide guidance on this aspect; indeed, the degree of protection obtained if the current standards are met is unknown, and perhaps cannot be determined (refs 11 and 12, app D). The vehicle noise problem is also a source of

1-1

concern in the private sector. The Federal Communications Commission (FCC) has performed research on the noise from civilian vehicles (refs 18 through 20, app D), opened a public Notice of Inquiry (ref 23, app D), and funded research on ignition noise suppression (ref 24, app D).

d. On 12 July 1977, the U. S. Army Test and Evaluation Command (TECOM), at the request of the U. S. Army Communications-Electronics Engineering Installation Agency (USACEEIA), assigned the responsibility for a feasibility study on the vehicular noise problem to the U. S. Army Electronic Proving Ground (USAEPG), Fort Huachuca, Arizona. Originally, the assignment included a multiphase program to be performed sequentially. Subsequent direction from the sponsor limited the task to the first phase of the initial multiphase program. The goal of this initial phase is to determine the feasibility of developing a better understanding of the cause and effect relationship between the radio noise from motor vehicles and the degradation such noise can cause to selected U. S. Army C-E systems. If this relationship can be established then the technical, economic, and schedule risks can be significantly reduced for decisions of the type mentioned above.

1.2 STUDY OBJECTIVE

The objective of this study is to review previous research, noise data, measurement standards, etc., relevant to the study of vehicle electromagnetic noise emissions.

1.3 SCOPE

a. This study is subdivided into the following areas:

(1) Review of the literature for germane material and the compilation of a bibliography (ref 25, app D, and app E).

(2) Selection of U. S. Army C-E systems representative of generic classes of systems which may be vulnerable to degradation by noise from vehicles (para 2.1).

(3) A review of available noise models and their input/output parameters which describe noise in terms consistent with the requirements of the various system performance models (para 2.2).

(4) A review of applicable models for degradation of the identified systems when operating in the presence of impulsive noise from motor vehicles, and the accuracy and status of validation of these models (para 2.3).

(5) A review of the available noise data required to determine the noise model parameters, and applicable noise data validation techniques (para 2.4).

(6) A review of available instrumentation and of the instrumentation required to obtain the required noise data (para 2.5).

(7) A summary of major findings and conclusions (para 2.6).

(8) Recommendations for filling the voids (para 2.7).

b. The functional relationship between noise data acquisition, validation, and communication system performance modeling is depicted in figure 1. This figure depicts the relationship of some measurable properties of noise to some user-relevant measure of system performance degradation. If this relationship can be established for C-E systems of interest, then meaningful cost-benefit analyses can be performed regarding the degree of noise suppression, and meaningful procurement standards and operational guidelines can be written.
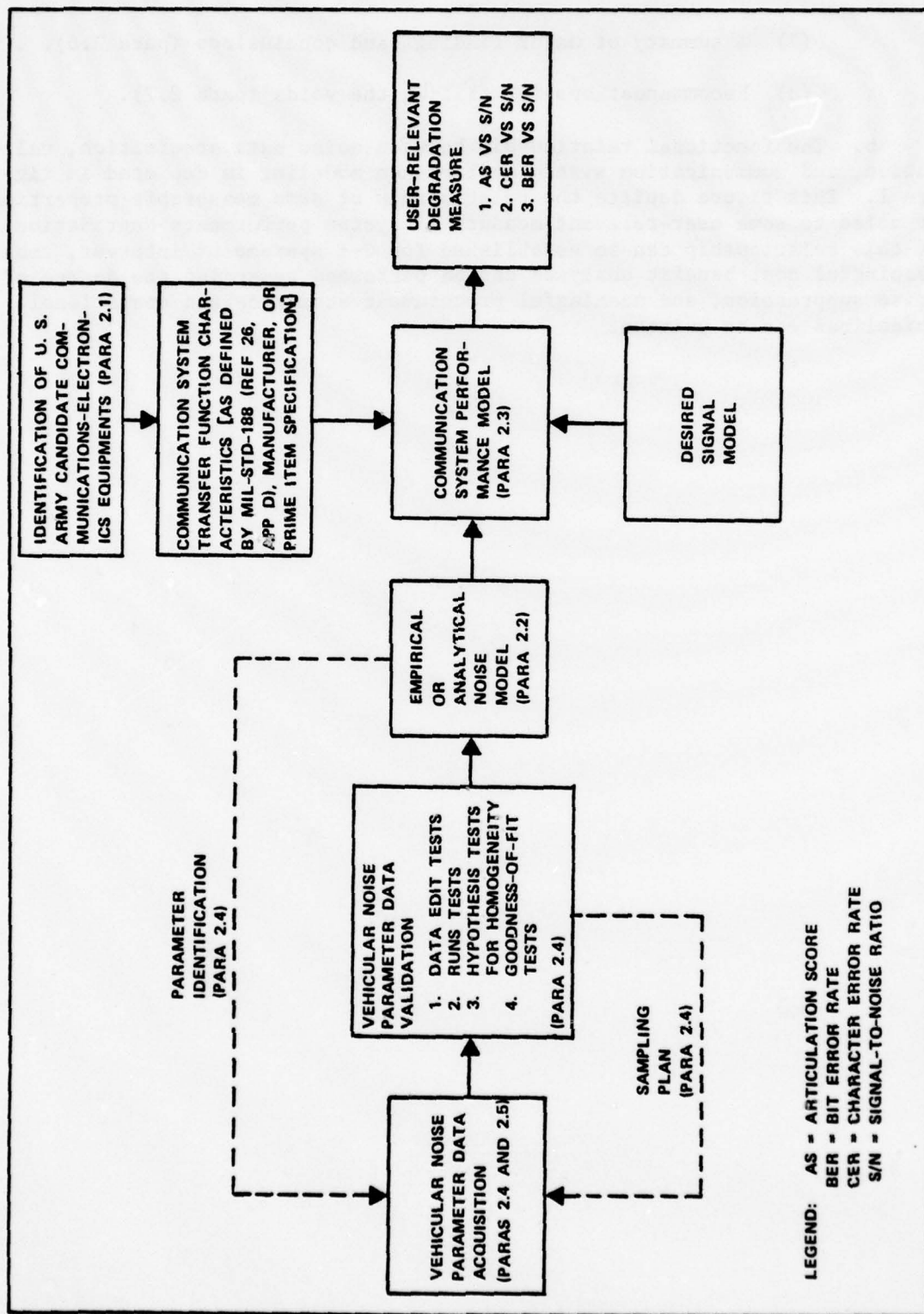
Figure 1. Vehicular noise information – model and communication system performance flow diagram.

LEGEND: AS = ARTICULATION SCORE
         BER = BIT ERROR RATE
         CER = CHARACTER ERROR RATE
         S/N = SIGNAL-TO-NOISE RATIO

1-4

SECTION 2 - DETAILS OF STUDY

2.1 CANDIDATE COMMUNICATION SYSTEMS

2.1.1 Objectives

The objectives of this subtask are to--

a. Identify some typical U. S. Army C-E equipments (and their associated transfer function characteristics) which perform the following functions:

(1) Transmitted signal radio frequency (RF) reception.

(2) Received signal demodulation.

(3) Signal decoding.

b. Develop a systematic mathematical terminology for communications transmitter-to-receiver signal flow and degradation due to additive noise.

2.1.2 Study Approach

a. For this study, U. S. Army C-E equipments were grouped within two major categories, as follows:

(1) C-E systems deployed as part of long-haul multichannel networks found in CONUS and Europe (e.g., DCA European backbone network). These equipments are normally installed in fixed plant facilities. They are either analog or digital and can handle both voice and data traffic.

(2) C-E systems deployed on the battlefield, usually on vehicles or in standard communication shelters. Similarly, these equipments are either analog or digital and provide either voice or data ground-to-ground or ground-to-air communications.

b. Transfer function characteristics were identified for each candidate C-E system. [The term "transfer function characteristic" is used in the same context as stated in MIL-STD-188C (ref 26, app D).] The overall communication system process is presented in figure 2. The receive sections of figure 2 are represented by the simplified block diagram shown in figure 3.

c. The received signal-plus-noise waveform r(t) can be represented as the sum--

$$r(t) = s(t) + N(t)$$

where s(t) is the desired signal at the receiver and N(t) is the additive noise at some point in the system. N(t) can be Gaussian or impulsive. Distortion of the original transmitted signal, s*(t), also occurs as the

ATMOSPHERIC NOISE

RF TRANSMISSION PROCESS NOISE

MODULATION PROCESS NOISE

ENCODER PROCESS

MODULATION PROCESS

RF TRANSMISSION PROCESS

TRANSMISSION PATH

MANMADE NOISE

PREDETECTION POINT

RF RECEIVING PROCESS

RF RECEIVING PROCESS NOISE

DEMODULATION PROCESS

DEMODULATION PROCESS NOISE

POST-DETECTION POINT

DECODER PROCESS

TRANSMITTED INFORMATION $s'(t)$

RECEIVED INFORMATION $r(t) = s(t) + N(t)$

Figure 2. Overall communication system transmit-receive process.

PREDETECTION
S/N OBSERVED
HERE

POST-DETECTION
S/N OBSERVED
HERE

USER OUTPUTS
AS
CER
BER

OUTPUT

IF

RECEIVER

TRANSMISSION
LINE

ANTENNA
CIRCUIT

LOSS-FREE ANTENNA
WITH AVAILABLE
EXTERNAL NOISE
kT_ab

ADDITIVE
NOISE

DESIRED
SIGNAL

PREDETECTION S/N
REFERRED HERE
FOR CALCULATION
(CCIR REPORT 413
REF 27, APP D)

LEGEND:
AS = ARTICULATION SCORE
BER = BIT ERROR RATE
CER = CHARACTER ERROR RATE
IF = INTERMEDIATE FREQUENCY
S/N = SIGNAL-TO-NOISE RATIO

Figure 3. Simplified block diagram of communications receiver.

2-3

signal propagates from the transmitter to the receiver. This type of distortion can be considered as multiplicative noise. It affects only the s(t) term, and one result can be intersymbol interference which can limit the performance of digital systems at very large signal-to-noise ratios. Multiplicative noise is mentioned briefly in paragraph 2.3, but a detailed treatment is beyond the scope of this feasibility study. A description of N(t) is contained in paragraph 2.2.

d. Deployment estimates were determined based on the type of equipment and its function.

2.1.3 Results and Analysis

Table I presents typical candidate strategic and tactical communication systems presently being fielded by the U. S. Army.

TABLE I. CANDIDATE TACTICAL COMMUNICATION SYSTEM MATRIX

Systems	1		2	3	4	5	6
Nomenclature	AN/VRC-12 Family		AN/GRC-106	RDS-80	AN/TSC-61A	AN/GRC-144	AN/PSC-1
	Non-Secure	Secure					
Function	Analog Voice	Digital Voice	Tactical (Voice & Data)	600 Channel MUX (Voice & Data)	Air Traffic Control (Voice)	12,24,48 Channel (Voice & Data)	Satellite Earth Terminal (Voice & Data)
Employment	Vehicles		Vehicles	Long Haul LOS	Tactical Airfields	Tactical/Fixed Communications	Manpack & Vehicles
Band & Frequency	VHF, 30-76 MHz		MF/HF, 2-30 MHz	SHF, 11 GHz	UHF & VHF (Various Radio Systems)	SHF, 4.5 GHz	UHF, 225-400 MHz
Modulation	Narrow-band FM Voice	Broad-band FM Voice	SSB Voice/RATT NCFSK	DQPSK	FM: Scrambler KY-8 AM: AN/ARC-51BX AN/GRR-23/24	PCM/FM	QPSK/CVSD (Voice) BPSK (Data)
Performance Measure	AS, BER		AS, CER, BER	AS, CER, BER	AS	AS, CER, BER	AS, BER
Receiver Proximity to Vehicles (Relative Scale*)	10		10	5-8	8-9	6-9	6-10
Relative Severity of Consequence of EMI (Relative Scale**)	7-10		7-10	10	8-10	7-10	7-10
Deployment Density	High (Tens of Thousands)	High	High (Thousands)	Low (Tens)	Medium (Hundreds)	Medium (Hundreds)	Medium (Hundreds)

*On a scale from 0-10; 10 implies receiver very close to vehicle traffic, while 0 or 1 implies receiver very far from vehicle traffic (see table C-1, ref 12, app D, for complete description).

**On a scale from 1-10, where 1 is least and 10 is greatest consequence.

AS = articulation score	MF = medium frequency (0.3-3 MHz)	
BER = bit error rate	MUX = multiplex	
BPSK = biphase shift keying	NCFSK = noncoherent frequency shift keying	
CER = character error rate	PCM = pulse code modulation	
CVSD = continuous variable slope delta	QPSK = quadriphase shift keying	
DQPSK = differential quadriphase shift keying	RATT = radioteletypewriter	
EMI = electromagnetic interference	SSB = single sideband	
FM = frequency modulation	UHF = ultrahigh frequency (300-3000 MHz)	
HF = high frequency (3-30 MHz)	VHF = very high frequency (30-300 MHz)	
LOS = line of sight		

2.2 VEHICULAR NOISE ANALYTICAL MODELS AND THEIR INPUT/OUTPUT NOISE PARAMETERS

2.2.1 Objectives

The objectives of this subtask are to--

a. Investigate and identify analytical noise models which may be used to model vehicular noise.

b. Identify the input/output noise parameters for these models.

c. Identify the advantages, disadvantages, and validation status for each analytical noise model.

2.2.2 Study Procedure

2.2.2.1 General

a. The probabilistic concepts of noise are too complex for a complete discussion here; many reports and books (refs 3, 28, and 29, app D) are presently available treating this subject in greater detail. Each of the noise sources identified in figure 2 can be modeled empirically or analytically (mathematically). For this brief introduction, the instantaneous random noise output of a narrowband* receiver (see fig. 3) can be defined by the following:

$$N(t) = v(t) \cos[2\pi f_c t + \phi(t)]$$

where

  f_c is the center tuned frequency of the receiver

  $v(t)$ is a random process describing the instantaneous envelope of the noise

  $\phi(t)$ is a random process describing the instantaneous phase of the noise

Figure 4A identifies each of the above quantities as functions of time.

b. For the simplest case, $N(t)$ can be considered to be white Gaussian noise** the instantaneous amplitude of which is described by the density function in figure 4B. Probability density functions describing $\phi(t)$ and $v(t)$ are presented in figures 4C and D, respectively. In practice, only parameters concerning the envelope $v(t)$ are considered for engineering applications and noise testing. Limited measurements (ref 8, app D) indicate that the uniform phase assumption is valid for automobile ignition noise.

---

*Narrowband processes are those which can be characterized by an envelope and phase. This results when the bandwidth of the receiving system is small compared to the center tuned (carrier) frequency, i.e., $BW_r < f_c$.
**White noise is characterized by constant amplitude power spectral density $|S(f)| = N_o$.

A. NOISE AT THE OUTPUT OF A NARROWBAND RECEIVER

RANDOMLY VARYING PHASE $\phi(t)$

RANDOMLY VARYING ENVELOPE $v(t)$

$N(t) = v(t) \cos [2\pi f_c t + \phi(t)]$

FREQUENCY APPROXIMATELY f_c
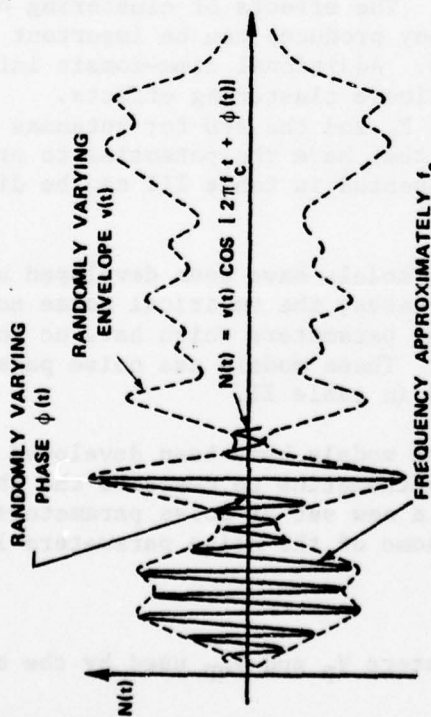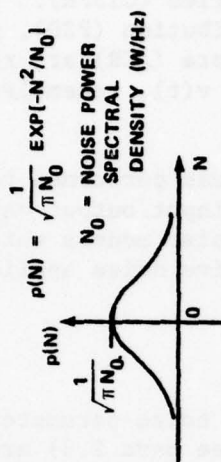
B. GAUSSIAN DENSITY FUNCTION DESCRIBING THE INSTANTANEOUS AMPLITUDE OF $N(t)$ AT THE OUTPUT OF A NARROWBAND RECEIVER.

$p(N) = \dfrac{1}{\sqrt{\pi N_0}} \, \text{EXP}[-N^2/N_0]$

N_0 = NOISE POWER SPECTRAL DENSITY (W/Hz)

$\dfrac{1}{\sqrt{\pi N_0}}$
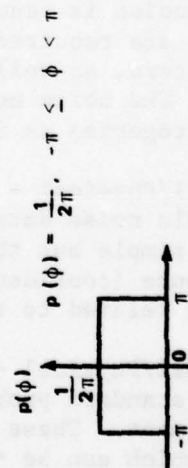
C. UNIFORM DENSITY FUNCTION FOR INSTANTANEOUS PHASE, $\phi(t)$, NOISE AT THE OUTPUT OF A NARROWBAND RECEIVER.

$p(\phi) = \dfrac{1}{2\pi}, \quad -\pi \leq \phi < \pi$

$\dfrac{1}{2\pi}$
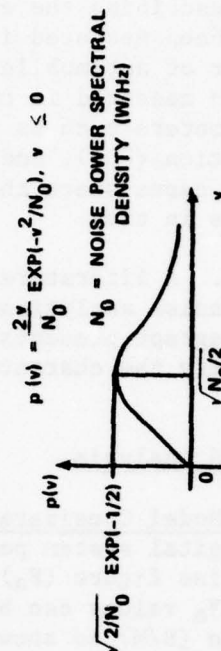
D. RAYLEIGH DENSITY FUNCTION DESCRIBING THE ENVELOPE, $v(t)$, OF THE NOISE PROCESS, $N(t)$, AT THE OUTPUT OF A NARROWBAND RECEIVER

$p(v) = \dfrac{2v}{N_0} \, \text{EXP}[-v^2/N_0], \quad v \geq 0$

N_0 = NOISE POWER SPECTRAL DENSITY (W/Hz)

$\sqrt{2/N_0} \, \text{EXP}[-1/2]$

$\sqrt{N_0/2}$

Figure 4. Noise and examples of its probabilistic descriptions.

c. Table II (ref 3, app D) presents various noise parameters which are employed in describing the envelope voltage, v(t). Historically, peak voltage (V_p) has been measured in the United States (SAE and DoD) as the primary descriptor of automobile ignition noise, whereas quasi-peak voltage (V_{qp}) has been measured in the other NATO countries (CISPR). It is evident that parameters such as pulse spacing distribution (PSD), pulse duration distribution (PDD), and average crossing rate (ACR) are required to describe those cases where the envelope voltage, v(t), resembles a series of impulses in time.

2.2.2.2 Specific. A literature survey and review was performed to investigate vehicular noise analytical models and their input/output parameters. The following paragraph presents a compilation of noise models which extend and further quantify the characterization of impulsive noise applicable to vehicle emissions.

2.2.3 Results and Analysis

2.2.3.1 General Model Considerations. The primary noise parameters required for the digital system performance models (see para 2.3) are external antenna noise figure (F_a) and the amplitude probability distribution (APD). The F_a values can be used to estimate the predetection signal-to-noise ratio (S/N) as shown in figure 3, and the APD can be used to estimate the probability that the noise exceeds the signal at the output of the predetection filter. The bit error rate (BER) of many systems can be computed using these noise parameters. The effects of clustering of noise bursts (and the bit error bursts they produce) can be important in deriving character error rates from BER's. Additional time-domain information about the noise is required to estimate clustering effects. Therefore, models are required to predict F_a and the APD for antennas and bandwidths of concern, as well as models that have the potential to predict clustering. The noise models as presented in table III can be divided into two major categories as follows:

a. Empirical/Physical - These noise models have been developed using presently available noise data. In most cases, the empirical noise models are analytically simple but they use noise parameters which have no known degree of confidence (confidence bounds). These models use noise parameters which can be related to those listed in table II.

b. Analytical/Physical - These noise models have been developed analytically using standard probabilistic mathematics to describe the physical noise environment. These models use a new set of noise parameters* (see table III) which can be related to some of the noise parameters listed in table II.

---

*"New" relative to the traditional parameters V_p and V_{qp} used by the automotive industry.

TABLE II. VARIOUS NOISE PARAMETERS AND THEIR DEFINITIONS

Parameter	Reference (app D)	Definition*	Mathematical Relation*
Quasi-Peak Voltage (V_{qp})	3, 11, 12	Measured output voltage value of $v(t)$ using a circuit with a short charging time and long discharge time	No general mathematical relation for random input waveforms; for deterministic waveforms see ref 32, app D
Peak Voltage (V_p)	3, 11, 12	Measured peak voltage value of $v(t)$ over interval T	Value of V_p is highly dependent on the interval T
Average Voltage (V_{av})	3, 12, 33, 34	Measured average voltage value of $v(t)$ over interval T	$V_{av} = \frac{1}{T} \int_0^T v(t)\, dt = \int_0^\infty v p(v)\, dv$
Root Mean Square Voltage (V_{rms})	3, 12, 33, 34	Measured rms voltage value of $v(t)$ over interval T	$V_{rms} = \sqrt{\frac{1}{T} \int_0^T v^2(t)\, dt} = \sqrt{\int_0^\infty v^2 p(v)\, dv} = \sqrt{P_N}$
Average Voltage Logarithm (V_{log})	3, 33	Measured logarithmic voltage value of $v(t)$ over the interval T	$V_{log} = \frac{1}{T} \int_0^T \log v(t)\, dt = \int_0^\infty \log v p(v)\, dv$
Amplitude Probability Distribution (APD)	3, 12, 33, 34	The probability that for interval T the voltage $v(t)$ exceeds a specified limit v_i	$\text{Prob}\,[v \geq v_i] = 1 - \text{Prob}\,[v < v_i]$ $\text{Prob}\,[v \geq v_i] = 1 - \int_0^{v_i} p(v)\, dv$
Pulse Spacing Distribution (PSD)	3, 12	The fraction of pulse spacings at level v_i that exceed a time limit τ_i	$\text{Prob}\,[\tau \geq \tau_i \mid v \geq v_i]$
Pulse Duration Distribution (PDD)	3, 12	The fraction of pulse durations at level v_i that exceed a time limit τ_i	$\text{Prob}\,[\tau \geq \tau_i \mid v \leq v_i]$
Noise Amplitude Distribution (NAD) -Average Crossing Rate (ACR) Characteristic	3, 12	Number of positive threshold crossings per second versus threshold level for the interval T	$C(v_i) = \frac{1}{2} \int_{-\infty}^\infty |\dot{v}|\, p(v_i, \dot{v})\, d\dot{v}$
Average Voltage Deviation (V_d)	3, 33, 34	The dB difference between V_{rms} and V_{av}	$V_d = 20 \log \frac{V_{rms}}{V_{av}}$
Quasi-Peak Voltage Deviation (Q_d)	3	The dB difference between V_{qp} and V_{rms}	$Q_d = 20 \log \frac{V_{qp}}{V_{rms}}$
Average-Logarithmic Voltage Deviation (L_d)	3, 33	The dB difference between V_{rms} and the antilog of V_{log}	$L_d = 20 \log \frac{V_{rms}}{10^{V_{log}}}$
Noise Power (P_N)	3, 35	The mean noise power available from a loss-free antenna due to an external source, determined over an interval T	$P_N = f_a kT_0 b = (T_a/T_0)\, kT_0 b$ $F_a = 10 \log f_a$ $P_N = \frac{1}{T} \int_0^T v^2(t)\, dt = \int_0^\infty v^2 p(v)\, dv$ $P_N = V_{rms}^2$
Power Spectral Density $S(f)$	3, 33	Power per unit bandwidth (b); Fourier transform of the autocorrelation function, $R(\tau)$, for the random noise process $v(t)$	$S(f) = \int_{-\infty}^\infty R(\tau) e^{-j2\pi f\tau}\, d\tau$ $R(\tau) = \lim_{T \to \infty} \frac{1}{T} \int_0^T v(t) v(t+\tau)\, dt =$ $\int_{-\infty}^\infty \int_{-\infty}^\infty v_1 v_2 p_2(v_1\, v_2, \tau)\, dv_1\, dv_2$

*Assumes stationarity over interval T.

TABLE III. NOISE ANALYTICAL MODELS

Model Name	Reference (app D)	Inputs	Outputs	Advantages	Disadvantages	Validation	Application
Hall	36	m, number of degrees of freedom of the regime process (χ^2-distribution with σ^2 variance) $\gamma = \sqrt{m} \, \sigma_i/\sigma$ σ_i^2 = variance of noise process	PDF of instantaneous amplitude, APD	Analytically tractable	Its unbounded second moment corresponds to infinite power	Fair fit with HF atmospheric noise and some manmade noise	Digital systems
Log-Normal-Omura	37	F_a, external antenna noise figure $V_d = 20 \log V_{rms}/V_{avg}$	APD	Relatively simple. Good fit to impulsive part of APD	Poor fit to low amplitude part of APD	Has been used with VLF atmospheric noise	Digital systems
Modified Log-Normal-Shohara	38	P_N, average noise power $V_d = 20 \log V_{rms}/V_{avg}$ ψ, ratio of total noise power to Gaussian background-noise power	APD	Relatively simple	ψ is not a commonly measured noise parameter	Fits VLF atmospheric noise APD's well. Not yet compared with manmade noise	Digital systems
Convolution	39	α, an empirical impulsiveness parameter γ^2, a measure of the ratio of impulsive to Gaussian noise	PDF of instantaneous amplitude, APD	Easily programmed	Parameters are not readily measurable although α, γ, and V_d are related	Proper selection of α and γ^2 gives good approximations to measured APD's for VLF and ELF noise	Digital systems
Middleton	30	A_g, impulsive index: average number of emission "events" times the mean duration of an event Γ_B, σ_G^2/Ω_{2B}: ratio of intensity of Gaussian noise to impulsive noise Ω_{2B}, intensity of impulsive noise A_α, effective impulsive index α, a factor dealing with density of noise sources and propagation of the noise N_I, the scaling factor ϵ_B, empirically determined "bendover" point of the APD	Characteristics function; PDF of instantaneous amplitude, APD	Analytically tractable and based on the physical processes of the noise itself	Seven parameters may intimidate some potential users	Excellent fit to atmospheric and manmade noise APD's (including ignition noise of SRI)	Digital systems
Average Power of Traffic Stream-Baran	16	Vehicle traffic conditions (traffic density, vehicle speed, distance to road)	F_a, external antenna noise figure averaged over the passing of many vehicles	Simple and easy to use	Does not provide detailed noise statistics	Compares well with measurements of ignition noise by SRI	Analog or digital systems
Cohen	40	Road-to-receiver geometry, vehicle speeds, ignition noise pulse strength, receiver impulse response, also several empirical parameters	APD	Relatively simple and easy to use	Provides APD at low probability end only. Does not trail off into Gaussian noise. Considers constant impulse strength	Good fit with measurements made by SRI	Digital systems

TABLE III. NOISE ANALYTICAL MODELS (CONT)

Model Name	Reference (app D)	Inputs	Outputs	Advantages	Disadvantages	Validation	Application
Spaulding	10,31	Road-to-receiver geometry, vehicle spacings and speeds, distribution of noise from individual vehicles	Mean and variance of the received noise power spectral density	Can be applied simply, for high traffic densities	Results are strongly dependent on the propagation loss assumption. Distribution of noise from individual vehicles has been measured at only a few frequencies	Fair fit to measured data at 20 and 48 MHz	Digital and analog systems
Crichlow Three-Moment	34	F_a, V_d, L_d	APD	Input parameters easily measured. Log of voltage can be approximated from V_d	Poor fit to Ignition noise APD's	Fits atmospheric noise quite well	Digital systems
Markov Regime	5,41	F_a, V_d, probability noise is in background noise regime, and Markov transition probability from background to impulsive regime. (First three available from APD.)	APD	Represents clustering effect of impulses explicitly. Analytically tractable	Markov transition probability not commonly measured	Initial check for ignition noise initiated but not completed-ref 41, app D	Digital systems

2.2.3.2 Noise Analytical Models

a. Several models for F_a are available (refs 10, 16, 30, and 31, app D). These models are all physical models which require some empirical inputs to obtain F_a estimates (as distinguished from purely empirical models). They involve road-to-receiver geometry and traffic density. The median F_a estimate produced can be used to estimate S/N's or it can be used as an input to one of the APD models to convert a relative APD to an APD with an absolute scale. The accuracy of some of these models (refs 16, 10, and 31, app D) has been spot checked during their development over a limited frequency range for a few types of antennas, but the models have not been validated in the scientific sense where predictions are made prior to data acquisition. One of the models (refs 9 and 31, app D) predicts the distribution of F_a values (as well as the median), assuming a Gaussian distribution.

b. The APD models can also be categorized as physical (refs 30 and 40, app D) and empirical (refs 5, 33, and 36-39, app D). Several features of these models are worth noting. The log-normal models (refs 37 and 38, app D) inherently predict APD's that increase in amplitude with decreasing probability, but at a rate which eventually becomes inappropriate for physical noise processes. Measured APD's for ignition noise "bend over" at the top (refs 8 and 9, app D), as predicted by Middleton's model (see fig. 2.4 of ref 30, app D). The Markov Regime Model (refs 5 and 41, app D) always predicts a bend-over. Having the proper bend-over is especially important in predicting the lower error rates for linear systems. The most important thing is to get the right APD for the system performance range of interest. For example, it is not important whether a system performance model gives erroneous answers for actual error rates of 10^{-12} if it gives reasonable predictions at 10^{-4} (and that happens to be the desired or required performance). As noted above, the high amplitude-low probability part of the APD is important for all linear digital systems; however, for a few linear systems the entire APD is important (e.g., DCPSK). For nonlinear systems (e.g., systems employing a clipper or limiter), the lower part of the APD is relatively much more important. The log-normal model is a poor choice for modeling nonlinear systems, and this is why Shohara developed the modified log-normal model (ref 38, app D), and Hall developed his model (ref 36, app D).

c. Little work has been done thus far in validation of APD models for individual automobiles or for streams of traffic. There are two aspects of model validation worth noting: (1) whether the model input parameters can be adjusted to give a good enough fit to measured APD's for a particular class of communication system, and (2) whether the model can predict (before measurements) the APD observed for a specified vehicle or traffic situation. Only the Cohen (ref 40, app D) and Middleton (ref 30, app D) models have demonstrated aspect (1) for a very limited sample of ignition noise data (selected examples from refs 8 and 9, app D). Some very preliminary checks (as yet unpublished) have been made for the Markov Regime model (ref 41, app D) for the same sample of ignition noise data. Middleton's model (ref 30, app D) has the most degrees of freedom (requires the

most parameters) and hence has the best potential to fit the entire APD. Whether this level of complexity is required depends upon the application. No tests of the very important overall prediction aspect have yet been made for any of the APD models.

d. Many of the above models have the potential to predict clustering of noise bursts and the resultant effect on character error rates (CER). A given APD can produce a certain BER but different CER's for some systems and it is for these cases that clustering may be an important consideration. The Markov Regime model, when using a mixture of two Gaussian distributions*, has the advantage that the amplitude statistics are Gaussian (but with different variances) for all time intervals (i.e., in both the impulsive and nonimpulsive intervals), and textbook solutions (see para 2.3 of app E and ref 25, app D) are available for the error rates for many systems which can be used to synthesize their average error rates.

e. It is worth noting that the parameter F_a (derived from V_{rms}, see ref 34, app D) is needed for all the models; however, none of the F_a, APD, or system performance models make use of the V_p parameter, which is the only parameter measured in MIL-STD-461A (ref 1, app D) and in the civil standard SAE J551e (ref 22, app D) referenced in MIL-STD-461A for administrative vehicles. An empirical relationship between peak field intensity (E_p) and quasi-peak field intensity (E_{qp}) has been used by the SAE and CISPR (ref 42, app D) to facilitate international trade in the automotive industry, as follows:

$$E_p = E_{qp} + 20 \text{ in dB} > 1 \text{ } \mu V/m/kHz$$

This relationship is intended to apply only to a single vehicle operating at 1500 rpm. There is no relationship between V_{qp} and communication system degradation, except for AM broadcast, and the 20-dB conversion is not a constant (ref 12, app D). It has even been shown that the 20 dB is not the appropriate conversion factor (ref 43, app D). There has been some analytical work on the relationship between V_{qp} and V_{rms} under certain assumptions (ref 44, app D) which indicate that a "typical" value of V_{qp} is approximately V_{rms} + 10 dB. Therefore, the closest empirical relationship between V_p and V_{rms} (to make an enlightened estimate on the relationship between V_{rms} and the MIL-STD-461A V_p parameter) for the same antenna and bandwidth is:

$$V_{rms} = V_p - 30 \text{ (dB}\mu V)$$

Care must be exercised regarding the method of calibration of each detector, and with the resulting units (refs 45 and 46, app D). The above expression assumes that the rms value of a sine wave was used for the calibration. Of course, F_a is related to the rms voltage at the terminals of an equivalent, lossless antenna (see fig. 3) as follows:

$$F_a = 20 \log V_{rms} - 10 \log R_r - 10 \log b + TL + ML + AL - 78.5 \text{ (in dB)}$$

---

*The model can use a non-Gaussian distribution for the low probability-high amplitude portion of the composite distribution (ref 5, app D).

where

V_{rms} is the open-circuit rms voltage, in dBμV, referred to receiver input

R_r is the antenna's input resistance (radiation resistance), in ohms

b is the noise power bandwidth, in Hz, of the system used to measure the noise voltage

TL is the insertion loss, in dB, of the transmission line between the antenna and its receiver

ML is the mismatch loss, in dB

AL is the loss in the antenna, in dB

It _may_ be possible to put some empirical bounds upon the relationship between V_p and F_a for individual vehicles. Of course, the relationship would not apply for measured noise from more than one vehicle without modification. In theory, two identical automobiles at the same distance would double F_a while leaving V_p unchanged.

2-14

2.3 DETERMINATION OF COMMUNICATION SYSTEM DEGRADATION DUE TO VEHICULAR
     NOISE

2.3.1 Objectives

The objectives of this subtask are to--

a. Identify the types of communication system performance analytical
models (and their associated noise parameters) which may be used to show
degradation from vehicular (impulsive) noise.

b. Identify the relative merits for each model.

2.3.2 Study Procedure

a. In determination of system performance in the presence of impul-
sive noise, there are two types of systems to consider--digital and analog.
For the digital system, the performance measures (e.g., BER) are always,
in principle, well defined and mathematically precisely determinable. How-
ever, for analog systems (e.g., voice), which include digital voice, the
required performance measure (e.g., AS) is subjective in nature and there-
fore quite difficult to obtain by objective means. For this reason, most
attention has been given to digital systems.

b. Techniques and models which could be applied to the determination
of communication system performance degradation from vehicular noise were
identified through a review of the literature pertaining to the subject.

2.3.3 Results and Analysis

2.3.3.1 Digital Communication Systems

a. There are two basic and effective techniques to analyze digital
systems in the presence of non-Gaussian noise. The first is to use a
Gaussian analysis, but with the distributions appropriate for impulsive
noise rather than the Gaussian distributions. In general, this means
that the APD of the received noise envelope is required. This technique
guarantees success (ignoring possible mathematical technical problems)
and is based on the geometric representation of digital systems. Arthurs
and Dym (ref 47, app D) present this approach in a very readable form,
and the majority of analyses have followed this procedure. Appendix A
is a short tutorial explanation of the "geometric" approach, along with
procedures for extending the results thus obtained for constant signals
to the results for fading signals. The "geometric" approach applies to
"ideal" systems using matched filter or correlation receivers; that is,
those receivers whose performance is known to be optimum in the presence
of Gaussian noise.

b. The second general approach corresponds to that used for fading
signals and makes use directly of the very extensive results available
for system performance in the presence of Gaussian noise. In this ap-
proach, the noise is treated as fading Gaussian noise, where the fading

distribution is the APD of the noise envelope. This technique is especially useful when considering linear receivers which depart from the "matched filter" ideal, but for which Gaussian results are known. Of course, one could, as before, start from the beginning and match the Gaussian analysis using the impulsive noise distribution, but this would require tedious derivations for each situation. The "fading Gaussian noise" approach is also particularly suited for analyzing the performance of receivers with various nonlinear devices such as limiters. Appendix B discusses this procedure in detail, including application to fading signals. In general, the results of such analyses for digital systems can be summarized as follows (see ref 3, app D, and ref therein for particular examples):

(1) For digital systems and constant signal, white impulsive noise is much more harmful (causes more errors) than Gaussian noise of the same energy at the higher S/N's while Gaussian noise is more harmful for the lower S/N's.

(2) When the envelope of the flat-fading signal has a Rayleigh distribution, Gaussian noise is more harmful at all S/N's. For diversity reception, however, impulsive noise is again more harmful at higher S/N's. For diversity reception, impulsive noise, and Rayleigh fading signals, the degree of statistical dependence between the noise on different diversity branches has a relatively minor effect on system performance for low orders of diversity. For nondiversity operation of a binary system with Rayleigh fading signal, the error probability for a large S/N is essentially independent of the additive noise statistics. Other flat fading situations (e.g., log-normal fading) do arise for which impulsive noise will cause more errors than Gaussian noise at some S/N's.

In addition to the above additive noise and flat-fading signal effects, systems are also subject to multiplicative noise. This form of signal distortion is sometimes termed frequency selective fading. In digital systems, the effect of multiplicative noise is generally to produce a BER threshold; that is, a value of BER which cannot be lowered by increasing signal power. For examples of this phenomenon, see references 5 and 48, app D, and appendix B.

2.3.3.2 Voice Communication Systems

a. The situation for the performance of voice systems, whether analog or digital, is somewhat more complex, since the required performance measure is a subjective measure. Few voice communication systems today are judged by the quality and intelligibility of the received speech; most are judged by some engineering parameter such as the post-detection (output) S/N (see fig. 3). For most forms of interference, including impulsive noise, such measures as output S/N have little to do with speech intelligibility, when considered alone. The most common procedure for determining the intelligibility of a voice system is the expensive and time-consuming method

2-16

involving trained speakers and listener panels that directly score the percentage of intelligible speech [articulation score see ref 49, app D].

b. Empirical estimates of AS as a function of audio S/N are available in the literature for some cases; however, most of these results pertain to Gaussian noise. One example exists for amplitude modulation (AM) voice in a 3-kHz bandwidth in the presence of both Gaussian and very impulsive noise (V_d = 12 dB) as a function of carrier-to-noise ratio (CNR)-- the predetection S/N (fig. 4.13 of ref 3, app D). If the relationship were developed empirically to relate AS to combinations of CNR and V_d (presented as AS versus CNR with V_d as a running parameter), then this would constitute a model for system performance. The required noise parameters would be F_a and V_d, where V_d can be determined for the system's bandwidth directly or by using a good bandwidth conversion algorithm for V_d measured in some other bandwidth. This technique has the best chance to work for AM [and single sideband (SSB)] systems (see table I).

c. One major type of modulation which currently lacks a good impulse noise effects model (and hence the noise parameter to be measured is unknown) is frequency modulated (FM) voice of the type used in the current AN/VRC-12 family. It is known that the time structure of the noise has significant impact on the performance, particularly for higher channel qualities. One system performance model for narrowband FM voice systems is the noise amplitude distribution (NAD) - ACR overlay technique. For this model, the noise parameter to be measured is the ACR (refs 12, 51, and 52, app D). The limited validations of this noise model (and system performance predictions) performed by the Motor Vehicle Manufacturers Association (MVMA) and General Electric (GE) have yet to be published. However, GE does use this model successfully to design commercial land mobile radio systems (ref 53, app D).

d. There has long been a need for an inexpensive, reliable, efficient, and objective method to evaluate the quality of speech. The most common methods have been the spectral weighting techniques, such as articulation index (AI), psophometric weighting, and speech communications intelligibility measure (SCIM) (ref 54, app D). These methods, while repeatable and simple, do not give a consistent relationship to AS. That is, each form of interference, type of modulation, and voice channel requires a separate and different transformation from AI (for example) to AS, the required measure. Therefore, the spectral weighting techniques could present difficulty when used to analyze the degradation of voice systems due to different types of interference and distortion (ref 54, app D).

e. A recently developed technique, based on linear predictive coding (LPC), is being evaluated to determine whether it can provide an objective measurement of voice intelligibility. This method (ref 55, app D) uses a performance measure (or metric) which seems to always bear the same relationship to AS, independent of the type of system, type of speaker, or

2-17

type of interference and distortion, including impulsive noise. In addition, this method can, in principle, be used with computer simulation of communication systems to predict expected performance (ref 56, app D).

2.3.3.3 Concluding Comments

a. Finally, it should be noted that, in general, such studies as the above obtain a single number (e.g., BER, AS, etc.) to describe system performance. A long-term average (see app A), such as error rate, gives a good measure of system performance only when considering stationary noise and signal processes (e.g., Gaussian noise and constant signal). Since the various forms of manmade noise are nonstationary random processes, and the signal processes are also, in general, nonstationary, information in addition to the error rate (or similar measure) is required to completely specify the performance of a given system. It has become common to give two additional measures: the percentage of time a given error rate or better will be achieved (termed "time availability") and the probability that a given system will achieve a specified time availability and error rate (termed "service probability" or "statistical confidence factor"). The service probability is designed to account for the probable errors in the prediction of the noise and signal distributions, their variations, and the like. Once an error rate or like measure has been obtained, the means of obtaining the time availability and service probability are well covered in the literature (refs 3, 27, and 34, app D).

b. For a quick reference, table IV lists typical systems, required input noise information, and appropriate references for determining performance in impulsive noise. Table IV is not meant to be all-inclusive, but when coupled with appendices A and B and the various references, does give a rather complete picture.

TABLE IV. COMMUNICATION SYSTEM PERFORMANCE ANALYTICAL MODELS

System Models	References (app D)	Required Noise Inputs	Output	Comments
NCFSK	57	APD, F_a	BER vs S/N	Assumes independent noise, so CER easily obtainable from BER. Except for very high speed systems, independence is probably a reasonable assumption.
NCFSK	34	APD, F_a, and their statistical variations.	BER vs S/N, time availability, and service probability	Reference 34 gives examples using NCFSK--the procedures for obtaining time availability and service probability are valid for any system.
CFSK PSK DCPSK ASK MSK	58 & app B 58, apps A,B 59 57, 58 37, 60	APD, F_a	BER vs S/N	Errors are not independent for DCPSK even with independent noise. Results reasonably well verified.
Above digital systems using other than matched filter detection but still "linear."	App B	APD, F_a	BER vs S/N	Appendix B uses the concept of "fading Gaussian noise" and requires further verification; i.e., comparison with rigorous analysis.
Above digital systems using nonlinear processing.	58, 61, & app B	APD, F_a	BER vs S/N	Some results reasonably well verified.

TABLE IV.   COMMUNICATION SYSTEM PERFORMANCE ANALYTICAL MODELS (CONT)

System Models	References (app D)	Required Noise Inputs	Output	Comments
Voice systems	54, 55	For AI, output signal and noise spectra	Nothing useful for impulsive noise	The LPC metric method needs further verification for impulsive noise.
		For LPC metric, Fa, APD, plus as yet undetermined information	AS vs S/N	
	12, 51	NAD (ACR) and isodegradation curves	dB degradation (dB of additional signal required to re-establish per-formance)	This empirical method has no firm basis in theory and has only been used by its originator (ref 51). Accuracy is unknown. Subjective measurement of receiver degradation is required.
	18, 19	Frequency, envi-ronment, type of station (base or mobile), and state of motion of mobile, and required subjec-tive channel quality	Degradation, re-quired signal in dB over that re-quired for com-batting set noise	Simple, if one assumes the envi-ronment is like one already mea-sured. Accuracy is unknown. Strictly qualitative and subjec-tive.

TABLE IV. COMMUNICATION SYSTEM PERFORMANCE ANALYTICAL MODELS (CONT)

System Models	References (app D)	Required Noise Inputs	Output	Comments
All of above with flat fading signal	62 & app A	BER vs S/N for constant signal plus signal fading distribution.	BER vs S/N AS vs S/N	
All of above with dispersive fading	44, 60	See references	BER vs S/N CER vs S/N	

AI – articulation index
APD – amplitude probability distribution
ASK – amplitude shift keying
BER – bit error rate
CFSK – coherent frequency shift keying
DCPSK – differentially coherent phase shift keying
S/N – signal-to-noise ratio
LPC – linear predictive coding
MSK – minimal shift keying
NCFSK – noncoherent frequency shift keying
PSK – phase shift keying

2.4 VALIDATION OF NOISE DATA SAMPLES AND DATA AVAILABILITY

2.4.1 Objective

The objective of this subtask is to present statistical validation methods which can be used to verify vehicular noise data and to identify the current state of vehicular noise data availability.

2.4.2 Study Procedure

Noise data acquisition produces a group of observations (see fig. 1) of a given noise parameter (or parameters), see table II. Communications system performance models generally require the computation of selected statistics. For example, to compute the average BER for a frequency shift keying (FSK) digital system it is useful to measure the amplitude of the envelope of the output of the predetection filter as a function of time (see paras 2.1 and 2.3, and figs. 2 and 3). The resulting noise data sample can be used to compute the APD, which, in turn, can be used to compute the BER. However, prior to the extraction of the desired statistics from the data sample it is necessary to perform some checks to ensure that the data sample can be used with confidence to extract the statistics so that the resulting conclusions (e.g., on average BER) will be valid. A literature search was performed to identify the required checks.

2.4.3 Results and Analysis

2.4.3.1 DATA EDIT Tests. This test identifies obviously erroneous noise parameter data values (e.g., values which fall outside a known range of possible values), and culls these values from a single test sample (ref 63, app D). Various parity checks are also used to spot erroneous noise data samples.

2.4.3.2 RUNS Test. This test will check the statistical independence of the individual samples (ref 64, app D). This check pertains to both the source and the sampling (e.g., sampling rate relative to the Nyquist rate for the filter bandwidth of interest). The assumption of independence has a large impact on the sample size required to describe the noise statistics with a given confidence (refs 64-66, app D).

2.4.3.3 Hypothesis Tests for Homogeneity. The test for homogeneity is basically a test of the hypothesis that the data samples were generated by the same underlying process mechanism (ref 64, app D). Specifically, this test entails developing a series of null hypotheses for each of the vehicular noise estimates and testing these hypotheses against a known probability distribution (e.g., χ^2-distribution) and the data sample to identify type I and II errors (ref 67, app D). This type of analysis determines whether the data sample can be used to estimate the desired noise parameter. Additionally, depending on the outcome of the analysis,

these tests can infer the stationarity or nonstationarity of the vehicular noise waveform. RUNS tests are also useful for checking stationarity (ref 63, app D).

2.4.3.4 Goodness-of-Fit Tests. These types of tests determine whether the noise parameter estimates can be described by an assumed probability distribution (i.e., pass the hypothesis test, for a given level of significance, that the samples were drawn from a specific sample space). Reference 64, appendix D, presents typical examples of these types of tests on data samples. It is especially important to test the hypothesis that the distribution is Gaussian (ref 63, app D). If such a test fails, then various distribution-free tests (ref 68, app D) may be of use.

2.4.3.5 Other Types of Noise Data Sample Tests. Several other types of tests are potentially useful prior to the computation of the desired statistics for any given system analysis. For example, tests for periodicities in the data are useful (e.g., Fourier transform).

2.4.3.6 Noise Data Availability

a. Some noise data are available in the open literature and additional data are available in technical reports (ref 25, app D, and app E). The applicability of most of these data to the evaluation of noise and/or system performance models or the evaluation of the degradation of specific systems of interest is very limited. The primary data required for the analysis of digital system performance are: (1) the average noise power (P_N) measured in the bandwidth of the predetection filter with an rms detector of sufficient dynamic range (or equivalent), and (2) the APD of the envelope of the noise output of the predetection filter. Measured values of the parameter F_a can be used, along with information on the receiving system, to compute the P_N mentioned above. Actually, measured values of the distribution of F_a versus frequency and distance from individual vehicle types are what is really needed, since there is considerable variability of the noise from different vehicles. The propagation effects for a given polarization (e.g., vertical) can be summarized for a given frequency band and distance interval as a distance scaling law so data obtained at different distances can be normalized to a reference distance (e.g., 10 m, the distance specified in the SAE and CISPR standards). Distributions of F_a (for a vertically polarized antenna near earth) for civilian vehicles in several countries for the frequency band 20-30 MHz are summarized in reference 15, appendix D, which contains the only known data of this type except for the data on 20 MHz and 48 MHz contained in reference 10, appendix D. Comparable F_a data for a population of military vehicles (or for data on civilian vehicles in other frequency bands) are presently not available, although a limited number of other measurements of F_a have been made (e.g., refs 4, 8, 10, and 16, app D).

b. Measured APD's for noise from single vehicles and from freeway traffic have been given by Shepherd, et al (ref 8, app D), and by Shepherd (ref 9, app D). The freeway data have been used by Middleton (ref 30,

2-23

app D) to check predicted APD's for his Class B (broadband) noise. This check represents one of the first published comparisons to date of a predicted and measured APD from ignition noise, although comparisons with other models have been presented (ref 41, app D). The APD model of Cohen (ref 40, app D) has also been compared (ref 69, app D) with these same data (ref 8, app D).

   c. Schulz and Southwick (ref 14, app D) measured APD's of V-8 ignition emanations of single vehicles and groups and noted the effects of bandwidth on averaged values. Their APD's are not directly comparable to those of Shepherd, et al (ref 8, app D) because of the method of calibration and data acquisition. While there are some pulse-height distributions of ignition noise from single automobiles (ref 70, app D), and even single cylinders (ref 71, app D), these results should not be confused with APD's of the type discussed in this report.

   d. The data mentioned above on ignition noise are of the type useful for estimating the performance of digital systems. The F_a data are useful for computing predetection S/N, sometimes called CNR for analog systems. To the extent that CNR can be correlated with AS or some other measure of system performance (e.g., a meaningful subjective estimate of channel quality), then the F_a data are useful for estimating the performance of analog systems. Figure 4.13 in reference 3, appendix D, presents word AS versus CNR for V_d = 1.049 dB (Gaussian noise) and V_d = 12 dB (very impulsive noise) for an AM voice system (SSB) in a 3-kHz bandwith. The only published data on F_a and V_d for ignition noise are references 8 and 9.

   e. The MVMA has performed several in-house studies of performance degradation to various types of systems (e.g., land-mobile radio and TV) caused by ignition noise. The results are not yet generally available in the literature, although there is an intent to file some additional information in FCC Docket 20654. It is not likely that significant amounts of F_a, V_d, or APD data will result from this effort.

   f. Data on V_p, V_{qp}, and average voltage (V_{av}) measurements of ignition noise are available (e.g., refs 15 and 17, app D); however (as noted in para 2.2), these parameters are not inputs to known system degradation models. It has been observed that V_{rms} data are more useful in estimating marginally useful land mobile radio (FM) circuits, V_{qp} data in estimating good quality circuits, and V_p data in estimating very high quality circuits (ref 53, app D). Requirements for additional data collection and identification are discussed in paragraph 2.7.

2-24

2.5 VEHICULAR NOISE PARAMETERS, TEST INSTRUMENTATION, AND METHODOLOGIES

2.5.1 Objectives

The objectives of this subtask are to--

a. Determine the most meaningful vehicular noise parameters.

b. Identify the test instrumentation and methodologies which may be used to measure vehicular noise emissions.

2.5.2 Study Procedure

a. Table V presents a listing of some of the noise parameters previously identified in table II. For each parameter listed, this table includes a series of bibliographic references, specification standards and limits, generic characteristics of instruments, and sources of off-the-shelf instrumentation with associated technical characteristics.

b. Certain basic concepts, identified below, must be kept in mind in making noise measurements.

2.5.3 Results and Analysis

a. The measurement of radiated noise and signals is in general required over a broad frequency range. Therefore, prior to detection, the noise and signal must be conditioned or transformed. This conditioning or transformation involves two steps: (1) frequency translation, and (2) bandwidth restriction (filtering). The frequency translation, if done without distortion, does not affect the characteristics of the signal plus noise envelope. The bandwidth restriction or filtering is, however, a much more complex operation which may, under certain ideal situations, have very little effect. However, in other situations filtering may have a significant effect. Although the bandwidth characteristics of the test instrument can be identified, the conditions most affecting the outcome of the measurement depend on the measured waveform's structure, which is unknown and unknowable. Because of this situation, it is always advisable to use a measuring instrument with an appropriate bandwidth. To determine the degradation of a specific candidate U. S. Army communications receiver, vehicular noise measurement data should be collected using test equipment receiver bandwidths which are as close as possible to the candidate receiver's bandwidth. Where possible, noise data should be collected for multiple bandwidth settings of the test equipment's receiver.

b. Voltage detectors can be categorized as follows: (1) quasi-peak, (2) peak, (3) average, and (4) true root mean square (rms)--see table V. Detector charge time, discharge time, integration time, and measurement interval T are important considerations when selecting a specific voltage detector. Peak and quasi-peak voltage detectors have fixed and asymmetrical charge and discharge times, whereas average and rms voltage detectors have symmetrical charge and discharge times. When measuring random

Noise Parameter (Detector)	Bibliographic Reference *	Specification (Limits)		Generic C	
		Document	Frequency	Organization	Frequency
Quasi-Peak Voltage (V_{qp})	61,62,65,71,86	SAE J551e	20 MHz–1000 MHz	CISPR (Publ 1)	0.15–30 MHz
		MIL-STD-461A	14 kHz–10 GHz		
		CISPR (Publ 9)	40 MHz–250 MHz		
				CISPR (Publ 2)	25–300 MHz
				CISPR (Publ 4)	300–1000 MHz
				ANSI (C63.3-1964)	UA
Peak Voltage (V_p)	27,61,62,65,71, 86,92	SAE J551e	20 MHz–1000 MHz	UA	UA
		MIL-STD-461A	14 kHz–10 GHz	UA	UA
		CISPR (Publ 9)	40 MHz–250 MHz	UA	UA
Average Voltage (V_{av})	20,27,45,79	MIL-STD-461A	14 kHz–10 GHz	ANSI (C63.3-1964)	UA
Rms Voltage (V_{rms})	27,45,65,79	UA	UA	UA	UA
Amplitude Probability Distribution (APD)	3,5,10,11,14,17,20, 25,29,30,36,42,49, 52,56,60,62,64,72, 73,74,75,79,87,90	UA	UA	UA	UA
Pulse Height Distribution (PHD)	25,47,79	UA	UA	UA	UA
Noise Amplitude Distribution (NAD) [Average Crossing Rate (ACR) Characteristic]	48,49,52,62	UA	UA	UA	UA
Voltage Deviation (V_d) $$V_d = 20 \log \frac{V_{rms}}{V_{av}}$$	2,3,20,41,58,79,85	CCIR 322 (atmospheric and galactic)	10 kHz–40 MHz	UA	UA
Noise Power (P_N)	7,15,41,50,58,60, 65,79	CCIR 322 (atmospheric and galactic)	10 kHz–100 MHz	UA	UA
		CCIR 258 (manmade)	250 kHz–250 MHz		

Note: UA – unavailable
        IFB – intermediate frequency 6–dB bandwidth
        CF – crest factor

*As contained in appendix E.
**U. S. Distributor: Epoch Enterprise, P.O. Box 17582,

TABLE V.   VEHICULAR NOISE PARAMETERS AND TEST INSTRUMENTATION

Generic Characteristics				Off-the-Shelf Equipments				
						Technical Characteristics		
Organization	Frequency	Dynamic Range	Other	Manufacturer	Nomenclature	Frequency	Dynamic Range	Other
CISPR (Publ 1)	0.15-30 MHz	30 dB ac, 12 dB ac	Charge time = 1 ms; discharge time = 160 ms	1. Singer Instrumentation	NM-17/27	10 kHz-32 MHz	160 dB	Charge time = 1 ms; discharge time = 600 ms
CISPR (Publ 2)	25-300 MHz	UA	UA	2. Singer Instrumentation	NM-37/57	30 MHz-1000 MHz	140 dB	Charge time = 1 ms; discharge time = 600 ms
CISPR (Publ 4)	300-1000 MHz	UA	UA	3. Singer Instrumentation	NM-25T	150 kHz-32 MHz	140 dB	Charge time = 1 ms; discharge time = 600 ms
NSI (C63.3-1964)	UA	UA	Charge time = 1 ms; discharge time = 600 ±120 ms	4. Fairchild	EMC-25	14 kHz-1000 MHz	150 dB	
				5. Stoddart Electro Systems	NM-30A NM-52A	20 MHz-400 MHz 375 MHz-1000 MHz	124 dB-164 dB 131 dB-145 dB	
IA	UA	UA	UA	1. Singer Instrumentation	NM-17/27	10 kHz-32 MHz	160 dB	Hold times = 0.05 s, 0.3 s, 3 s
IA	UA	UA	UA	2. Singer Instrumentation	NM-37/57	30 MHz-1 GHz	140 dB	Hold times = 0.05 s, 0.3 s, 3 s
IA	UA	UA	UA	3. Singer Instrumentation	NM-25T	150 kHz-32 MHz	140 dB	Slideback
				4. Fairchild	EMC-25	14 kHz-1000 MHz	150 dB	
				5. Rohde and Schwarz	HFU 100.1066.02	25 MHz-1300 MHz		
				6. Stoddart Electro Systems	NM-30A NM-52A	20 MHz-400 MHz 375 MHz-1000 MHz	124 dB-164 dB 131 dB-145 dB	Slideback
				7. Norma Messtechnik GmbH, Vienna, Austria**	U-Functionmeter	10 Hz-2 MHz	1 mV-300 V	CF ≥ 14
NSI (C63.3-1964)	UA	UA	Charge time ≤ 1/5 IFB; discharge time ≤ 1/5 AFB	1. Singer Instrumentation	NM-17/27	10 kHz-30 MHz	160 dB	
				2. Singer Instrumentation	NM-37/57	30 MHz-1000 MHz	140 dB	
				3. Singer Instrumentation	NM-25T	150 kHz-32 MHz	140 dB	
				4. Stoddart Electro Systems	NM-30A NM-52A	20 MHz-400 MHz 375 MHz-1000 MHz	124 dB-164 dB 131 dB-145 dB	
				5. Norma Messtechnik GmbH**	U-Functionmeter	10 Hz-2 MHz	1 mV-300 V	CF ≥ 14
IA	UA	UA	UA	1. Singer Instrumentation	NM-26T	150 kHz-32 MHz	140 dB	Time constant = 0.1-100 s
				2. Richard Brancker Research, Ltd	Model 895 V_{rms} Converter	20 MHz-1000 MHz	0 dBμV-40 dBμV	Time constant = 1 s, 4 s, 20 s; CF = 25 dB
				3. Norma Messtechnik GmbH**	U-Functionmeter	10 Hz-2 MHz	1 mV-300 V	CF ≥ 14
IA	UA	UA	UA	1. Norma Messtechnik GmbH**	Probability Meter	10 Hz-1 MHz	30 mV-1000 V	UA
IA	UA	UA	UA	UA	UA	UA	UA	UA
IA	UA	UA	UA	UA	UA	UA	UA	UA
IA	UA	UA	UA	1. Singer Instrumentation	NM-26T	150 kHz-32 MHz	140 dB	UA
				2. Richard Brancker Research Ltd	Model 895 V_d Converter	20 MHz-1000 MHz	0 dB-40 dB	Time constant = 1 s, 4 s, 20 s; CF = 25 dB
IA	UA	UA	UA	1. Hewlett Packard (HP)	HP 342A Noise Figure Meter	30,60,70,105, 200 MHz	5.2 dB noise source, 0-15 dB → ∞; 15.2 dB noise source, 3-30 dB → ∞	BW = 1 MHz; input impedance = 50 ohms
				2. Hewlett Packard (HP)	HP 436A Power Meter	100 kHz-18 GHz	50 dB	UA

Enterprise, P.O. Box 17582, Tucson, AZ 85731

waveforms such as manmade noise, these time constants may greatly influence a quantitative measurement. Therefore, it is always important to understand the operation, electrical characteristics, and method of calibration for a specific detector.

2.5.3.1 Quasi-Peak Voltage

a. The quasi-peak voltage detector (refs 72 and 73, app D) is time-dependent, with fixed charge and discharge times. As indicated in table V, the ANSI and CISPR detectors have a constant charge time of 1 millisecond (ms) for different frequency bands. The discharge times for these detectors, however, are different (see table V) and are a function of frequency. Because of the 1-ms charge time, this detector will indicate a measured value dependent on the impulse rate of the input waveform.

b. An example of this impulse rate dependency is evidenced in the EMC-25 field intensity meter (FIM) when used in the quasi-peak detection mode. A change of 45 dB occurred, for constant amplitude pulses, when the input waveform's impulse rate was increased from 10 kHz to 1 MHz (see ref 74, app D). It is, in general, difficult to relate the output of this type of detector to an input which is a random impulsive waveform. However, it has been shown that estimates of the quasi-peak values can be derived from an APD under certain assumptions (ref 44, app D).

2.5.3.2 Peak Voltage. The peak voltage detector is also time-dependent, with a fast charge time and a very long discharge time. As a result, changes of impulse rate will not affect the peak detector reading. An example of this is when the EMC-25 is in the peak detection mode. Input pulses of constant amplitude with rates from 100 Hz to 500 kHz caused a meter reading change of 0 dB within ±1 dB (ref 74, app D). For random waveforms, the measured value of peak voltage is a function of the measurement (observation) interval T.

2.5.3.3 Average Voltage. The average voltage detector is sometimes called a "carrier detector." The average voltage switch position on some commercially available meters is labeled field intensity (FI). For random waveforms, the average voltage has been defined in table II. Unfortunately, most FIM's using "average" detectors do not measure the average voltage because of logarithmic IF's, dynamic range limitations, and calibration procedures. The average voltage when used by itself is not a particularly useful measure of random impulsive noise. However, when used in conjunction with the rms voltage (para 2.5.4.4), it provides a measure of the impulsiveness of random noise environments (para 2.5.4.7).

2.5.3.4 Rms Voltage

a. The rms voltage is one of the most useful voltage parameters which can be measured since it is directly related to the average power of the input waveform (see table II). The rms detector is required to measure signal-to-noise ratios.

2-29

b.   Some commercially available rms voltage detectors cannot be used to make accurate rms voltage measurements for impulsive waveforms due to limited dynamic range capabilities (i.e., small crest factor—CF). Crest factor is defined to be the ratio of the waveform crest (peak or maximum) voltage value for which the detection system response is linear (or can be calibrated) to the rms voltage value of the waveform (i.e., $CF = V_p/V_{rms}$ for a detection system with linear response).

c.   One instrument of particular interest is the U-functionmeter. This meter will measure ± peak, average, and rms voltages and has a minimum CF of 14 (23 dB) at full scale. This instrument, by means of a novel analog-to-digital conversion process, performs the actual mathematical calculation required to obtain each voltage parameter. The difficulty with conventional rms meter design is the squaring operation which creates dynamic range limitation problems in analog circuits. The U-functionmeter design performs the squaring in a digital circuit and avoids this dynamic range problem.

2.5.3.5 Amplitude Probability Distribution (APD)

a.   The APD, as shown in table II, is simply the complement of (or one minus) the cumulative distribution function (CDF), which is described in basic probability textbooks (refs 3 and 75, app D). There are several instruments on the market today which will measure the CDF from which the APD can be calculated. Most correlators will also measure the CDF of various stationary input waveforms.

b.   The APD parameter appears to be the most useful since most of the noise parameters listed in tables II and V can either be calculated or closely approximated from recorded APD data. In the past, APD measurements of noise have been made only by a few investigators. Various techniques have been used to collect APD data, ranging from analog recording and digital recording (ref 8, app D) to hardware threshold detectors. A novel APD detector designed by R. A. Southwick is being fabricated for the USAEPG. This detector features the selection of a number of preset probabilities and the resultant determination of the corresponding exceeded amplitude voltage (threshold) level. In addition, broadband general purpose APD measurement devices are being built, for use with the U. S. Army Communications Electronic Engineering Installation Agency's (USACEEIA's) transportable automated EMC measurement systems (TAEMS—see refs 76 and 77, app D), by the Institute for Telecommunication Sciences (ITS).

2.5.3.6 Noise Amplitude Distribution (NAD). The NAD parameter is a method of presenting average crossing rate (ACR) data characteristics as a function of threshold level. NAD is not, however, a distribution of a random variable. Most APD measurement devices have the capability of measuring the ACR characteristic. Empirical evaluation of communication system performance degradation can be performed with this method using a set of "isodegradation" curves as demonstrated in references 51 and 53, appendix D. However, this technique for predicting communication system performance has never been validated.

2-30

2.5.3.7 <u>Voltage Deviation (V_d)</u>. The voltage deviation parameter, V_d, provides a measure of the noise impulsiveness of the environment. V_d is given by the following equation:

$$V_d = 20 \log \frac{V_{rms}}{V_{av}}$$

Both V_{av} and V_{rms} have been discussed previously. V_d can be calculated by first measuring V_{rms} and V_{av} separately, then using the above equation. Direct measurement of V_d can be made with the Model 895 V_d Converter measurement instrument, with Singer NM-26T (see table V), or with any other meter with a V_d function.

2.5.3.8 <u>Noise Power (P_N)</u>. Noise power (P_N) has been specified by the U. S. Government (ref 35, app D) as the basic parameter for the measurement of radio noise. The measurement procedures as discussed in paragraph 2.5.4.4 for V_{rms} apply since P_N is proportional to V_{rms}^2 (see table II).

2.5.3.9 <u>Miscellaneous Parameters</u>. There are other noise parameters which have been used for various special purposes and for which references can be found (see table II for examples).

2.6 SUMMARY OF MAJOR FINDINGS AND CONCLUSIONS

a. Currently there is no ongoing program to evaluate and resolve
the overall problem of communication system performance degradation
caused by vehicular noise emissions. Various parties in both industry
and government have investigated certain aspects of this problem. How-
ever, no single party is undertaking the task to organize and control
the various splintered investigations which have been completed or are
planned for future implementation. Because of the complexity of this
overall problem, a need exists to develop an implementation plan for fu-
ture efforts, with a list of tasking priorities, and to establish a group
to monitor these efforts.

b. The preceding paragraphs (paras 2.1 through 2.5) identify various
candidate U. S. Army communications systems, vehicular noise parameters
and analytical models, and communication system performance analytical mod-
els. Each of these subjects are summarized individually in tables within
each paragraph. The following presents a summary of the major findings
and voids which have been identified for the example communication systems
listed in table I. This was performed by examining the information con-
tained in tables II through V and applying this information to the infor-
mation contained in table I. The applicable documents, table V, and voids
were then summarized on a system-by-system basis as shown in table VI.

c. The major findings and conclusions of this feasibility study
are--

(1) A detailed impulsive noise data base for environments to
support the utilization of analytical models is not available.

(2) Limited instrumentation to measure noise parameters rele-
vant for digital communication system models either exists or is now being
procured by the Army.

(3) At the present time, test beds (refs 78 and 79, app D)
do not consider the effects of impulsive noise on systems and equipments
(see table I). The test beds, however, do provide vehicle types on which
there are mounted certain transmitters and receivers. Therefore, it is
possible to derive vehicle(s) disposition (i.e., density and map location)
for a specific scenario time. The test beds therefore could be used to
support a large-scale analysis of impulsive noise effects.

(4) Analytical models to determine BER versus S/N and CER ver-
sus S/N for digital communication systems are relatively well developed
and validated for most of these systems. Further, the required noise pa-
rameters have been determined for use with these models.

(5) There are no analytical models to determine AS versus S/N
for analog (voice) communication systems, although several crude empirical
models exist in the literature. The required noise parameters have not
been determined.

TABLE VI. SUMMARY OF PRESENT VEHICULAR NOISE DATA AND MODELS WHEN APPLIED TO CANDIDATE U. S. ARMY COMMUNICATIONS EQUIPMENTS

	1 AN/VRC-12 Family		2 AN/GRC-106		3 RDS-80	4 AN/TSC-61A	5 AN/GRC-144		6 AN/PSC-1	
	Nonsecure	Secure	Tactical		600 Channel MUX	Air Traffic Control	Tactical Fixed Communications		Satellite Earth Terminal	
	Analog Voice (FM)	Digital Voice (CVSD/FM)	Voice (SSB)	RATT (NCFSK/SSB)	LOS Voice and Data (Digital DQPSK)	Tactical Airfields (Voice, AM, FM)	Voice (PCM/FM)	Data (PCM/FM)	Voice	Data
System Performance Model	UA	UA	UA	Refs 3, 34, and 57, app D, and apps A and B	Ref 59, app D, and app B	UA	UA	App B	UA	Refs 58 and 59, app D, and apps A and B
Noise Model	UA	UA	UA	Table III	Table III	UA	UA	Table III	UA	Table II
Instrumentation	PA	PA	PA	Table V	Table V	PA	PA	Table V	PA	Table V
Noise Model Input Parameter Values (data base)	UA	UA	UA	UA	UA	UA	UA	UA	UA	UA
Physical Environment (Deployments) — Tactical	SCORES Europe I, Sequence 4, Test Bed (ref 78, app D) / Combat Scenario Europe I, Sequence 2A (ref 79, app D)	SCORES Europe I, Sequence 4, Test Bed (ref 78, app D) / Combat Scenario Europe I, Sequence 2A (ref 79, app D)	SCORES Europe I, Sequence 4, Test Bed (ref 78, app D) / Combat Scenario Europe I, Sequence 2A (ref 79, app D)	SCORES Europe I, Sequence 4, Test Bed (ref 78, app D) / Combat Scenario Europe I, Sequence 2A (ref 79, app D)	Not Applicable	SCORES Europe I, Sequence 4, Test Bed (ref 78, app D) / Combat Scenario Europe I, Sequence 2A (ref 79, app D)	SCORES Europe I, Sequence 4, Test Bed (ref 78, app D) / Combat Scenario Europe I, Sequence 2A (ref 79, app D)		SCORES Europe I, Sequence 4, Test Bed (ref 78, app D) / Combat Scenario Europe I, Sequence 2A (ref 79, app D)	
Physical Environment (Deployments) — Long Haul	Not Applicable		Not Applicable		UA	Not Applicable	Not Applicable		Not Applicable	

SCORES - Scenario Oriented Recurring Evaluation System.
UA - unavailable
PA - partially available

Information on the above findings is summarized in table VI, which identifies the voids on a system-by-system basis using the example systems listed in table I.

d. The prescribed measurements of automobile ignition noise include peak field strength measurements as defined in MIL-STD-461A and SAE J551e (which also permits quasi-peak field strength measurements). These noise parameters have not been shown to bear any quantitative relationship to the degradation of communications system performance. In fact, the peak measurement is even insensitive to the rate of occurrence of the impulses and will give the same reading for any impulse rate ranging from a very few to many hundreds of impulses per second.

2.7 RECOMMENDATIONS

2.7.1 General

This report summarizes the present status regarding the modeling and measurement of ignition noise from motor vehicles. It also identifies the types of models, parameters, and measurement instrumentation and methodologies presently available which can be used to determine the degradation caused by ignition noise to Army C-E systems and equipments. The three main voids are the following: (1) voice system performance models, (2) a noise data base, and (3) meaningful measurement standards and limits for ignition noise. A summary of specific recommendations to solve the problems associated with these three voids is provided in the following paragraphs.

2.7.2 System Performance Models for Voice Systems

a. There are three known potentially useful approaches (not necessarily considered models) in the area of degradation to determine voice-channel intelligibility. One is the FCC technique of measuring degradation directly for each given type of system and in each environment of interest. Another is the ACR overlay technique, an empirical graphical method for comparing a measurement of the noise against subjectively derived curves of receiver degradation. The third is the LPC analysis method, in which a computer is used to compare a degraded voice signal against an identical, but undegraded, voice signal. In this latter method, as in the FCC method, the noise environment's effect upon the particular communication system is measured, but not the noise environment itself. It is recommended that--

(1) The ACR overlay technique be carefully evaluated to determine whether there is a promising relationship between degradation of voice reception quality and the subjectively determined AS.

(2) The LPC technique be similarly evaluated, and also the relationship between the LPC parameter and measure(s) of the noise environment be investigated and compared with the subjectively determined AS.

b. The FCC, ACR, LPC, and AS scoring techniques should be used to evaluate the performance of the AN/VRC-12 family of radios under controlled manmade noise conditions.

c. The accuracy of the noise measurement techniques and system performance prediction techniques currently used by the EMETF and other Army agencies for evaluating analog voice systems' performance should be re-evaluated on the basis of the results of the above recommended test programs.

2.7.3 Radio Noise Data Base

a. Two types of noise data are required: (1) measured noise data on individual Army and civilian vehicles, and (2) measured noise data on

tactical and strategic environments which include typical vehicle deployments.

b. It is recommended that the USACEEIA TAEMS van(s) be used to measure the noise parameters P_N, V_d, APD, and possibly ACR as a function of frequency and bandwidth for electromagnetic emissions from individual Army and civilian vehicles available at Fort Huachuca and other CONUS locations. The data collected will provide inputs to the noise models, listed in table III, which pertain to digital system performance.

c. After it has been determined what measured noise parameters will be required as input to the analog and digital voice communication system models, these parameters should also be measured in a tactical battlefield scenario. The noise system parameters P_N, V_d, and APD should be measured simultaneously with the analog model input parameters, and communication system performance should also be recorded simultaneously for each generic type of communication system in the battlefield environment. These types of data should also be obtained for strategic environments (e.g., military posts, camps, and stations).

d. The radio noise data should be acquired, whenever possible, on a noninterfering basis with the primary TAEMS mission at the various sites at which the TAEMS is deployed.

e. The APD devices under procurement by CEEIA and USAEPG should be used at the same location and time so that measurement results can be compared when measuring the same noise environment.

f. Required accuracies for noise parameter measurements should be determined empirically and (where possible) analytically.

2.7.4 Meaningful Standards for Automotive Ignition Noise

a. The current ignition noise standards (MIL-STD-461A and SAE J551e) are primarily used by the Army during the procurement of _new_ tactical and administrative vehicles. The usefulness of these standards should be studied in the context of relating the degree of suppression (and its cost) to an assumed degree of improved communication system performance of several Army C-E system(s). Standards for vehicles in service should also be included.

b. The empirical relationship, if any, between V_p and P_N should be determined for some example cases to assess the merit of retaining the relatively easy-to-measure V_p parameter in future military standards. If there is a relationship, an analysis should be performed to determine whether V_p data provide an upper bound on the degradation of any systems of interest to DoD. Even if V_p cannot provide exact predictions of system performance, this parameter should be examined to determine its validity and possible use as a meaningful limit. Also, other easy and inexpensive-to-measure parameters should be explored for their potential use in estimating upper bounds on degradation.

2-36

2.7.5 Instrumentation

Table V presents the instrumentation currently available to measure the various noise parameters. In addition, instrumentation described in paragraph 2.5 is in the process of being developed for future use in the field. With the advent of microprocessor-controlled instrumentation, the measurement of statistical signal parameters can now be done by relatively simple-to-operate field-usable instruments. The development of this technology should be further investigated and exploited so as to develop instruments for the measurement of more meaningful noise parameters.

2.7.6 Validation of Noise Environment Models and Digital System Performance Models

a. While the noise and system performance models exist for most digital systems, additional validation measurements should be performed to define the degree of confidence in these models.

b. Predictions should be made of the noise for environments of interest to the Army and for the performance of selected digital systems operating in these environments. The noise parameters and system performance should then be measured simultaneously in the selected example environments, and a measure of confidence should be developed for both the models and the predictions.

c. Existing data should be utilized to check existing models (e.g., the Markov Regime model).

2.7.7 Deployment Data

a. The existing data on the numbers of vehicles, by type, that are likely to be operating in the vicinity of communication receivers have not been assembled in a form required as input to the environmental noise models. The statistics of the distances from the vehicles to the victim receivers are required for an accurate description of the noise environment.

b. The deployment data on military vehicles (and possibly some civilian vehicles) should be assembled in the form required for environmental noise models for selected example tactical and strategic scenarios.

c. To help fill long haul communications systems and equipment and vehicular noise voids, consideration should be given to identifying the potential problems involved in providing a test bed with Defense Communications Agency (DCA) and World Wide Military Command and Control Communication System (WMC^{3}S) node points. Secondly, consideration should be given to providing some idea of vehicle(s) disposition (i.e., vehicle density and map location) for a specific geography and time frame identified by the test bed; this analysis can be done manually with the test bed data.

2.7.8 Quick-Response Data Base

The information on the degradation caused by ignition noise should eventually be assembled (to the extent practicable) in a set of parametric curves or charts (or equivalent) to permit a quick-look-up for a quick-response capability.

SECTION 3 - APPENDIXES

APPENDIX A - SLOW FLAT FADING DESCRIPTION BY A. D. SPAULDING - GEOMETRIC APPROACHES, TUTORIAL

C O P Y

BI-1. SYSTEMS EVALUATION FOR SLOW-FLAT FADING

A. D. Spaulding

BI-1.1. INTRODUCTION .

In this section we will develop the simple technique to
determine the performance of a telecommunications system with
a slow-flat fading signal once a performance characteristic
is known for the constant signal. The "slow" in slow-flat
fading means the signal amplitude fades slowly enough in time
that the signal can be regarded as constant over some time
period of interest (such as the time of a signal element in
a digital system). The "flat" refers to the spectral behavior
of the fading, and implies that the entire signal spectrum
fades up and down uniformly so as not to distort the signal.

The physical processes that cause fading fall into two
broad catagories: (1) absorption and other large volume
effects, which result in a random signal normally called
scatter; (2) the other category is comprised of numerous
specular modes of propagation. The separation of the modes
may take place at sharp boundaries of charged particles or
reflections from isolated objects, etc. We have an assort-
ment of distinct paths that the wave fronts may take in
propagating from the transmitter to the receiver. This
phenomenon is commonly called multipath and each path may
contain some specular and scatter contributions. In any
case, the fading signal received at the receiver becomes
random and can be treated only in statistical terms.

In order to understand how a system's performance is
degraded by the slow-flat fading signal compared with the
performance for a constant signal of the same average power,
and how the degree of degradation can be easily calculated,

we will first consider a simple, but practical example. This
will enable us not only to understand the technique, but also
to see why the technique will not work for other kinds of fading
signals (for example, frequency selective fading, leading to
signal distortion).

We will analyze the performance of a binary coherent
phase shift keying (CPSK) digital system first, when the
signal is constant, and then, from the probability of error
characteristic obtained for this constant signal, we will
obtain the system performance for slow-flat fading signals.
We will do this for all the types of slow-flat fading signals
generally considered, starting at the very beginning and
analyzing the system's performance using a geometrical
approach. This will enable us to picture what is going on
in the signal-receiving process.

BI-1.2.   CONSTANT SIGNAL PERFORMANCE

To represent a digital system geometrically, we make use
of the following fact:

Any finite set of physical waveforms of duration T,
say $S_1(t)$, $S_2(t)$, ..., $S_m(t)$, may be expressed as
a linear combination of k orthonormal waveforms
$\phi_1(t), \phi_2(t), ... \phi_k(t)$, where $k \leq m$.

That is, each signal, $S_i(t)$ can be written as

$$S_i(t) = a_{i1}\phi_1(t) + a_{i2}\phi_2(t) + ... + a_{ik}\phi_k(t) , \quad (BI-1)$$

where the coefficients a_{ij} are given by

$$a_{ij} = \frac{1}{T} \int_0^T S_i(t)\phi_j(t) \, dt.$$

Here the basic waveforms, $\phi_j(t)$, being orthonormal means that

$$\frac{1}{T}\int_0^T \phi_i(t)\phi_j(t)dt = 1 \quad i = j$$
$$= 0 \quad i \neq j \; .$$

While the above representation looks similar to the familiar Fourier expansion of a waveform, it is different in two important respects. The waveforms $\phi_i(t)$ are not restricted to sine and cosine waveforms, and (BI-1) is exact, even though only k terms are used.

Because of the above, our signaling waveforms, $S_i(t)$, can be represented in the k-dimensional signal space, $\phi_j(t)$, with coordinates given by the a_{ij}. For example, consider a set of signals for which k = 2, then the signals, $S_i(t)$, are given by vectors in the space $\phi_1(t)$, $\phi_2(t)$ as in figure BI-1.

$$S_1(t) = a_{11}\phi_1(t) + a_{12}\phi_2(t)$$
$$S_2(t) = a_{21}\phi_1(t) + a_{22}\phi_2(t)$$
$$\vdots$$
$$S_i(t) + a_{i1}\phi_1(t) + a_{i2}\phi_2(t)$$
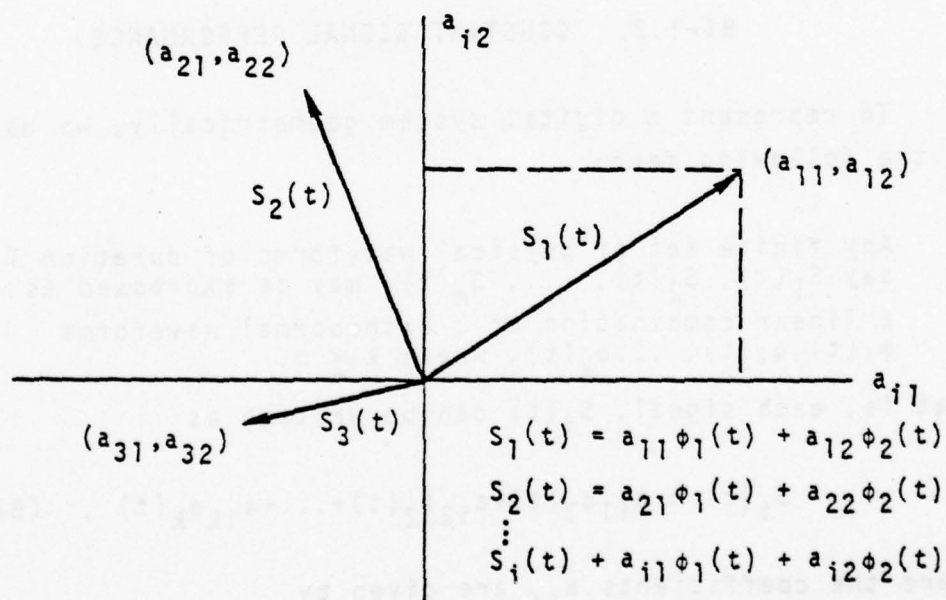
Figure BI-1. *Signals represented as vectors in a signal space, k = 2.*

A-4

As we shall see, the above representation not only allows visualization of what is actually going on in the receiving process, but also allows the variable, t, time to be removed from the problem. Our signals are now represented by simple vectors in ordinary Cartesian coordinates. That is, each signal is now represented by a <u>point</u> in the signal space with coordinates a_{ij}. All the rules of ordinary geometry apply, for example, the "distance" between signals is simply the ordinary distance between the corresponding signal points.

Digital receivers, actually, by various means, compute the coordinates of a received signal and then make a decision based on these coordinates. One obvious receiver implementation is shown in figure BI-2. The actual physical implementations of the digital receiver may be, as in figure BI-2, a matched filter form, etc., but all these forms accomplish precisely the same thing, i.e., to compute the signal coordinates, a_{ij}, and then make a decision as to which signal was sent, based on these a_{ij}.

Figure BI-2. Product integrators used to calculate the signal space coordinates of signal $S_i(t)$.

The additive noise, which interferes without signal and causes the receiver to make errors when it tries to decide which one of the m-signalling waveforms was transmitted, also is represented by a point in the receiver's signal space. If $n(t)$ is the received 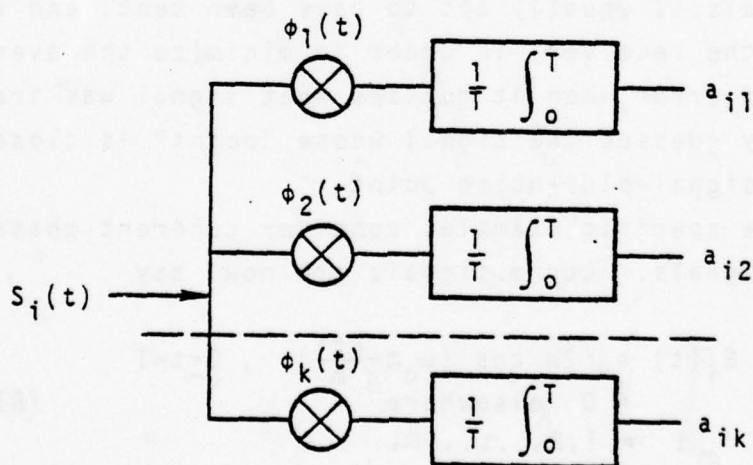random-noise waveform, then it (like the signal) goes through the product integrators (or whatever), with the result that, as far as the receiver is concerned, the interfering noise is given by

$$n(t) = n_1\phi_1(t) + n_2\phi_2(t) + \ldots + n_k\phi_k(t) . \qquad (BI-2)$$

Therefore, if the receiver received noise only, the noise would also be represented by a point in the receiver's signal space, the noise coordinates given by n_1, n_2, ..., n_k.

Each of our m signals is represented by a unique point in the signal space. When signal plus noise is received, the result is a point (signal-plus-noise point) that can be anywhere in the signal space, depending on the noise. If each of our m signals is equally apt to have been sent, and are of equal power, the receiver, in order to minimize the average probability of error when it guesses what signal was transmitted, simply guesses the signal whose "point" is closest to the received signal-plus-noise point.

To take a specific example, consider coherent phase-shift-keyed signals. Our m signals are now, say

$$\begin{aligned} S_i(t) &= \sqrt{2W} \cos \left(\omega_0 t + \frac{2\pi i}{m}\right) , \quad 0 \leq t < T \\ &= 0 \quad \text{elsewhere} \qquad (BI-3) \\ i &= 1, 2, \ldots, m, \end{aligned}$$

where W is the power in $S_i(t)$ (Watts), and
$\omega_0 = 2\pi\ell/T$, for some fixed integer ℓ.

We can choose, then, for our basic waveforms

$$\phi_1(t) = \sqrt{2} \cos \omega_0 t$$
$$\phi_2(t) = \sqrt{2} \sin \omega_0 t$$

Note that our signal space is two-dimensional (k = 2) no matter what m is.

Consider m = 2, now

$$a_{11} = \frac{1}{T} \int_0^T \sqrt{2W} \cos (\omega_0 t + \pi) \sqrt{2} \cos \omega_0 t \, dt = -\sqrt{W}$$

$$a_{12} = \frac{1}{T} \int_0^T \sqrt{2W} \cos (\omega_0 t + \pi) \sqrt{2} \sin \omega_0 t \, dt = 0$$

Likewise, $a_{21} = \sqrt{W}$, $a_{22} = 0$. Therefore, the space and the points representing the two signals are as shown in figure BI-3. The point (n_1, n_2) corresponding to additive noise alone is also shown on figure BI-3.
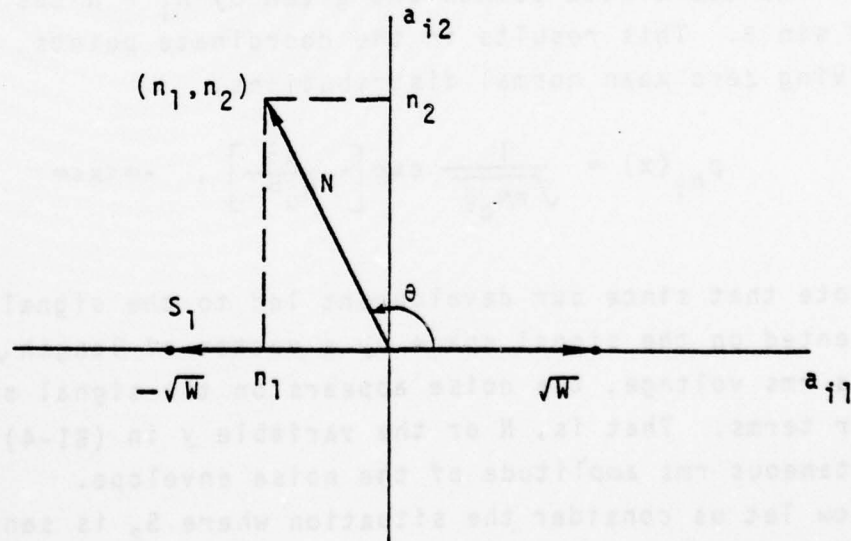
Figure BI-3. The signal space and signal points for binary CPSK, and the noise point (n_1, n_2).

Let the interfering noise be zero mean, white Gaussian, such as it would be if the noise were galactic or receiver front-end noise. N, the noise amplitude after it goes through the receiver and appears on the signal space (fig. BI-3), is Rayleigh distributed. Its probability density function is

$$p_N(y) = \frac{2y}{N_o B} \exp\left[-\frac{y^2}{N_o B}\right], \quad y \geq 0. \qquad (BI-4)$$

This says that the probability that the noise amplitude N has a value in the range Y - dy/2 and y + dy/2 is given by $p_N(y)dy$, where N_o is the noise power spectral density (Watts/Hz) and B is the bandwidth (Hz), i.e., $N_o B$ is the noise power. The phase angle θ is uniformly distributed, i.e., its probability density function is

$$p_\theta(x) = \frac{1}{2\pi}, \quad -\pi < x \leq \pi,$$

i.e., θ has equal probability of being anything between $-\pi$ and π. The coordinate points are given by $n_1 = N \cos \theta$ and $n_2 = N \sin \theta$. This results in the coordinate points, n_1 and n_2, having zero mean normal distributions,

$$p_{n_1}(x) = \frac{1}{\sqrt{\pi N_o B}} \exp\left[-\frac{x^2}{N_o B}\right], \quad -\infty < x < \infty \qquad (BI-5)$$

Note that since our development led to the signal being represented on the signal space by a vector of length $\sqrt{W}$, i.e., a rms voltage, the noise appears on the signal space in similar terms. That is, N or the variable y in (BI-4) is the instantaneous rms amplitude of the noise envelope.

Now let us consider the situation where S_2 is sent and we want to compute the probability that the receiver will decide S_1, and thus make an error. The situation is shown in

figure BI-4. If the resultant signal-plus-noise point lies
in the shaded region (the region whose points are closest to
the S_1 point), then the receiver will decide S_1, and make an
error. This will happen whenever $\sqrt{W} + n_1$ is less than zero,
or p_e = probability of error given that S_2 is transmitted =
probability that $\sqrt{W} + n_1 < 0$. The probability, or likelihood,
that $\sqrt{W} + n_1 < 0$ depends on the probability distribution of n_1.
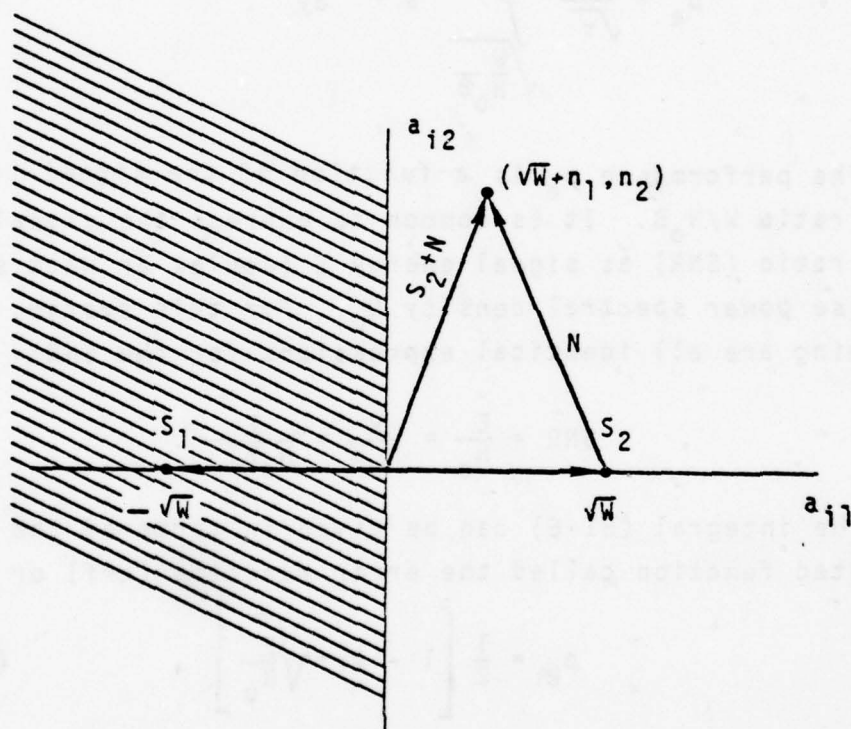
Figure BI-4. The signal-plus-noise point, given
that S_2 was transmitted.

In our case

$$p_e = \text{prob}\left[\sqrt{W} + n_1 < 0\right] = \text{prob}\left[n_1 < -\sqrt{W}\right],$$

or, from (BI-5)

$$p_e = \int_{-\infty}^{-\sqrt{W}} \frac{1}{\sqrt{\pi N_0 B}} \exp\left(-\frac{x^2}{N_0 B}\right) dx \quad,$$

or

$$p_e = \frac{1}{\sqrt{\pi}} \int_{\sqrt{\frac{W}{N_0 B}}}^{\infty} e^{-y^2} dy \quad . \tag{BI-6}$$

The performance p_e is a function of the signal-to-noise ratio $W/N_0 B$. It is common to express the signal-to-noise ratio (SNR) as signal energy E (Joules or Watt seconds) to noise power spectral density N_0. For this system, the following are all identical expressions for the SNR:

$$\text{SNR} = \frac{E}{N_0} = \frac{W}{N_0 B} = \frac{E}{N_0 B T} \quad .$$

The integral (BI-6) can be given in terms of the standard tabulated function called the error function (erf) or

$$p_e = \frac{1}{2}\left[1 - \text{erf}\sqrt{\frac{E}{N_0}}\right] , \tag{BI-7}$$

where

$$\text{erf}(x) = \frac{2}{\sqrt{\pi}} \int_0^x e^{-y^2} dy \quad .$$

Let us look more closely at what the above result (BI-6) actually says. If we have in, say the ith bit, the signal

A-10

level represented by $\sqrt{W}$, and the noise level (in this case represented by n_1), there will or will not be an error in this i^{th} bit, depending on the size of n_1. The integral in (BI-6) says that we are taking an average over an infinity of such i^{th} bits, weighted according to the probability or liklihood that n_1 is of proper size to cause an error. That is, p_e in (Bi-6) represents an _average_ probability of error given that S_2 is sent. If p_e is 10^{-3}, say, then out of m such bits, with m being very, very large, essentially m x 10^{-3} of these bits will be in error. Of course, there is no way of telling which bits will be in error, only the average number. We have considered the above case in which only S_2 was sent. If we repeat for the signal S_1, we obtain the same result. So the probability of error, p_e (BI-6) is the average probability of error for the system.

All digital systems can be put in the above framework and their performance for a constant signal level and for arbitrary additive noise calculated (although, perhaps not so easily as above). Note that for the noise, we required knowledge of the noise _as_ _seen_ _by_ _our_ _receiver_, how big it was, i.e., its spectral density, N_0, and the probability density of its amplitude. Note also that the performance turned out to be a function of the signal-to-noise ratio E/N_0 (or $\frac{W}{N_0 B}$).

BI-1.3. FADING SIGNAL PERFORMANCE

We now consider the case where the signal is not constant but fading. Suppose, however, that our signal is not distorted by the fading and that the fading is slow enough that we can consider the signal constant over an appropriate period of time (T seconds in our example). For our example, we still have the same "signal space" representation of the system, but now our two signals are given by (see (BI-3))

$$S_1(t) = -\sqrt{2W_j} \cos \omega_0 t \ , \ 0 \le t \le T \qquad \text{(BI-8)}$$

$$S_2(t) = \sqrt{2W_j} \cos \omega_0 t \ , \ 0 \le t \le T$$

where the subscript j denotes the signal level in the jth bit. Note that the only change we have allowed is in the signal amplitude and we require W_j to be constant over the time period occupied by bit j. Having pointed out what, precisely, the "slow-flat" fading rules are, we generally now drop the subscript j, and simply say that the signal amplitude varies according to some fading distribution. This says that now the signal amplitude, just as the noise before, is random and we can only specify the likelihood or probability of it having particular values.

Previously (see fig. BI-3), as we went from bit to bit in our bit stream, the signal points on the a_{i1} axis remained fixed, while the noise point of interest (the coordinate n_1) moved randomly up and down the a_{i1} axis. We computed the average probability of error by averaging over many, many situations (bits) taking into account the probability of n_1 having values which would cause errors.

Now with the fading signal, the signal point also moves randomly up and down the a_{i1} axis as we go from bit to bit. Figure BI-5 shows the situation for three successive bits, considering signal S_2.

As before with the noise, to obtain the average probability of error, we must average over many such bits, taking into account now, the variable signal point (i.e., the probability distribution of the signal amplitude) as well as the variable noise point. This means that our average must now consider both the signal distribution and the noise distribution. Fortunately, this can be accomplished quite easily using the following rule from probability theory:
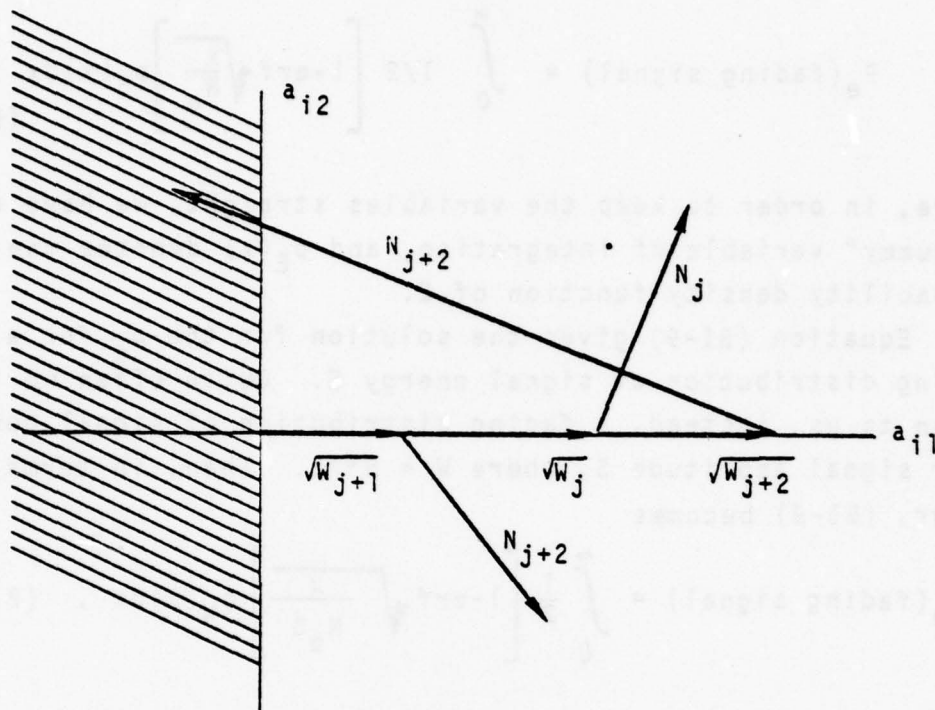
Figure BI-5. Signal plus noise, signal fading.

$$P[A] = \int_{-\infty}^{\infty} P[A|B=x] \, p_B(x) \, dx \ ,$$

that is, the probability of event A is given by the proba-
bility of event A, given that B has the value x, averaged
over all values that B can have.

For our system, we have calculated the performance,
given a signal energy E (or power, W) namely, p_e. The above
says that for fading signal, we need only multiply the
constant signal performance by the probability density function
of the fading signal energy and then average (integrate) over
all possible values of the signal energy. Therefore, from
(BI-7), we have

$$P_e(\text{fading signal}) = \int_0^\infty 1/2 \left[1 - \text{erf} \sqrt{\frac{x}{N_o}} \right] p_E(x)dx \quad , \tag{BI-9}$$

where, in order to keep the variables straight, we have used a "dummy" variable of integration, and $p_E(x)$ denotes the probability density function of E.

Equation (BI-9) gives the solution for the p_e for a fading distribution of signal energy E. Quite often we have given to us, instead, a fading distribution of signal power W or signal amplitude S, where $W = S^2/2$. Then, in terms of power, (BI-9) becomes

$$p_e(\text{fading signal}) = \int_0^\infty \frac{1}{2} \left[1 - \text{erf} \sqrt{\frac{x}{N_o B}} \right] p_W(x)dx \quad , \tag{BI-10}$$

where $p_W(x)$ is the fading distribution of signal power W. Note that, of course, (BI-9) and (BI-10) are identical in form. For signal amplitude S, (BI-9) becomes

$$p_e(\text{fading signal}) = \int_0^\infty \frac{1}{2} \left[1 - \text{erf} \sqrt{\frac{x}{2N_o B}} \right] p_S(x)dx \quad , \tag{BI-11}$$

where $p_S(x)$ denotes the distribution of signal amplitude. In (BI-10) the variable of integration x represents signal power W, while in (BI-11), the variable of integration x represents signal amplitude S ($W = S^2/2$).

The question now becomes, what $p_W(x)$ or $p_S(x)$ should we use? Let us first consider the case of a signal whose amplitude fades according to the Rayleigh distribution:

$$p_S(x) = \frac{x}{W_o} e^{-x^2/2W_o} \quad , \tag{BI-12}$$

where W_o denotes the mean power of the signal; i.e., the mean value of W. Of course, for constant signal, W_o = W. We will see later why the Rayleigh distribution is sometimes a good one to use for multipath signals.

Equation (BI-11) now gives us

$$p_e = \frac{1}{2} \int_0^\infty \left[1 - erf \frac{x}{\sqrt{2N_o B}} \right] \frac{x}{W_o} e^{-x^2/2W_o} dx \quad . \quad (BI-13)$$

This integral is easily evaluated (especially with a good table of integrals) to give the known result

$$p_e = \frac{1}{2} \left(1 - \frac{\sqrt{\frac{W_o}{N_o B}}}{\sqrt{\frac{W_o}{N_o B} + 1}} \right) \quad . \quad (BI-14)$$

Again, our result came out in terms of the SNR. As discussed previously, the signal power to noise power ratio, $W_o/N_o B$ is equal to the signal energy to noise power spectral density ratio, E_o/N_o, (E_o = mean value of E) for this system.

What we have shown is that the performance of any system with slow flat-fading signal can be calculated using the system performance characteristic in constant signal and the probability distribution of the fading signal. For example, if we had available for an analog system (such as voice) some constant signal performance characteristic (such as articulation index) as a function of signal-to-noise ratio, then we could compute the performance for fading signal as above. We would need to be sure, however, that all the assumptions inherent in "slow" and "flat" were met or were reasonable approximations to the actual physical situation.

In summary, if $g_c(W/N_oB)$ denotes the performance for constant signal, and if $p_W(x)$ denotes the probability density of the signal power W, then the performance of the system in fading signal, $g_f(W_o/N_oB)$, is given by the average over all possible values of W,

$$g_f(\dot{W}_o/N_oB) = \int_{\text{all } W} g_c(x/N_oB)p_W(x) \, dx \, . \qquad (BI-15)$$

If $p_S(x)$ is the probability density of the signal amplitude S,

$$gf(W_o/N_{\hat{o}}B) = \int_{\text{all } S} g_c(x^2/2N_oB) \, p_S(x) \, dx \, . \qquad (BI-16)$$

Consider now the cases where either the "slow" assumption, or the "flat" assumption, or both, is not valid. Our receiver will still calculate a signal point no matter what kind of distorted signal the receiver receives. Now, however, the signal points will move randomly and rapidly all over the signal space and the computations of the statistics of such motion will be extremely difficult. Also, the signals are usually spread in time (also frequency), resulting in the received signals occupying more than their allotted (0,T) time slot. The result is that, if we are looking at bit j, for example, there is some signal from bit j-1 still going on, causing interference, i.e., intersymbol interference. This, as well as other problems, indicates why the straight-forward approach given in (BI-15,16) cannot be used. For this reason we like to use slow-flat fading approximations whenever possible. The procedures required for system performance calcu-lations in the case of "slow and flat" not being valid are covered in subsequent sections.

BI-1.4 FADING SIGNAL DISTRIBUTIONS

When the signal is propagated from the transmitter to the
receiver, it is modified by the propagation media. Quite
often the signal travels to the receiver via one, two, or any
number of separate paths. If the signal from each of these
multipaths is represented by a signal vector, then the receiver
sees the vector sum of these signal vectors. The phase angle
between any two such vectors is generally, on the average,
uniformly distributed, i.e., the phase angle has equal chance
of being anything between $-\pi$ and π radians. We are interested
then in the probability distribution of the amplitude (or
power) of the received signal, i.e., the above vector sum.

As mentioned earlier, each path may have some specular and
scatter contributions. Scatter comes from large volume effects,
and means the signal is scattered into many, many small signal
vectors. That is, it is equivalent to multipath with many,
many paths such that none of these many, many received signal
vectors dominate the others (i.e., sticks out like a "sore
thumb"). If we have such a sum of many more or less equal-
sized vectors with uniform phase between them, then the
amplitude of the vector sum has a Rayleigh distribution.
Figure BI-6 (from Nesenbergs, 1967) shows the probability-density
function of n equal-sized vectors for n = 1, 2, 3, 4, and 6
along with the Rayleigh limit ($n\to\infty$). We see that the "many
many" above need only be 5 or 6 before the Rayleigh distribu-
tion is a reasonable approximation. In other words, the
situation where we have, say 6 or more distinct paths, and
the signal components from these paths are essentially equal,
then the received signal amplitude is approximately Rayleigh
distributed.

Suppose, instead, that we have one specular path (due, for
example, to a direct line-of-sight path) and a scatter path,

or, equivalently, a number of other paths from which the received signals are more or less equal and small compared to the main signal. An example of one such situation would be "constant groundwave plus Rayleigh fading skywave". There are, of course, many other possibilities. In this case, the received signal amplitude has a Nakagami-Rice distribution,

$$p_S(x) = \frac{x}{\alpha} \exp\left[\frac{-x^2 + 2\beta}{2\alpha}\right] I_0 \left(\frac{\sqrt{2\beta}\,x}{\alpha}\right) \qquad (BI-17)$$

where α is the power in the Rayleigh vector, β is the power in the constant vector, and I_0 is the zero-order modified Bessel function.

If, as before, N_0 denotes the noise power spectral density, then the signal-to-noise ratio is

$$\frac{W}{N_0 B} = \frac{\alpha + \beta}{N_0 B} \quad . \qquad (BI-18)$$

The distribution of signal amplitude for the general case of the sum of any number of such Nakagami-Rice vectors and resulting special cases is given by Nesenbergs (1967).

Consider the case where we have a direct ray and a single other path, resulting from a ground reflection. The probability density for the received signal power, W, is then

$$p_W(x) = \frac{1}{\pi} \frac{1}{\sqrt{4k^2 \gamma_0^2 - (x - (k^2 + 1)\gamma_0)^2}} \quad ,$$

$$\gamma_0 (1-k)^2 \leq x \leq \gamma_0 (1+k)^2 \quad . \qquad (BI-19)$$

where γ_0 is the power of the direct ray and k is the voltage-amplitude ratio of the reflected-to-direct ray (reflection coefficient). The total mean power in the received signal is $\gamma_0(1+k^2)$, or the signal-to-noise ratio is

$$\frac{W}{N_o B} = \frac{Y_o(1+k^2)}{N_o B}$$ (BI-20)

Experimental observations of received fading-signal amplitudes over various communication circuits have shown that the signal amplitude, when expressed in decibels, can sometimes be approximated by a normal distribution. That is, the signal amplitude has a log-normal distribution. If, for the signal amplitude, S, we let $Y = 20 \log S$, then

$$p_Y(y) = \frac{1}{\sigma\sqrt{2\pi}} e^{-\frac{1}{2}\left(\frac{y-\mu}{\sigma}\right)^2} \quad , \quad -\infty < y < \infty \quad , \quad$$ (BI-21)

where μ is the mean value of Y(dB) and σ is the standard deviation (dB). The signal distribution for use in (BI-16) is then

$$p_S(x) = \frac{8.686}{x\sqrt{2\pi\sigma^2}} e^{-\frac{1}{2}\left(\frac{20\log x - \mu}{\sigma}\right)^2} \quad , \quad 0 \leq x < \infty \quad .$$ (BI-22)

For log-normal fading signal, the σ is usually given in terms of the "fading range". The fading range is the difference (in dB) between the upper and lower decile values. The upper decile is that value which is exceeded only 10 percent of the time, and the lower decile is that value which is exceeded 90 percent of the time. In terms of the fading range, 2.54 σ = fading range. The average received signal power is

$$W_o = 10^{0.1\mu + 0.0115\sigma^2}$$ (BI-23)

and the signal-to-noise ratio is $W_o/N_o B$.

The above distributions (BI-12, 17, 19, and 22) pretty well cover all the signal distributions that are generally considered for slow-flat fading. Which one to use depends on the particular kind of propagation path one is interested in. The

above distributions of the fading signal say nothing as to how "fast" the signal fades up and down. Therefore, consideration must be given to more than the fading distribution when trying to decide if a slow-flat assumption is valid.

BI-1.5.   EXAMPLES AND REFERENCES

In this section we will give the results for our example system (CPSK) for all of the fading distributions considered above. An example for a voice system will also be given.

Figure BI-7 shows the results for the binary CPSK system for constant signal (BI-7), Rayleigh fading signal (BI-14), Nakagami-Rice fading (BI-17) with the power of the constant vector 10 dB above the average power of the Rayleigh vector, Nakagami-Rice fading with the power of the constant vector equal to the average power of the Rayleigh vector, and log-normal fading (BI-22), using a 13.4-dB fading range. Note that Rayleigh fading also has a 13.4-dB fading range.

Figure BI-8 shows the results for the binary CPSK system for the case of constant signal vector plus reflected signal vector. Results are given for constant signal (k=0), and for k = 0.2, 0.6, 0.8, and 0.9. We see from figures BI-7 and BI-8 that a very wide range of system performances can be obtained depending on the particular kind of signal fading present.

In order to show the results of using (BI-16) for a voice system, figure BI-9 is included. It shows the performance of a double-sideband AM system in white Gaussian noise and Rayleigh-fading signal. The calculations, via (BI-16), are from the performance in constant signal for a 5.2-kHz IF bandwidth (Cunningham et al., 1947). The performance is given in terms of the phonetically balanced word articulation index.

For the nature of fading signals, extensive bibliographies (Nupen, 1960; Salaman, 1962) are available. A historically significant survey was performed by the National Bureau of Standards (NBS, 1948). A number of good comprehensive texts are also available (Davies, 1965, for example).

The representation of digital systems in geometric terms is covered quite well by Arthers and Dym (Arthers and Dym, 1962). Performance characteristics for systems in fading signal and in nonGaussian impulsive noise (as well as Gaussian noise) are available (Bello, 1965; Conda, 1965; Halton and Spaulding, 1966; Akima et al., 1969; Akima, 1970; etc.

The following list of references includes additional references not cited above. The list is hardly complete, but will provide a great deal of additional information concerning the characterization of the fading channel, and the performance of a wide variety of systems with both constant and fading signal.
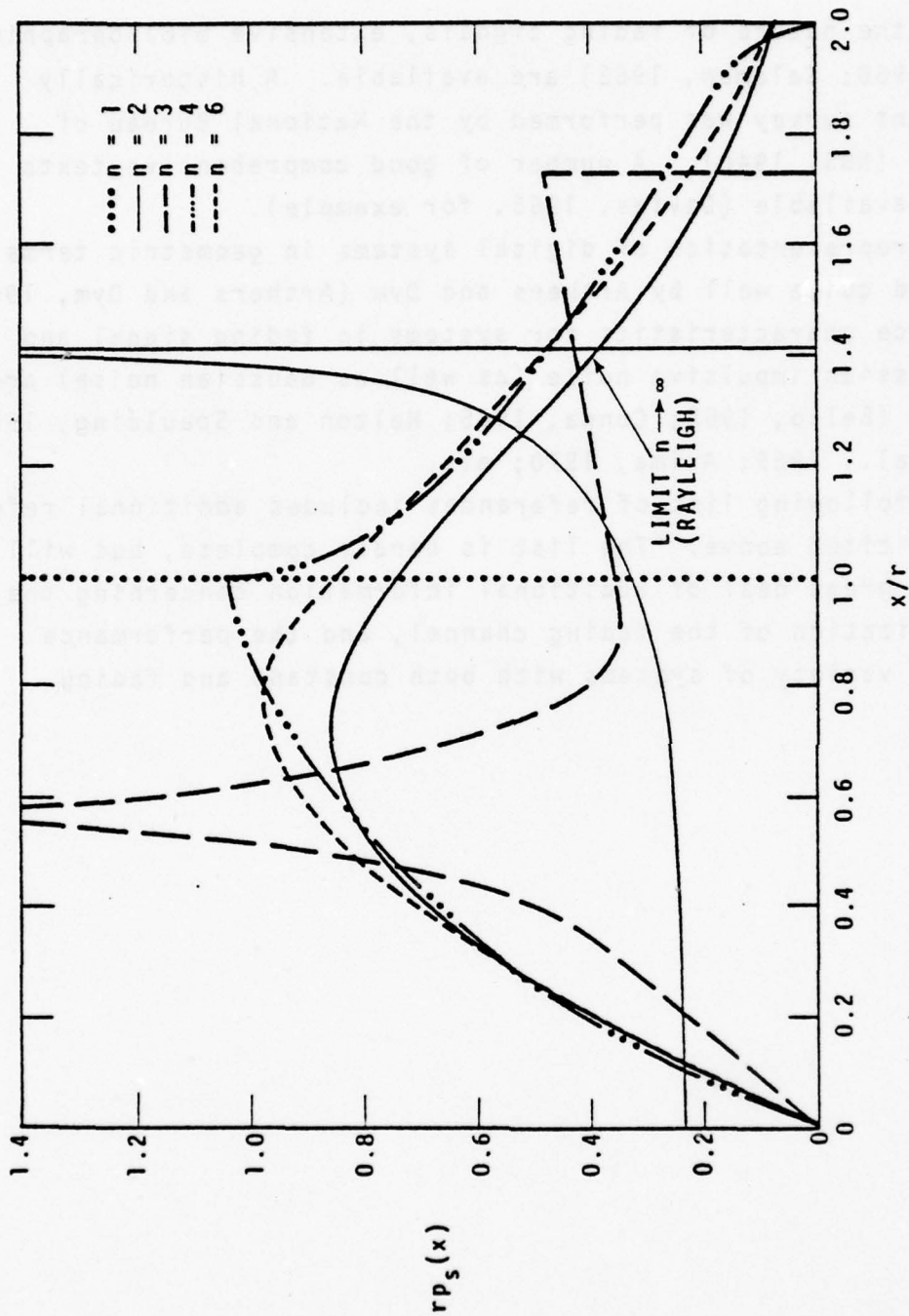
Figure BI-6. Amplitude probability density for sum of n equi-power constant signal vectors. The density functions are given in normalized form where r^2 = total signal power = nr_1^2, r_1^2 = power in each of the n-signal vectors.
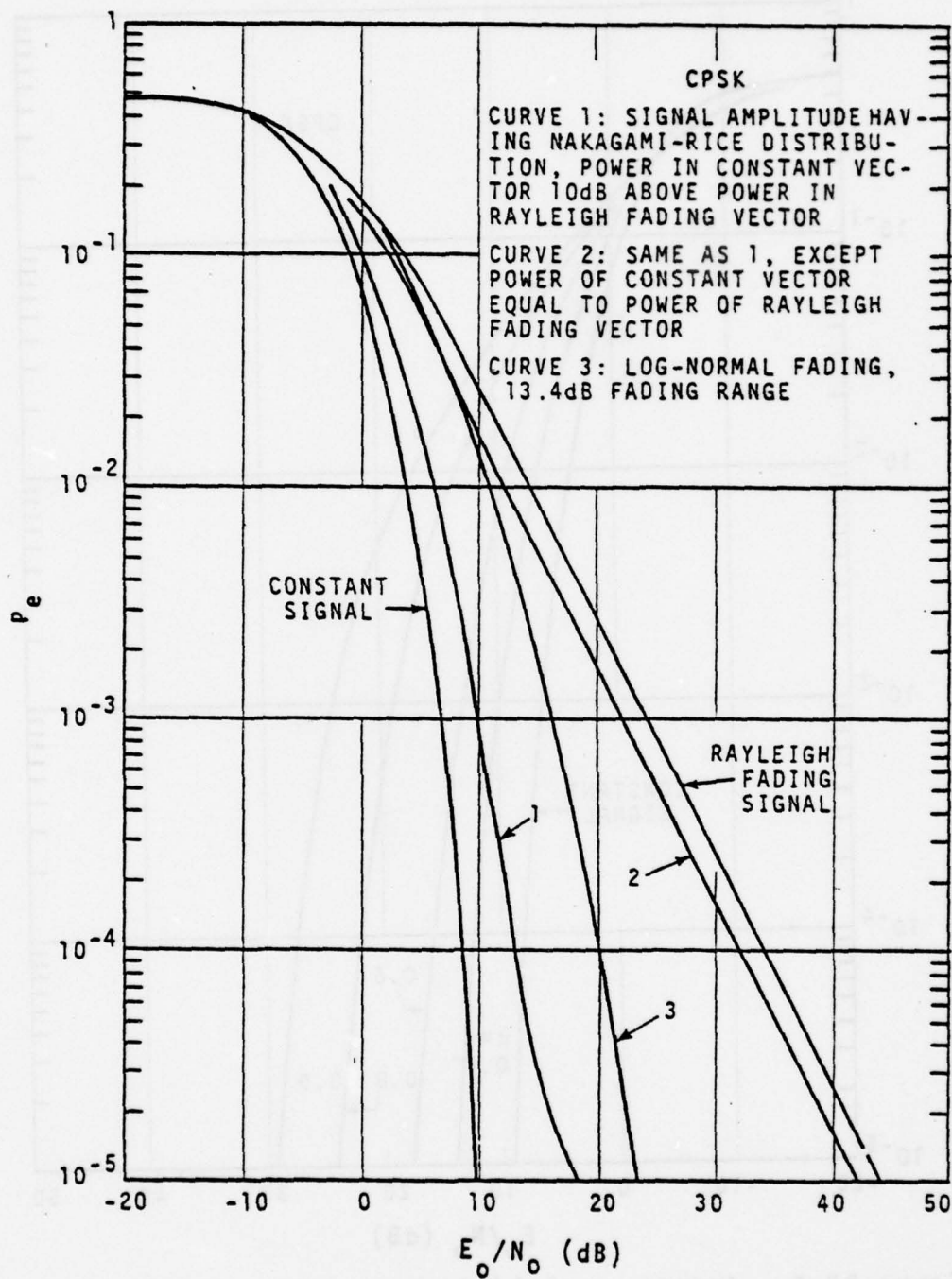
Figure BI-7. Average probability of error vs. signal
    energy to noise power spectral density ratio for
    constant signal and various types of fading signals
    for a binary coherent phase shift keying system.
    The noise is Gaussian.
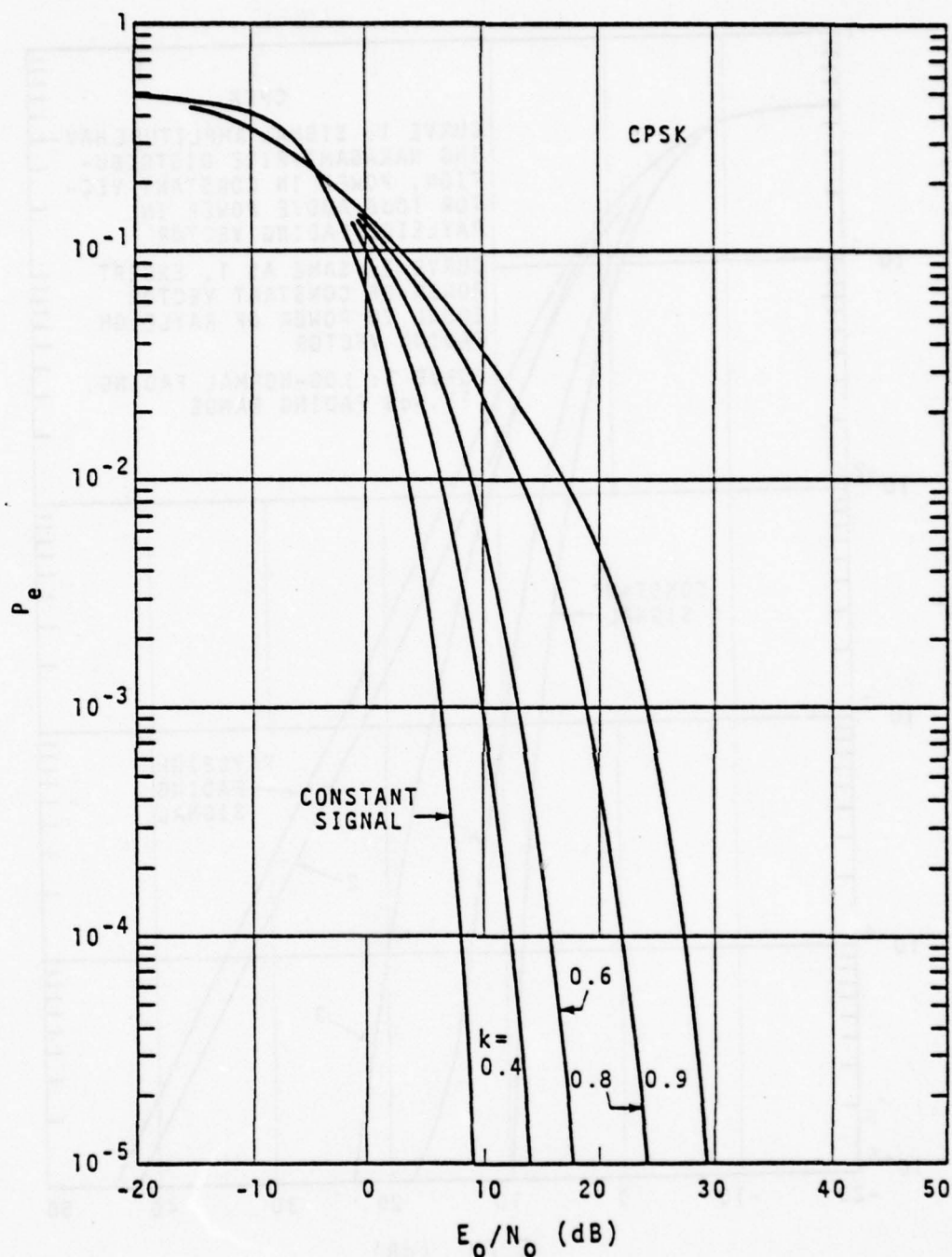
Figure BI-8. Average probability of error vs. signal energy to noise power spectral density ratio for constant signal and fading signal, where the fading signal is composed of a constant signal vector plus a reflected vector with reflection coefficient k. The noise is Gaussian.

A-24
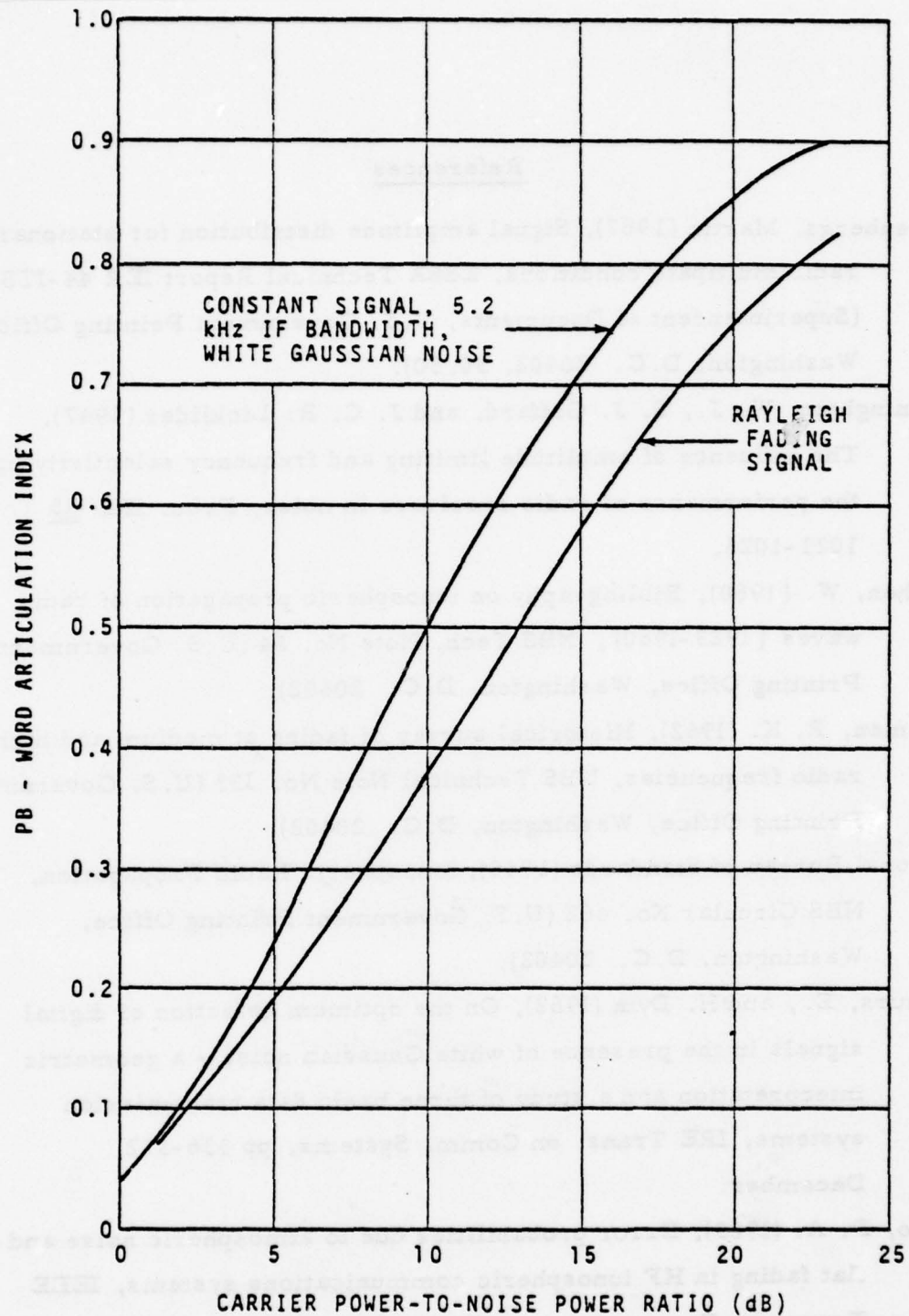
Figure BI-9. *Phonetically balanced word articulation
index vs. carrier power-to- voice power ratio for
DSB-AM constant signal and Gaussian noise (after
Cunningham et al., 1947) and for Rayleigh-fading
signal.*

References

Nesenbergs, Martin (1967), Signal amplitude distribution for stationary radio multipath conditions, ESSA Technical Report IER 44-ITSA 44 (Superintendent of Documents, U.S. Government Printing Office, Washington, D.C. 20402, $0.50).

Cunningham, W. J., S. J. Goffard, and J. C. R. Licklider (1947), The influence of amplitude limiting and frequency selectivity upon the performance of radio receivers in noise, Proc. IRE 35 1021-1025.

Nuphen, W. (1960), Bibliography on ionospheric propagation of radio waves [1923-1960], NBS Tech. Note No. 84 (U.S. Government Printing Office, Washington, D.C. 20402).

Salaman, R. K. (1962), Historical survey of fading at medium and high radio frequencies, NBS Technical Note No. 133 (U.S. Government Printing Office, Washington, D.C. 20402).

National Bureau of Standards (1948), Ionospheric Radio Propagation, NBS Circular No. 462 (U.S. Government Printing Office, Washington, D.C. 20402).

Arthurs, E., and H. Dym (1962), On the optimum detection of digital signals in the presence of white Gaussian noise - a geometric interpretation and a study of three basic data transmission systems, IRE Trans. on Comm. Systems, pp 336-372, December.

Bello, P. A. (1965), Error probabilities due to atmospheric noise and flat fading in HF ionospheric communications systems, IEEE Trans. on Communications Technology, Vol. 13, No. 3, pp 266-279.

Conda, A. M. (1965), The effect of atmospheric noise on the probability
of error for an NCFSK system, IEEE Trans. on Communications
Technology, Vol. 13, No. 3, pp 280-283.

Halton, J. H., and A. D. Spaulding (1966), Error rates in differentially
coherent phase systems in non-Gaussian noise, IEEE Trans. on
Communications Technology, Vol. COM-14, No. 5, pp 594-601.

Akima, H., G. Ax, and W. M. Beery (1969), Required signal-to-noise
ratios for HF communication systems, ESSA Technical Report
ERL 131-ITS 92 (U.S. Government Printing Office, Washington,
D.C. 20402, $0.60).

Akima, H. (1970), Modulation studies for IGOSS, ESSA Technical
Report ERL 172-ITS 110 (U.S. Government Printing Office,
Washington, D.C. 20402, $0.55).

Additional References

Florman, E. F., and J. J. Tary (1962), Required signal-to-noise ratios, RF signal power, and bandwidth for multichannel radio communications systems, NBS Technical Note 100 (U.S. Government Printing Office, Washington, D.C. 20402, $1.00).

Gierhart, G. D., R. W. Hubbard, and D. V. Glen (1970), Electro-space planning and engineering for the air traffic environment, Report No. FAA-RD-70-71 (U.S. Government Printing Office, Washington, D.C. 20402, $2.25).

Hubbard, R. W., D. V. Glen, and W. J. Hartman (1970), Modulation characteristics critical to frequency planning for the aeronautical services, ESSA Technical Memorandum ERLTM-ITS 232, FAA Contract No. FA67-WAI 134 (FAA Systems Research and Dev. Services, Spectrum Plans and Programs Branch RD-510, Washington, D.C. 20553).

Farrow, J. E., R. E. Skerjanec, and A. P. Barsis (1971), A discussion of performance predictions and standards for tropospheric tele-communications systems, Office of Telecommunications Technical Memorandum 62.

Salaman, R. K., Gene Ax, and A. C. Stewart (1971), Radio channel characterization, Telecommunications Technical Memorandum, OT/ITSTM 27.

APPENDIX B – DETECTION ANALYSIS TECHNIQUES – INFORMAL NOTES PROVIDED BY A. D. SPAULDING

RESULTS OF INTERIM HF
DETECTION ANALYSES

1.   INTRODUCTION.

This report summarizes the performance of standard
communication signals transmitted through a channel subjected to a
number of different disturbances. Among the digital signals, we
treat frequency-shift keying (FSK), phase-shift keying (PSK), and
amplitude-shift keying (ASK). The signals can be multi-level
(M-ary), as well as two-level (binary) and can be phase-
coherent or noncoherent. Analog signals of interest include
conventional amplitude modulation (AM), signal sideband (SSB),
double sideband (DSB), frequency modulation (FM) and pulse-
position modulation (PPM). Although the above modulation
techniques are not all-inclusive, most conventional techniques
are accounted for. Furthermore, the methodology employed here
makes extensions to other techniques straight-forward.

We assume that the signals pass through a channel that
introduces Gaussian noise, interference, non-Gaussian (atmospheric)
noise, Rician fading, and distortion due to rapid and frequency
selective fading. Again, our list of deleterious effects is not
all-inclusive but many of the commonly encountered disturbances
are included.

Performance will depend on the type of receiver
(detector) that is used. We are interested in a number of

1.　　　　-- Continued.

different detectors including both phase coherent and noncoherent. Furthermore, the summary includes descriptions and performance of optimum detectors.

It is clear that we need to develop equations for a very large number of cases since we are interested in most modulation types and most forms of signal degradation. Furthermore, we should be flexible enough to incorporate additional signals of interest that may arise or modifications in the models of deleterious effects (for example, fading with a distribution other than the assumed Rician). We also seek consistency between results for different signals, as it would be irrational to predict good performance with some signals and poor performance with others because of differing assumptions used in the derivations. The analysis must be capable of handling a wide variety of detection techniques and should provide insight into good techniques. Our problem is further compounded by the paucity of results in the literature for certain deleterious effects such as non-Gaussian noise.

We have developed an approach that satisfies all of the constraints of the preceding paragraph. Our approach consists of first obtaining the performance in the simplest of all cases; additive, white, Gaussian noise. The performance is then successively perturbed to account for non-dispersive fading and non-Gaussian noise and, finally, dispersive fading.

1. _____ -- Continued.

The above approach is used to determine the performance
of conventional detection techniques in Section 2, the structure
of optimum detectors in Section 3, and the performance of
advanced technology detectors in Section 4. Admitadly, the
distinction between conventional and advanced technology
detection techniques is not sharp. For purposes of this report,
advanced technology detectors include receiver structures that
approach optimality when the disturbance consists of more than
just Gaussian noise.

2.   PERFORMANCE OF STANDARD RECEIVERS.

2.1   Performance in Additive, White, Gaussian Noise.

2.1.1   Binary Modulation.

In the case of binary modulation, we know that one of two possible signals, denoted s_1 and s_2, has been transmitted. Our task is to decide which is the correct one.* When the only disturbance to the system is additive, white, Gaussian noise, we have a case which has been extensively treated in the literature. The probability of error depends on three factors:

1. E/N_o, the energy-to-noise density at the input. If we define the system bandwidth as $1/T$, where T is the bit duration, then E/N_o is equal to the signal-to-noise ratio.

2. ρ, the normalized correlation coefficient or inner product of the two signals which measures how different the two signals are from each other. By definition,

$$\rho = (1/E) \int_0^T s_1(t)\, s_2(t)\, dt$$

3. The type of detector. It will be shown in Section 3 that the optimum detector is a correlator, or

_____

*This formulation of the problem is referred to as bit-by-bit detection. Performance can be improved through error coding in which multiple bits are examined before a decision is reached. Error coding is beyond the scope of this report; we confine our attention to bit-by-bit detection.

2.1.1   -- Continued.

                matched filter. It will turn out that many other
                detectors perform nearly as well.

For the moment, assume that a correlator is used as the detector.
It can be shown that the probability of error is given by [1-3]

$$P_e = (1/2) \text{ erfc } (a/\sqrt{2}) = $$

where $a = [E/N_o (1-\rho)]^{1/2}$ (2-1)

$$\text{erfc}(z) = (2/\sqrt{\pi}) \int_z^\infty e^{-t^2} dt = 1 - \text{erf}(z)$$

Since erfc(z) is a tabulated function, we need only determine the
inner product, ρ, in order to relate the probability of error to
E/N_o or to S/N. Since erfc(z) is a monotonically decreasing func-
tion of z, we should make "a" as large as possible. This can be
done by making E/N_o as large as possible or ρ as small as
possible consistent with the restriction $-1 \leq \rho \leq +1$. Equations
for ρ are given in Table 2-1 together with the value of the
parameter that minimizes ρ, and a reference for the result.

          In our terminology, PSK is phase-shift keying; that
is, the transmitted carrier is abruptly shifted in phase (or not
shifted) at the end of each binary digit. Similarly, in FSK, the
frequency is shifted and in ASK, the amplitude is shifted. The
later is often called on-off keying (OOK) and requires twice the

B-6

Table 2-1.   Correlation Coefficients for Binary Systems

Binary Signal	Equation for Correlation Coefficient (ρ) (Definition of Symbols under Table)	Optimum Value of Parameter	ρ for Optimum Value of Parameter	Reference Numbers
PSK	$\rho = \cos \phi$	$\phi = \pi$	-1	1,4
FSK	$\rho = \dfrac{\sin(\omega_2 - \omega_1)T}{(\omega_2 - \omega_1)T}$	$\Delta f = \dfrac{0.71}{T}$	-0.22	1,2
ASK	$\rho = 0$	---	0.	--
PSK-PM & PSK-FM	$\rho = J_0(K)$	$K_1 = 3.83$	-0.4028	5
FSK-PM & FSK-FM	$\rho = J_0(\beta_1)J_0(\beta_2)$	$\beta_1 = 3.83$; $\beta_2 = 0$ or, $\beta_2 = 0$; $\beta_1 = 3.83$	-0.4028	6
ASK-PM & ASK-FM	$\rho = J_0(\beta_2 - \beta_1)$	$\beta_2 - \beta_1 = 3.83$	-0.4028	6

where

ϕ = phase angle between the two signals (radians).

$\omega_{1,2}$ = transmitted angular frequencies (radians/sec),

T = pulse length (seconds),

Δf = difference in transmitted frequencies (cps) $= \dfrac{\omega_2 - \omega_1}{2\pi}$.

$K_1 = [\beta_1^2 + \beta_2^2 - 2\beta_1\beta_2 \cos \phi]^{1/2}$,

$\beta_{1,2}$ = modulation index of signal on final carrier,

$J_0(x)$ = Bessel function of the first kind.

2.1.1   -- Continued.

transmitted energy during the on times in order to have the same
average E/N_o as the others. If the carrier phase, frequency,
or amplitude is not directly shifted, but rather the phase,
frequency or amplitude of a subcarrier is shifted and the
subcarrier is phase or frequency modulated onto the carrier, we
have PSK-PM, FSK-PM, or ASK-PM as noted in Table 2-1.

        Detectors other than correlators are often used in
common practice. Equations for the probability of error with these
detectors are summarized in Table 2-2, together with restrictions
on the value of the parameters and appropriate references.

        Some curves for the probability of error are shown in
Figure 2-1. We see that correlation detection is typically 1-3
dB better than other detectors for the same signal.

2.1.2   M-ary Modulation.

        When one of M possible signals is transmitted, we have
a generalization of the binary case. Assuming that correlation
detection is used and the correlation coefficients between all
pairs of signals are identical, the probability of error is given
by[13]

$$P_e = 1 - \int_{-\infty}^{\infty} \phi(z) \, [\overline{\Phi}(z+\sqrt{2}\,a)]^{M-1} \, dz$$

where $\phi(z) = (1/\sqrt{2\pi}) \exp(-z^2/2)$ (2-2)

Table 2-2.   Equations for Non-Matched-Filter Detection of Binary Signals

Modulation	Detection	Probability of Error	Optimum Value of Parameter	Reference Number
PSK	Phase comparison with preceding bit	$P_e = \frac{1}{2} \exp\left(-\frac{E}{N_o}\right)$	$\phi = \pi$	4
PSK	Discriminator	$P_e = \frac{1}{2} \exp\left(-0.81 \frac{E}{N_o}\right)$		7
FSK	Discriminator	$P_e = \frac{1}{2} \exp\left(-0.61 \frac{E}{N_o}\right)$	$\Delta f \approx \frac{0.8}{\tau}$	8
FSK	Envelope Detection	$P_e = \frac{1}{2} \exp\left(-0.50 \frac{E}{N_o}\right)$	$\Delta f > \frac{1}{\tau}$	9,10
ASK	Envelope Detection	$P_e = \frac{1}{2} \left[1 - Q\left(\sqrt{\frac{2E}{N_o}}, b_o\right)\right] + \frac{1}{2} \exp(-b_o/2^2)$	$b_o \approx \sqrt{2 + \frac{E}{2N_o}}$	11,12

where Q=Marcum Q Fnct

b_o=Threshold

$P_e \approx \frac{1}{2} \exp\left(-0.25^2\right)E/N_o)$

Note: For PM or FM subcarrier systems where the first stage of demodulation is a phase detector, the performance is the same as a non-subcarrier system degraded by $2J_1^2(\beta)$ where J_1=Bessel function and β is the modulation index. Degradation is 1.7 dB for the optimum β of 1.84 (except ASK is degraded approximately 4.7 dB). A sin ϕ detector obtains the sine of the phase angle and may be implemented as a phase-locked loop. See Reference [6].

B-9

LEGEND

A MATCHED FILTER PSK
B DIFF. COHERENT PSK
C DISCRIMINATOR PSK
D MATCHED FILTER FSK
   OPT. FREQ. SEPARATION
E MATCHED FILTER WIDEBAND
   FSK AND MATCHED FILTER
   ASK
F DISCRIMINATOR FSK
G ENVELOPE ASK
H ENVELOPE FSK
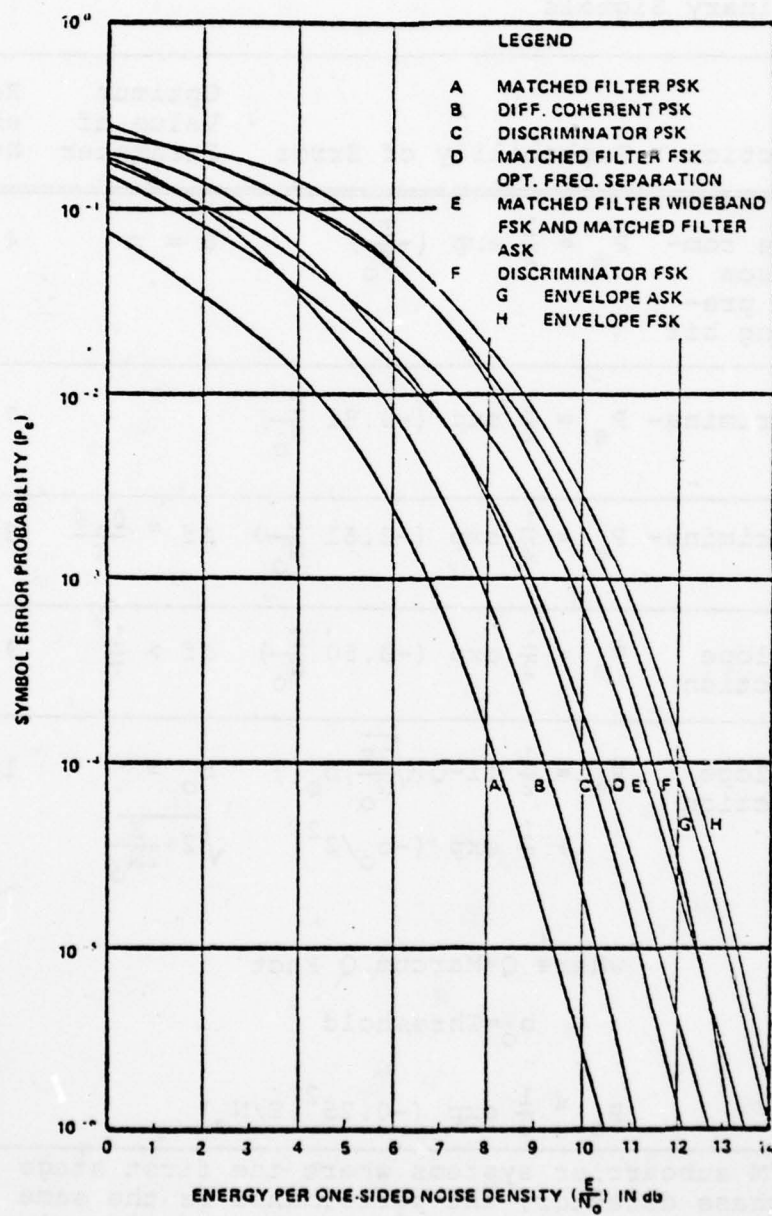
Figure 2-1. P_e for Typical Binary Systems.

2.1.2   -- Continued.

$$\Phi(z+a) = \int_{-\infty}^{z+a} \phi(y) \, dy$$

$$a = [(E/N_O)(1-\rho)]^{1/2}$$

Equation (2-2) is the appropriate generalization of Equation (2-1). Values for the correlation coefficient are given in Table 2-3. As can bee seen from Table 2-3, the correlation coefficient for a number of modulation techniques is zero.

We have plotted results for $\rho = 0$ in Figure 2-2. Note that the appropriate parameter is $\frac{E/n}{N_O}$, the energy per bit per noise density since there are $n = \log_2 M$ bits per symbol.

Equation (2-2) is limited to the case where all pairs of correlation coefficients are identical. It can also be used to bound results by selecting the largest or the least value. When M>3, it is impossible to select correlation coefficients that are all equal in the case of MPSK and MASK. Instead, for MPSK we have for large S/N[4].

$$P_e = 2[1-\Phi(\sqrt{2E/N_O} \sin \pi/M)] \qquad (2-3a)$$

and for MASK we have[14]

$$P_e = 2(M-1)/M [1-\Phi(\sqrt{E/N_O/(M-1)^2})] \qquad (2-3b)$$

Results are plotted in Figures 2-3 and 2-4.

Table 2-3.   Correlation Coefficients for M-ary Systems

M-ary Signal	ρ for Optimum Parameter (minimum ρ)	Condition for Minimum ρ	Reference Number
MFSK	$\rho = 0$	$\Delta f = \dfrac{0.5\,m}{T}$; m = integer	2
MFSK-PM & MFSK-FM	$\rho = 0$	β = 2.405 or 5.520 or 8.654 or ... for all β's	6
MPSK-PM & MPSK-FM	$\rho = 0$	$2\beta \sin \phi/2 > 50$	6
MASK-PM & MASK-FM	$\rho = 0$	$\beta_2 - \beta_k > 50$	6

where

Δf = frequency separation,

β = modulation index,

ϕ = phase angle between adjacent subcarrier signals.
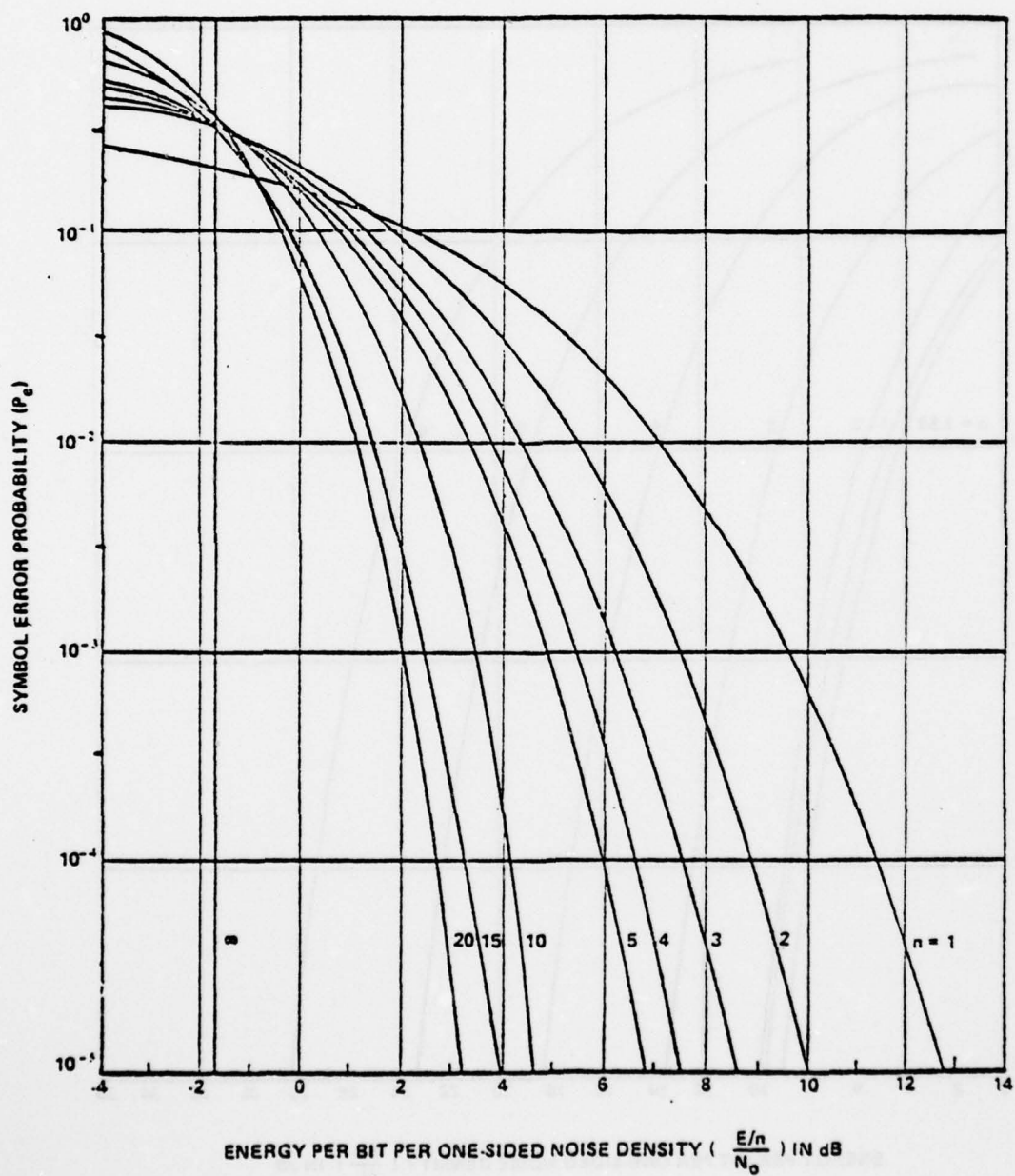
Figure 2-2. P_e for Orthogonal M-ary Modulation with Correlation Detection
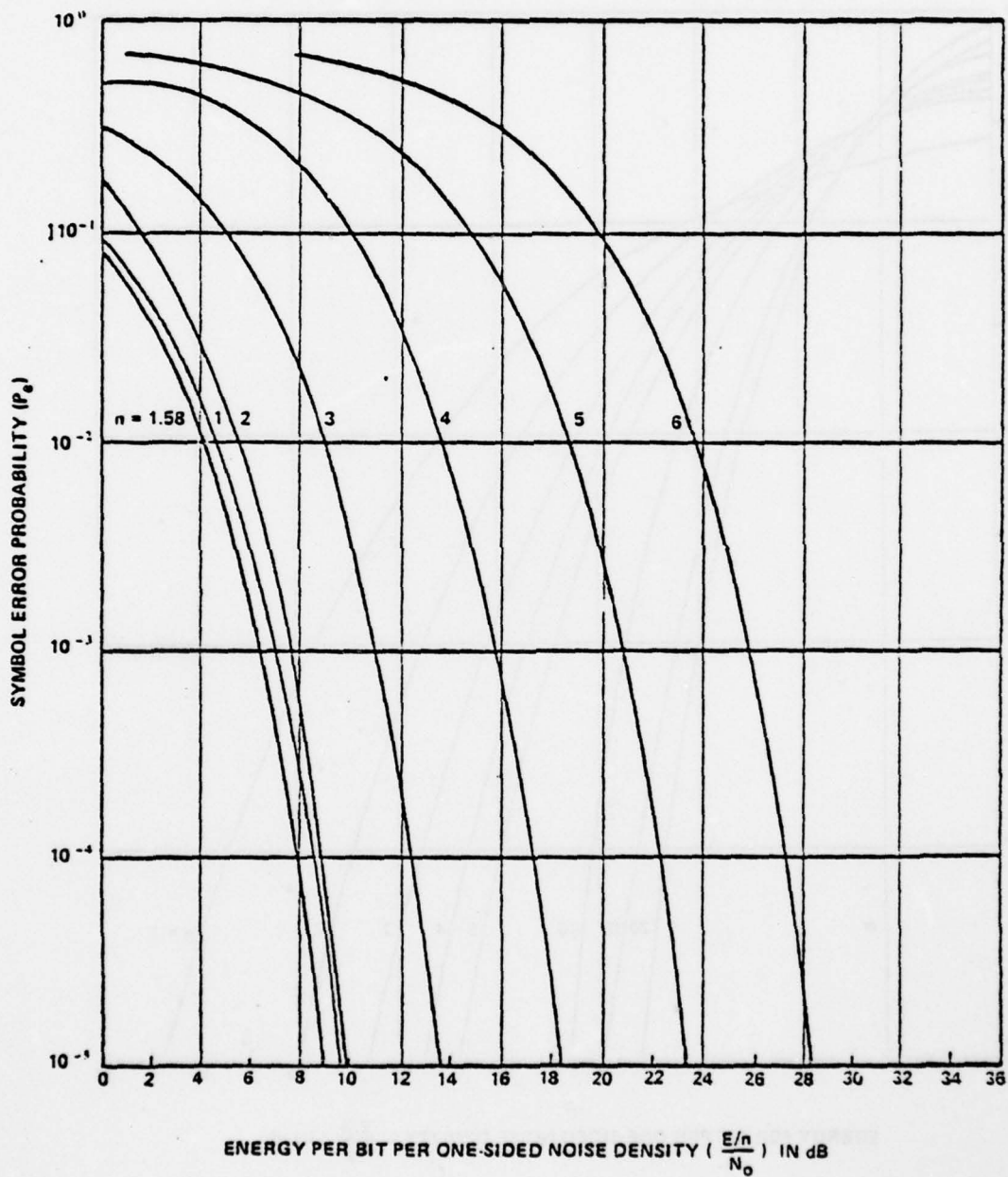
Figure 2-3. P_e for Correlation Detection of MPSK
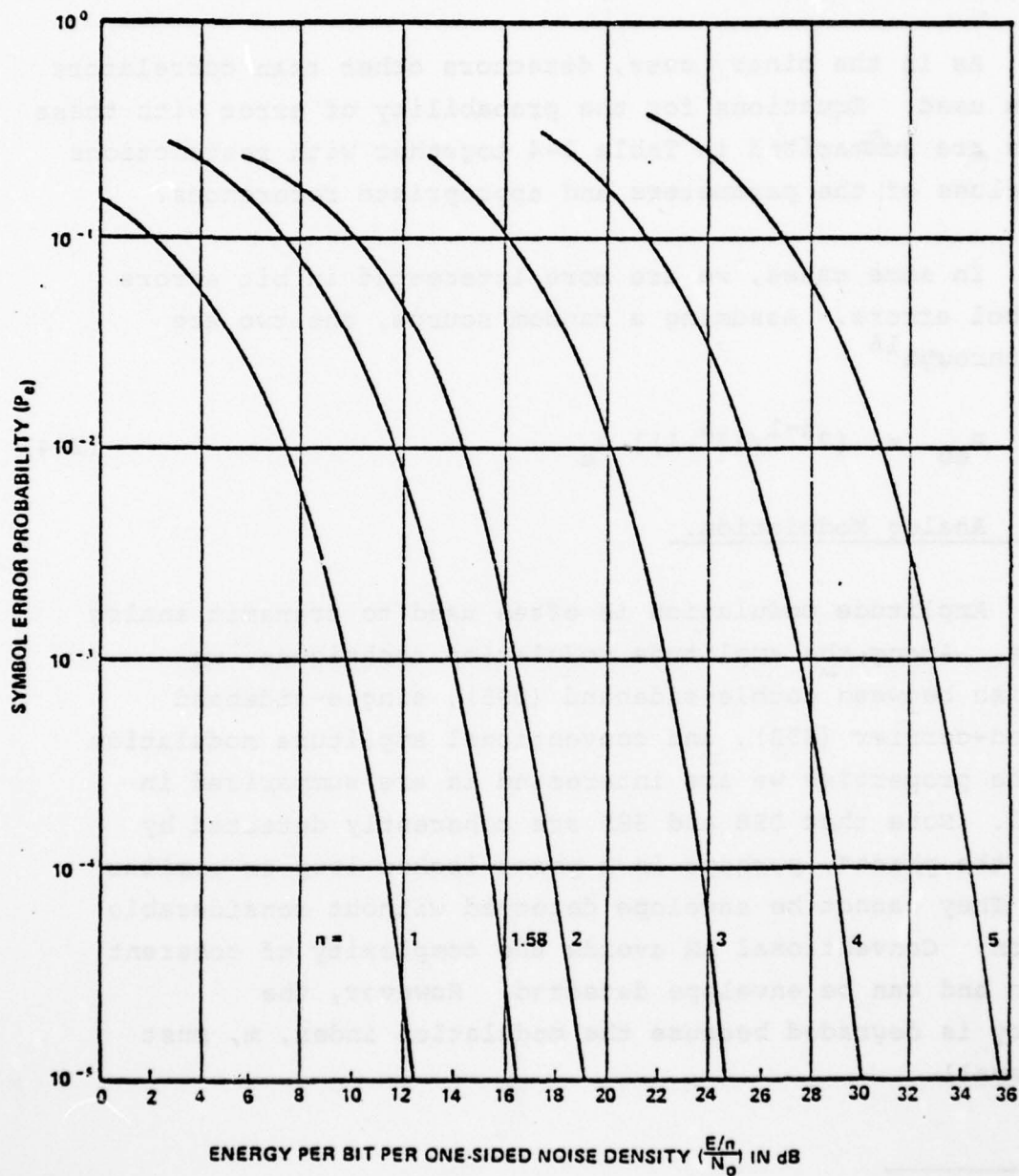
Figure 2-4. P_e for Correlation Detection of MASK

As in the binary case, detectors other than correlators are often used. Equations for the probability of error with these detectors are summarized in Table 2-4 together with restrictions on the values of the parameters and appropriate references.

In some cases, we are more interested in bit errors than symbol errors. Assuming a random source, the two are related through[16]

$$P_{eb} = [2^{n-1}/(2^n-1)] P_e \tag{2-4}$$

2.1.3 Analog Modulation.

Amplitude modulation is often used to transmit analog waveforms. Among the amplitude modulation techniques, we distinguish between double-sideband (DSB), single-sideband suppressed-carrier (SSB), and conventional amplitude modulation (AM). The properties we are interested in are summarized in Table 2-5. Note that DSB and SSB are coherently detected by tracking the phase*, perhaps in a phase-locked loop or similar device. They cannot be envelope detected without considerable distortion. Conventional AM avoids the complexity of coherent detection and can be envelope detected. However, the efficiency is degraded because the modulation index, m, must be kept small.

---

*For voice modulation, a tracking error of 20-30 Hz has been found to be tolerable.

Table 2-4.   Equations for Non-Matched-Filter Detection of
              M-ary Signals.

Modulation	Detector	Probability of Error (Optimum Parameters)	Reference Number
MFSK	Envelope Detector	$P_e = \frac{1}{M} \exp(-\frac{E}{N_o}) \sum_{k=2}^{M} (-1)^k$ $\binom{M}{k} \exp(\frac{E}{kN_o})$	13,15
MPSK	Phase Comparison	$P_e = 2[1-\underline{\Phi}(2\sqrt{E/N_o} \sin \frac{\pi}{2M})]$ for large S/N	4
MASK	Envelope Detector	$P_e \doteq 2P_e$ of binary case with E/N_o multiplied by $\frac{n}{(M-1)^2}$	

Note: For PM and FM subcarrier systems where the first stage of
demodulation is a sin ϕ detector, the performance is the same as
a non-subcarrier system degraded by $2J_1^2(\beta)$ where J_1 = Bessel
function and β is the modulation index. Degradation is 1.7 dB
for the optimum β of 1.84 (except ASK is degraded approximately
4.7 dB. A sin ϕ detector obtains the sine of the phase angle
and may be implemented as a phase-locked loop. See Reference [6].

Table 2-5.   Amplitude Modulation Techniques

Modulation	Transmitted Waveform	Detector	$\dfrac{(S/N)\,out}{(S/N)\,in}$
DSB	$g(t)\,\cos\omega_c t$	Coherent	1
SSB	$g(t)\,\cos\omega_c t$ $-\hat{g}(t)\,\sin\omega_c t$	Coherent	1
AM	$[1+g(t)]\,\cos\omega_c t$	Envelope	$E[g^2(t)]$

where $g(t)$ = modulating waveform,

$\hat{g}(t)$ = Hilbert Transform of $g(t)$

$E[g^2(t)]$ = Expected value of modulation squared;

$E[g^2(t)] < 1$

ω_c = radian carrier frequency.

Note: Noise power is measured in the bandwidth $0 < f \leq f_m$ where f is the modulation bandwidth. Results are from Reference [16,17].

2.1.3   -- Continued.

        The analysis of frequency modulation (FM) is much more
complicated than that of any of the amplitude modulation systems
since FM is inherently a nonlinear operation. A number of different
analyses have been performed using slightly different approaches.
All of the analyses agree in the above threshold regions, that is,
when the S/N is large. However, there is some disagreement in the
below threshold region, although the disagreement is generally minor.
We favor the so-called Rice "click" analysis[18] for three reasons:

        1.   It is the only analysis that includes the effect
              of modulation on the noise.

        2.   Results are reasonably consistant with experiments.

        3.   The equations can be readily applied to a great
              variety of cases.

Using Equation (3-8-25a) of Reference (12), the output S/N of
FM using the Rice "click" analysis is;

$$S/N = \frac{3 \beta^2 (B/f_m) \, C/N}{1 + 4 \sqrt{3} \, \rho (B/f_m)^2 \, \text{erfc} \, \sqrt{C/N}} \qquad (2-5)$$

where   S/N = Output signal-to-noise ratio
         C/N = Input signal-to-noise ratio
                 (also termed carrier-to- noise ratio)

2.1.3 -- Continued.

$$B = \text{Half the RF bandwidth}$$
$$f_m = \text{Modulating frequency}$$
$$\beta = \text{Modulation index; } \beta \approx B/f_m - 1$$

When the input signal-to-noise ratio is large, the denominator becomes unity and we have the usual formula for S/N in the above threshold region. Equation (2-5) was derived for the case where it is assumed that the modulation has no impact on the noise. However, Rice has shown that the ratio of the number of clicks with Gaussian modulation to the number of clicks with no modulation is

$$\frac{N_{+Gauss}}{N_{+Unmod}} = \frac{e^{-C/N}(1+2a_oC/N)^{1/2}}{\sqrt{\pi C/N} \text{ erfc } \sqrt{C/N}} \qquad (2-6)$$

where $\quad a_o = \Delta^2/r^2$

$$\Delta = \text{rms frequency deviation (Hz)}$$

$$r = \frac{2B}{\sqrt{12}} \quad \text{for rectangular filter}$$

The output S/N is then given by Equation (2-5) with the second term of the denominator multiplied by Equation (2-6).

1·0 2·8 2·5
5·0 3·15 2·2
5·6 3·5
6·3
1·1 4·0 2·0
4·5
1·8
1·25 1·4 1·6
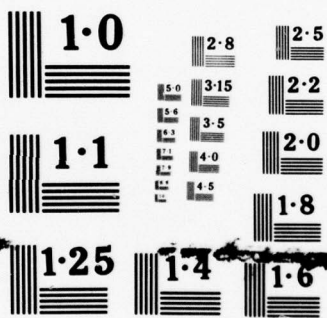
NATIONAL BUREAU OF STANDARDS

2.1.3 -- Continued.

Another analog modulation technique of interest is pulse-position modulation (PPM). Like FM, PPM expands the bandwidth and realizes an improvement in S/N, but exhibits a threshold effect. PPM can be analyzed by using the concepts of "stretch" factor and "probability of anomoly". Using these concepts the output S/N is given approximately by[1].

$$\frac{S}{N} = \left[3(12/\pi^2)\ 1/\beta^2\ N_o/2E + 3(2/3)\ (\beta-1)\ \frac{e^{-E/2N_o}}{\sqrt{2\pi}\ E/N_o} \right]^{-1} \qquad (2-7)$$

where β = modulation index = W/W_m -2

E/N_o = Energy-to-noise density

W = RF transmission bandwidth

W_m = modulation bandwidth

2.2 Performance in Interference.

Interference may be modeled as an additive noise process. In general, interference is neither white nor Gaussian. However, it is often reasonable to consider the interference to be white and Gaussian for the following reasons:

1. When the desired signal is narrow band, interference is often white across that band

2.2 _____ -- Continued. __

    2.   Non-white noise can be passed through a whitening
       filter with no loss in signal detectability[1] for
       optimum detection.

    3.   Some individual interfers will be Gaussian if they
       are received over a fading channel that randomizes
       the signals.

    4.   Even if the individual interferers are not
       Gaussian, the composite can be close to Gaussian
       since as few as 6 equal-amplitude sinusoids have
       a distribution that is close to Gaussian[12].

    5.   For a specified mean-square value, the Gaussian
       distribution has the largest entropy of any
       distribution[19]. Consequently, the Gaussian
       distribution is in some sense a worst case as it
       has the maximum uncertainty. Furthermore, the
       Gaussian distribution has a large area under the
       tail of the curve, and this area is the key to
       error probability calculations.

    6.   In the absence of an experimental measurement, the
       actual distribution is unknown. Consequently,
       we must assume a probability distribution and we
       might as well assume one that is both analytically
       tractable and, at the same time, is in some
       sense a worst case, or at least a very unfavorable
       case.

2.2   -- Continued.

7.   If the white, Gaussian assumption is not made,
each case must be treated separately i.e., each type
of signal and each type of interference requires
a separate analysis. Examples of such analyses
are given in References (20-26). Frequently, the
results differ only slightly from what would
have been obtained using the white, Gaussian
assumption; an example, taken from Jones[26] is
shown in Figure 2-5.

2.3   Performance in Flat-Flat Fading.

The signals of interest will experience fading. In this
section, we assume that the fading is slow relative to the time it
takes for the signal to vary significantly and we assume that the
fading is not frequency selective. This type of fading has been
termed flat-flat, i.e., flat in frequency and flat in time. A
model for this type of fading is a slowly varying attenuator.

We can readily calculate the performance of a communica-
tion system in flat-flat fading by making use of the results in
additive, white, Gaussian noise. Since the flat-flat fading
channel alters the received signal strength, it alters the input
signal-to-noise ratio by the same amount. The output performance
also varies. It is clear that the average output performance is
obtained by averaging the performance over the variations in
input signal-to-noise ratio.
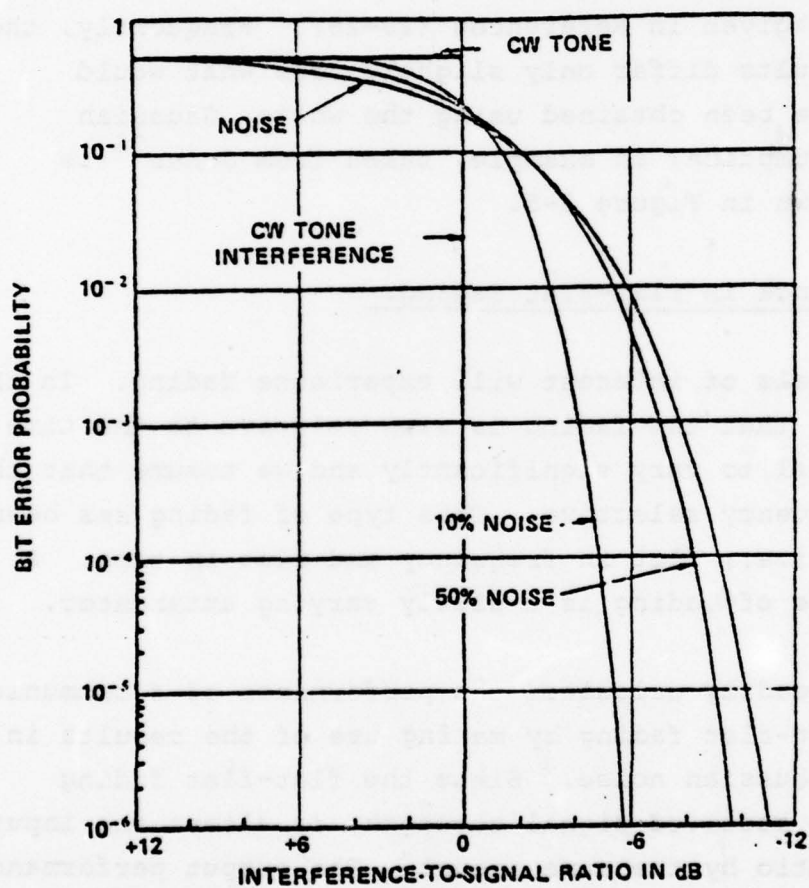
Figure 2-5.   FSK and DPSK Errors in Interference

B-24

2.3   -- Continued.

        As a specific example, suppose that we have noncoherent
FSK in a Rayleigh fading channel.* The probability of error
is [16]

$$P_e = \int_0^\infty [1/2 \; e^{-(1/2)\rho}] \cdot [(1/\rho_o) \; e^{-\rho/\rho_o}] \; d\rho \qquad (2\text{-}8a)$$

$$P_e = 1/(2+\rho_o) \qquad (2\text{-}8b)$$

where ρ = signal-to-noise ratio, a variable
         ρ_o = average value of ρ

In the remainder of this report we use ρ to denote the variable
signal-to-noise ratio rather than signal correlation coefficient.

        Note that in Equation (2-8a) the first term in brackets
under the integral sign is the probability of error in additive,
white, Gaussian noise which can be denoted as $P_{e,G}(\rho)$. The
second term is the probability distribution of the fading and can
be denoted as $p_{f,R}(\rho)$. Consequently, we can write Equation
(2-8a) as

$$P_{\dot{e},F} = \int_0^\infty P_{e,G}(\rho) \cdot p_{f,R}(\rho) \; d\rho \qquad (2\text{-}9)$$

---

*Probability distributions for the Rayleigh, Rician, and log-
 normal distributions used in Section 2 are detailed in Appendix A.

B-25

2.3 -- Continued.

If we have some modulation technique other than noncoherent FSK,
we merely substitute the appropriate probability of error in white,
Gaussian noise into Equation (2-9) For $P_{e,G}(\rho)$. Consequently,
all of the results of Section 2.1 can be applied readily to the
flat-flat fading case. If the fading is given by the Rice
distribution we use the appropriate probability density

$$P_{f,N}(\rho) = \frac{(1+\gamma)}{\rho_o} e^{-\gamma} e^{-(1+\gamma)\rho/\rho_o} I_o(\sqrt{4\gamma(1+\gamma)\rho/\rho_o})$$

(2-10)

where γ = Power of the specular component divided by the
power of the random signal component

$I_o(\cdot)$ = modified Bessel function

in place of the Rayleigh density

$$P_{f,R}(\rho) = (1/\rho_o) e^{-\rho/\rho_o}$$

(2-11)

Similarly, if the fading is described by any other distribution we
can use the appropriate distribution in Equation (2-9) together
with the error probability of the appropriate technique in
additive, white, Gaussian noise.

2.3   -- Continued.

        Equation (2-9) provides a good general result. The
appropriate integral can be evaluated numerically. However, closed
form solutions to the integral are known for a number of special
cases. These solutions are summarized in Table 2-6.

2.4   .   Performance in Non-Gaussian Noise.

        One method of handling non-Gaussian noise is to consider
it to be time-varying Gaussian noise. That is, we visualize the
noise as Gaussian but at certain times, under disturbed conditions,
the noise power increases. Taking this viewpoint, we determine
the probability distribution of the increase in power over nominal
and average the performance over this distribution which is not
necessarily Gaussian. The averaging method is analogous to our
handling of fading. For fading, we average the signal over the
probability of signal strength while for non-Gaussian noise we
average the noise over the probability of noise power.
Consequently, we write

$$P_E = \int_0^\infty P_{E,F}(\rho) \; w(\rho,\bar{\rho}) \; d\rho \qquad (2-12)$$

where

   $P_{E,F}$ = probability of error in additive white Gaussian
             noise and fading

   $w(\rho,\bar{\rho})$ = probability distribution of the noise amplitude
             (envelope variations).

B-27

Table 2-6. Closed Form Error Rates in Fading

Modulation	Fading	Error Probability	Reference
Coherent PSK	Rayleigh	$P_e = 1/2 \left(1 - \frac{1}{\sqrt{1 + 1/\zeta_o}}\right)$	12,16
Diff. Coh. PSK	Rayleigh	$P_e = \frac{1}{2 + 2\zeta_o}$	12,16
Coherent FSK	Rayleigh	$P_e = 1/2 \left(1 - \frac{1}{\sqrt{1 + 2/\zeta_o}}\right)$	12,16
Noncoherent FSK	Rayleigh	$P_e = \frac{1}{2 + \zeta_o}$	12,16
Coherent ASK Optimum Threshold	Rayleigh	$P_o = 1/2 \left(1 - \frac{1}{\sqrt{4 + 4/\zeta_o}}\right)$	12
Coherent ASK Fixed Threshold	Rayleigh	$P_o = 1/2 - 1/4 \left[\text{erfc}\left(\frac{-b_o}{\sqrt{2}\sqrt{1 + 1/\zeta_o}}\right) + \exp\left(\frac{-b_o^2}{2(1 + \zeta_o)}\right) \right]$ where b_o = threshold (function of ζ_o)	12
Noncoherent ASK Fixed Threshold	Rayleigh	$P_e = 1/2 \left(1 - \exp\left(\frac{-b_o^2}{2}\right) \frac{1}{1 + \zeta_o}\right) + 1/2 \exp\left(\frac{-b_o^2}{2}\right)$ where b_o = threshold and $b_{o,opt} = \sqrt{2\left(1 + 1/\zeta_o\right) \ln\left(1 + \zeta_o\right)}$	12
FSK	Nakagami-Rice	$P_e = Q(ac,bc) - 1/2 (1 + b) e^{-(a^2 + b^2)c^2/2} I_o (abc^2)$ where $Q(\cdot)$ = Marcum Q function and $a,b,c,$ differ for coherent or noncoherent	27

	Coherent	Noncoherent
a	$1 - \mu$	1
b	$1 + \mu$	1
c	$\sqrt{2\gamma_o^2 \frac{E}{N_o}}$	$\sqrt{\gamma_o^2 \frac{1}{4} \frac{(1 + \mu)^2}{\mu} \cdot 2 \frac{E}{N_o}}$

2.4 -- Continued.

Assuming that the non-Gaussian component is due to atmospheric
noise (thunderstorm activity) it is approximately log-normal.
The probability density can then be written (see Appendix A) as

$$w\,(\rho,\bar{\rho}) = \frac{1}{\sqrt{0.46\pi V_d/\rho}}\,\exp\left[\frac{-(\log_e\,\sqrt{\bar{\rho}/\rho}\,+\,0.23\,V_d)^2}{0.46\,V_d}\right] \quad (2\text{-}13)$$

where V_d = voltage deviation, defined as the root mean
square envelope relative to the average envelope
expressed in decibels; $20\,\log_{10}\,[E_{rms}/E_{av}]$

Equation (2-12, and 2-13) then enable us to calculate the
probability of error for any of the modulation techniques
considered in Section 2-1 when its noise is non-Gaussian.

The above approach to non-Gaussian noise can be justified
on several grounds. We can argue that physically the noise from a
lightning discharge is Gaussian noise since it comes from the
movement of a large number of electrons. Furthermore, regardless
of the statistics at its origin, the noise tends toward Gaussian
as it is propagated since the channel is random. However, the
magnitude of the Gaussian noise coming from the discharge varies
in accordance with the magnitude and locality of the discharge and
the non-Gaussian appearance of the noise is due to the distribution
of the received magnitude of the discharges. Our method assumes

2.4 -- Continued.

precisely this time-varying magnitude of Gaussian bursts. We can also argue that an atmospheric noise simulator has been constructed by taking Gaussian noise and passing it through an amplifier with a variable gain.[28] Probability distributions with the noise simulator closely matched distributions of true atmospheric noise and measured error probabilities also showed good agreement. Finally, we can justify our approach on the grounds that error probabilities derived by this method closely match error probabilities derived by other methods as well as experimental error probabilities[29].

Although we have offered justification for the validity of our approach, we admit that there is no firm theoretical reason for calling the approach correct. We are using this method rather than other methods[29] because it is simple and easy to apply. Specifically, we prefer the described approach for the following reasons:

1. It is the only approach we are aware of that can be applied to all modulation techniques. Other approaches require tedious derivations to be repeated for each of the many modulation techniques we are dealing with. Furthermore, the different results will be consistant since the same assumption is made.

2. Other approaches will also require assumptions although they are often buried in the mathematics. We have no reason to believe these other approaches will yield more accurate results.

2.4   -- Continued.

3.   Our approach can handle any distribution of noise, we merely use the new distribution in place of Equation (2-13). Thus, if we measure the atmospheric noise and find it is not log-normal, we can use the measured distribution in place of Equation (2-13). There is no need to rederive results although obviously we will have to redo the machine computations with the measured distribution.

4.   In general, optimum receivers for non-Gaussian noise are nonlinear. In Section 4 we shall see that our approach can be used with nonlinear receivers. We are aware of no other method that gives believable answers for nonlinear receivers in atmospheric noise

5.   This approach has been used successfully by Stein[12] (Sect 10-12), Omura and Shaft,[29] and Conda[30].

2.5   Performance in Dispersive Fading.

When the time duration between fades is not very much greater than the time duration of a signalling element, or when the coherent bandwidth of the medium is not very much greater than the signal bandwidth, the signal is distorted by the propagation medium. We refer to this as dispersive fading. Since dispersive fading introduces distortion, its principle effect is to set a limit on performance regardless of the

2.5   -- Continued.

signal-to-noise ratio. This limitation is generally referred to
as an irreducible error or asymptotic error.

        Figure 2-6 shows an example of the probability of error
calculated for a particular modulation technique in the presence
of dispersive fading[31]. Note that the actual error is closely
approximated by two curves representing the performance in non-
dispersive fading and the asymptotic error. An even closer
approximation is obtained by simply adding the errors from the
two sources. We shall adopt the approach of calculating the
irreducible error and adding it to the error in the absence of
dispersive fading. Our reasons for doing this follow:

    1.   A complete calculation taking into account all
          of the deleterious effects simultaneously has never
          been performed to our knowledge for even a single
          modulation technique.

    2.   Calculating the errors separately allows us to
          determine which deleterious effect limits
          performance; consequently we know what type of
          inproved detector is needed.

    3.   Accuracy limitations imposed by this method are no
          greater than limitations imposed by other
          assumptions (such as the correlation functions)
          that must be made due to lack of knowledge about
          the medium.

BINARY ERROR PROBABILITY

10^{-1}

10^{-2}

10^{-3}

$P_e (\infty)$

10^{-4}

10^{-5}

ACTUAL PROBABILITY
OF ERROR CURVE

ASYMPTOTIC ERROR

PROBABILITY OF ERROR
FOR A TIME-AND-FREQUENCY-
FLAT CHANNEL

0   10   20   30   40   50

SIGNAL—TO—NOISE RATIO (dB)
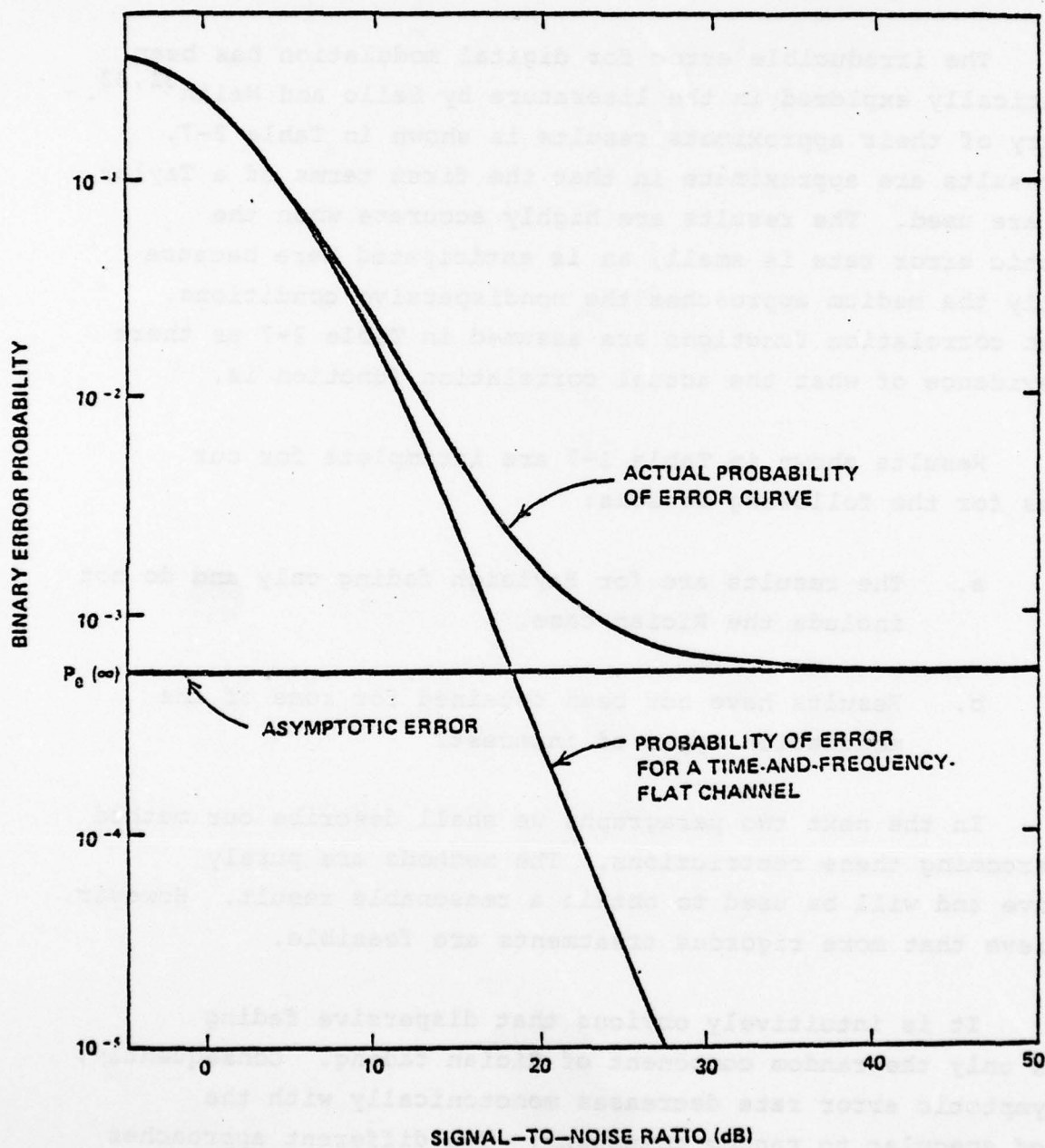
Figure 2-6.   Determination of the Probability-of-Error Curve By
the Residual Error and the Flat-Flat Probability-
of-Error Curve

B-33

2.5   -- Continued.

        The irreducible error for digital modulation has been
systematically explored in the literature by Bello and Nelin[32,33].
A summary of their approximate results is shown in Table 2-7.
Their results are approximate in that the first terms of a Taylor
series are used. The results are highly accurate when the
asymptotic error rate is small, as is anticipated here because
generally the medium approaches the nondispersive conditions.
Gaussian correlation functions are assumed in Table 2-7 as there
is no evidence of what the actual correlation function is.

        Results shown in Table 2-7 are incomplete for our
purposes for the following reasons:

        a.   The results are for Rayleigh fading only and do not
              include the Rician case.

        b.   Results have not been obtained for some of the
              modulation types of interest.

        In the next two paragraphs we shall describe our method
for overcoming these restrictions. The methods are purely
intuitive and will be used to obtain a reasonable result. However,
we believe that more rigorous treatments are feasible.

        It is intuitively obvious that dispersive fading
affects only the random component of Rician fading. Consequently,
the asymptotic error rate decreases monotonically with the
ratio of specular to random component. Two different approaches

Table 2-7.   Asymptotic Error

Modulation	Detection	Fading	Probability of Error
Noncoherent FSK	Noncoherent	Time Selective	$P_0 = \left[2 + \dfrac{1-a^{-1}(4+1/2-2^{-1})}{4a/2^{-3}}\right]^{-1}$, $a = \dfrac{2^2(BT)^2}{\log_e 2}$
PSK	Diff. Coh.	Time Selective	$P_1 = [2 + 2/a]^{-1}$
Noncoherent FSK	Noncoherent	Freq. Selective	$P_2 = (1/4)P_1 + (1/2)\,P_2\,P_1 = \left[2 + \dfrac{8d^2}{2^2}(1-2/r)\right]^{-1}$
			$P_2 = \left[2 + \dfrac{1-\frac{1}{2}\frac{d^2}{\sqrt{r}}}{2d/r^2}\right]^{-1}$
PSK	Diff. Coh.	Freq. Selective	$P_3 = (1/4)P_3 + (1/2)P_4 \, P_3 = \left[2 + \dfrac{1-4d/r\sqrt{r}}{\frac{4d^2}{2^2}}(1-1/r)\right]^{-1}$
			$P_4 = \left[2 + \dfrac{2(1-bd)}{4d^2} + \dfrac{4d^2}{2^2}\dfrac{}{(1-1/r)^{-2}}\right]^{-1}$

Note that this is Bello's result rather than the Bailey and Lindenlaub correction.[33]

$a^2 = \dfrac{-^2(B_f T)^2}{\log_e 2}$

$d^2 = \dfrac{1}{T B_c}$

T = bit length

B_f = bandwidth of fading spectrum (half power)

B_c = correlation bandwidth of medium (half power point)

2.5 -- Continued.

can be taken to account for the improvement under specular
conditions. In one approach, we first assume that the random
component produces an effective signal-to-distortion ratio (S/D)
which we evaluate by substituting the asymptotic error for
Rayleigh conditions into the equation for non-dispersive fading
and solve for ρ (which is interpreted as S_r/D). Next, we add
the signal power in the specular component to the signal power
in the random component to obtain $(S_s+S_r)/D$ and use the resulting
value in the error equation for non-dispersion conditions to
obtain a new asymptotic error rate proportional to $\exp(-(S_s+S_r)/D)$.
In the other approach we merely multiply by $e^{-\gamma}$ to obtain a
result proportional to $\exp[-(S_r/D) - \gamma]$. This last result can
be written as

$$e^{-(S_r/D + \gamma)} = e^{-(S_r/D + S_s/S_r)} \tag{2-14a}$$

$$e^{-(S_r/D + \gamma)} = e^{-[(S_r^2 + DS_s)/D \cdot S_r]} \tag{2-14b}$$

$$e^{-(S_r/D + \gamma)} = e^{-[(S_r + D S_s/S_r)/D]} \tag{2-14c}$$

For all cases of interest $D/S_r < 1$ and the second approach yields
a more conservative answer. Consequently, we recommend the
second approach which merely consists of multiplying the
asymptotic error by $e^{-\gamma}$. It is obvious that the recommended
approach yields the correct answer at the two extreme cases of

2.5   -- Continued.

Rayleigh fading and no fading. It also agrees with Stein's
recommendations for modifying Rayleigh results to fit Rician
cases. A rigorous approach to the Rician case would involve
applying Bello's[34] general formula to specific cases or application
of Stein's[12] general formula along lines similar to Fralick[35].

        The principal digital modulation technique missing from
Table 2-7 is amplitude-shift-keying. From the point of view of
distortion, ASK resembles FSK more than PSK since the signal is
either present or absent in a filter. Consequently we will use the
results of FSK for ASK. However, the decision region for ASK is
half that of FSK; consequently the performance of ASK in dispersive
fading will be worse than FSK. We therefore recommend quadrupling
the asymptotic error rate of FSK when calculating performance of
ASK. The reason for quadrupling is that the decision region is
halved, corresponding to a decrease of 6 dB and the error rate
for non-dispersive fading is proportional to signal-to-noise
ratio.

        We also note that M-ary modulation is missing from
Table 2-7. Decision regions for MASK and MPSK are reduced to
approximately 1/M-1 and sin π/M times the former values. Since
this corresponds to a reduction in voltage and the error curves
are approximately linear, we multiply the asymptotic error by
$(M-1)^2$ and $1/\sin^2 \pi/M$ for MASK and MPSK respectively. We note
that for the special case of quaternary PSK, our method predicts
a doubling of the error rate relative to binary PSK, a result that

2.5   -- Continued.

is in good agreement with exact computations made by Gaarder[36].
We do not use Gaarder's results for this special case because we
wish to keep our assumptions consistent among the different
modulation methods. MFSK differs from MASK and MPSK in that the
decision region is unaltered by M-ary modulation, assuming
that the additional frequencies are spaced wide enough to maintain
orthogonal signalling. Since the decision region is unaltered, we
anticipate that the irreducible error for MFSK will be the same
as for the binary FSK.

         Discriminator detection of PSK and FSK is not included in
Table 2-7. We could use the results of Sifford, et al.[37] for
discriminator detection of FSK (no results are available for PSK);
however, since we wish to keep results consistent, we use non-
coherent detection rather than discriminator detection. Performance
between the two is comparable.

         Analog modulation is handled differently for each
modulation technique. The only results we are aware of for AM
were obtained by Boorstyn and Schwartz[38] who show that the
irreducible mean-squared error with an optimum linear receiver
is given by

$$\overline{\varepsilon^2} = \frac{1/\gamma}{1+1/\gamma} \qquad (2-15)$$

2.5   -- Continued.

where γ is the ratio of the power in the specular component divided
by the random component. This result is intuitively pleasing
as it indicates that the error is proportional to the intensity
of fading i.e., the channel in improving unwanted AM which is
detected. The output signal-to-distortion ratio can be taken as
the reciprocal of the mean squared error. We shall use Equation
(2-15) for all forms of amplitude modulation i.e., SSB, DSB
and conventional AM. Note that the result is valid for Rician
as well as Rayleigh fading. However, the result is valid for
slow nonselective fading.

        The effect of dispersive fading on analog FM is
enormously more complicated than AM. As an example, a computation
of the S/D caused by frequency selective fading resulted in an
equation that could be printed only on a fold-out page[37]. This
equation included some simplying assumptions and represented the
asymptotic error for Rayleigh fading--Rician fading would be even
more complicated. Consequently, without apology, we use a simpler
approximate result derived by Bello and Nelin[39],

$$D/S = 1.2 (2\pi\Delta)^4 f_d^2 f_m^2 / 4 \qquad\qquad (2-16)$$

where Δ = time delay (seconds)
           f_d = frequency deviation
           f_m = highest modulating frequency

2.5 _____ -- Continued.

Equation (2-16) is approximately valid for frequency-selective
Rayleigh fading. To convert the result to Rician fading we
arbitrarily multiply Equation (2-16) by the ratio of the random
power divided by the specular power. The resulting equation
agrees with a result obtained by Medhurst[40] for two specular
components except for the absence of the multiplicitive
constant 1.2. Medhurst's result assumed a large ratio of desired
to undesired power and further assumed the worst case phase
relationship.

Pulse-position modulation (PPM) is quite analogous to
MFSK in that multiple time slots are available rather than
multiple frequency slots. For lack of more precise results
we can apply the results of MFSK to PPM, interpreting asymptotic
error as an equivalent signal-to-distortion ratio.

In all of the analog techniques the distortion-to-
signal ratio and noise-to-signal ratio can be added to obtain
a composite result.

6.   REFERENCES.

1.   J.M. Wozencraft and I.M. Jacobs, *Principles of Communication Engineering*, Wiley 1967.

2.   V.A. Kotel'nikov, *The Theory of Optimum Noise Immunity*, McGraw-Hill, Chapter 4; 1959.

3.   W.M. Siebert, "Statistical Decision Theory and Communications: The Simple Binary Decision Problem," Chapter 8 of E.J., Baghdady, (editor), *Lectures on Communication System Theory*, McGraw-Hill; 1961.

4.   C.R. Cahn, "Performance of Digital Phase-Modulation Communication Systems," *IRE Trans. on Comm. Sys.*, vol. CS-7 pp. 3-6; May, 1959.

5.   J.A. Develet, Jr. "A Note on Demodulation of PCM/PM Signals with Switching Type Phase Detectors," *IRE Trans. on Space Elect. & Telemetry*, vol. SET-8, pp. 39-43; March, 1962.

6.   P.D. Shaft, "Analysis of M-ary Modulated Subcarrier Systems" First IEEE Annual Communications Convention Conference Record, pp. 89-94; Boulder Colo. June 1965.

7.   A.A. Meyeroff., and W.M. Mazer, "Optimum Binary FM Reception Using Discriminator Detection and IF Shaping," *RCA Review*, vol. 22, pp. 698-728; December, 1961.

6. _____ -- Continued.

8.   P.D. Shaft, "Error Rate of PCM-FM Using Discriminator
        Detection," *IRE Transactions on Space Electronics and
        Telemetry*; Vol SET-9 pp. 131-137 December, 1963.

9.   C.S. Weaver, "A Comparison of Several Types of
        Modulation," *IRE Trans. on Comm. Sys.*, vol. CS-10,
        pp. 96-101; March, 1962.

10.   S. Reiger, "Error Probabilities of Binary Data
        Transmission Systems in the Presence of Random Noise,"
        1953 IRE Nat'l. Conv. Record, Pt. 8, pp. 62-79.

11.   W.R. Bennett, "Methods of Solving Noise Problems,"
        Proc. IRE, vol. 44, pp. 609-638; May, 1956.

12.   M. Schwartz, W.R. Bennett, and S. Stein, *Communication
        Systems and Techniques*, McGraw-Hill, 1966.

13.   A.H. Nuttall, "Error Probabilities for Equicorrelated
        M-ary Signals Under Phase Coherent and Phase Incoherent
        Reception," *IRE Trans. on Inf. Theory*, vol. IT-8, pp.
        303-314; July, 1962.

14.   C.R. Cahn, "Combined Digital Phase and Amplitude
        Modulation Communication Systems," *IRE Trans. on
        Comm. Sys.*, vol. CS-8, pp. 150-155; September, 1960.

6.   -- Continued.

15.   S. Reiger, "Error Rates in Data Transmission,"
        Proc. IRE, vol. 46, pp. 919-920; May, 1958.

16.   S. Stein and J.J. Jones, *Modern Communication
        Principles with Application to Digital Signaling*,
        McGraw-Hill 1967.

17.   D. J. Sakrison, *Communication Theory: Transmission of
        Waveforms and Digital Information*; Wiley 1968.

18.   S.O. Rice, "Noise in FM Receivers" Chapter 25 in
        Proceedings Symposium of Time Series Analysis,
        M. Rosenblatt (ed.); Wiley 1963.

19.   W.W. Harman, *Principles of the Statistical Theory of
        Communication*, McGraw-Hill 1963.

20.   I. Plusc, "Investigation of Frequency Modulation Signal
        Interference," *Proc. IRE*, Vol. 35, pp. 1054-1059
        (October 1947).

21.   R.G. Medhurst, "FM Interfering Carrier Distortion:
        General Formula," *Proc IEE*, Vol. 109B, pp. 149-150
        (March 1962).

22.   F.G. Splitt, "Comparative Performance of Digital Data
        Transmission in the Presence of CW Interference,"
        IEEE Transactions on Communication Systems, Vol. CS-10,
        pp. 169-177 (June 1962).

6.   -- Continued.

23.   A.S. Rosenbaum, "PSK Error Performance in Gaussian Noise
        and Interference," *Bell System Technical Journal*,
        Vol. 48, pp. 413-442 (February 1969).

24.   V.K. Prabhu, "Error Rate Considerations for Coherent
        Phase Shift Keyed Systems with Co-Channel Interference"
        Bell Syst. Tech. J., Vol. 48, pp. 743-768 (March 1969).

25.   V.F. Volteras, "Quadrature Detection PSK System and
        Interference," RCA Review, Vol. 29, pp. 122-140
        (March 1968).

26.   J.J. Jones, "FSK and DPSK Performance in a Mixture
        of CW Tone and Random Noise Interference" *IEEE Trans.
        on Comm. Tech.*, Vol COM-18, pp. 693-695, October 1970.

27.   G.L. Turin, "Error Probabilities for Binary Symmetric
        Ideal Reception Through Nonselective Slow Fading and
        Noise" *Proc IRE*, vol 46, pp. 1603-1619; September 1958.

28.   R.F. Linfield and C.D. Beach, "High Performance
        Reliable VLF Component of the Naval Advanced
        Communications System, Final Research Report 34-R-8,
        Vol. I, Contract NObsr-85360, DECO Electronics, Inc.,
        Boulder, Colorado (March 1965).

29.   J.K. Omura and P.D. Shaft, "Modem Performance in VLF
        Atmospheric Noise" *IEEE Trans. on Communication Technology*,
        Vol. COM-19, pp. 659-688; October 1971.

6.   -- Continued.

30.   A.M. Conda, "The Effect of Atmospheric Noise on the Probability of Error for NCFSK Systems," *IEEE Trans. Communication Technology*, Vol. COM-13, pp. 280-284 (September 1965).

31.   N.T. Gaarder, "An Examination of Selected HF Phase Modulation Techniques" Technical Report 2, Part III, SRI Project 4172 Stanford Research Institute, Menlo Park, California; February 1965.

32.   P.A. Bello and B.D. Nelin, "The Influence of Fading Spectrum on the Binary Error Probabilities of Incoherent and Differentially Coherent Matched Filter Receivers" *IEEE Trans. on Comm. Systems*, Vol. CS-10, pp. 160-168; June 1962; (Corrected pg. 169; June 1963)

33.   P.A. Bello and B.D. Nelin, "The Effect of Frequency Selective Fading on the Binary Error Probabilities of Incoherent and Differentially Coherent Matched Filter Receivers" *IEEE Trans. on Comm. Systems*, Vol. CS-11, pp. 170-185; June 1963; (Corrected pg. 230; December 196). Also see comments by Bailey and Lindenlaub pp 749-751, October 1968.

34.   P.A. Bello "Binary Error Probabilities Over Selectively Fading Channels Containing Specular Components", *IEEE Trans. on Comm. Tech.* Vol. COM-14, pp. 400-406; August 1966.

6. _____ -- Continued._

35.   S.C. Fralick, "Modem Performance Over LF/VLF Channels"
          Special Tech. Report 2, SRI Project 8078, Stanford
          Research Institute, Menlo Park, Calif, August 1970.

36.   N.T. Gaarder, "An Error-Rate Expression for HF DPSK
          Communication Systems" Tech. Report 3, SRI Project 4172,
          Stanford Research Institute, Menlo Park, Calif.
          August 1964.

37.   B.M. Sifford, H.N. Shaver, P.D. Shaft and J.L. Ramsey,
          "Performance and ECM Vulnerability Analysis of
          Troposcatter Multichannel Data Transmission Systems"
          Tech. Report 6, Part I, SRI Project 4172, Stanford
          Research Institute, Menlo Park, Calif., May 1966.

38.   R.R. Boorstyn and M. Schwartz: Performance of Analog
          Demodulators in a Fading Environment" *IEEE Trans. on
          Comm. Tech.*, Vol. COM-16, pp. 45-51; February 1968.

39.   P.A. Bello and B.D. Nelin, "The Effect of Frequency
          Selective Fading on Intermodulation Distortion and
          Subcarrier Phase Stability in Frequency Modulation
          Systems" *IEEE Transactions on Communications Systems*,
          Vol. CS12, pp. 87-101; March 1964.

40.   R.G. Medhurst, "Echo Distortion in Frequency Modulation
          Frequency Division Multiplex Trunk Radio Systems"
          Electronics and Radio Engineering, pp. 253-259;
          July 1959.

6. -- Continued.

41. T. Kailath, "Optimum Receivers for Randomly Varying Channels" in *Proc 4th London Symp. on Inf. Theory.* Butterworth 1961.

42. T. Kailath, "Adaptive Matched Filters" in *Mathematical Optimization Techniques*, (R. Bellman, editor) California, Press 1963.

43. A.J. Viterbi, *Principles of Coherent Communication*, McGraw-Hill 1966.

44. O. Ye. Antonov, "Optimum Detection of Signals in Non-Gaussian Noise" *Radio Engineering and Electronic Physics*, Vol 12, pp 541-548, April 1967.

45. J.E. Evans and A.S. Griffiths, "Design of an ELF Noise Processor" 1972 IEEE Conference on Engineering in the Ocean Environment, Newport, R.I., September 1972.

46. A.S. Griffiths, "ELF Noise Processing" Techn. Report 490, Lincoln Lab. MIT; 13 January 1972 (AD 739 907).

47. A. Papoulis, *The Fourier Integral and Its Applications*, McGraw Hill, 1962.

48. H.L. Van Trees, *Detection, Estimation, and Modulation Theory, Part I*, Wiley, 1968.

49. S. Zacks, *The Theory of Statistical Inference*, Wiley, 1970.

6.   -- Continued.

50.   C.R. Rao, *Linear Statistical Inference and Its Application*, Wiley, 1965.

51.   H.L. Van Trees, *Detection, Estimation, and Modulation Theory, Part II*, Wiley, 1971.

52.   A.N. Kolmogorov, "Interpolation and Extrapolation of Stationary Random Sequences," *Bull, Acad, Sci., U.S.S.R., Ser. Math.*, 5, 1941.

53.   N. Wiener, *Extrapolation, Interpolation and Smoothing of Stationary Time Series*, Wiley, 1949.

54.   R.E. Kalman, "A New Approach to Linear Filtering and Prediction Problems," *J. Basic Engineering*, Vol. 82, pp. 34-45, March 1960.

55.   R.E. Kalman and R.S., Bucy, "New Results in Linear Filtering and Prediction Theory," *J. Basic Engineering*, Vol. 83, pp. 95-108, March 1961.

56.   T. Kailath, "An Innovations Approach to Least-Squares Estimation Part I", *IEEE Trans. on Automatic Controls*, Vol. AC-13, pp. 646-654, December 1968.

57.   T. Kailath and P. Frost, "An Innovations Approach to Least-Squares Estimation Part II," *IEEE Trans. on Automatic Controls*, Vol. AC-13, pp. 655-660, December 1968.

6.   -- Continued.

58.   P. Frost and T. Kailath, "An Innovations Approach to
           Least-Square Estimation, Part III," *IEEE Trans. on
           Automatic Control*, Vol. AC-16, pp. 217-226, June 1971.

59.   T. Kailath and R.A. Geesey, "An Innovations Approach to
           Least-Square Estimation Part IV," *IEEE Trans. on
           Automatic Control*, Vol. AC-16, pp. 720-726, December
           1971.

60.   R.A. Geesey and T. Kailath, "An Innovations Approach to
           Least-Square Estimation Part V, submitted to *IEEE Trans.
           on Automatic Control*.

61.   T. Kailath, "The Innovations Approach to Detection and
           Estimation Theory," *Proc. IEEE*, Vol. 58, pp. 680-695,
           May 1970.

62.   P. Frost, "Nonlinear Estimation in Continuous Time
           System," Ph.D. Dissertation, Stanford Univ., Stanford
           Calif. 1968.

63.   A.J. Viterbi, "Phase-Locked Loop Dynamics in the Presence
           of Noise by Fokker-Planck Techniques," *Proc. IEEE*,
           Vol. 51, pp. 1737-1753, December 1963.

64.   H.L. Van Trees, "Analog Communication Over Randomly-Time-
           Varying Channels," *IEEE Trans. on Inf. Theory*, Vol 12,
           pp. 51-63, January 1966.

6.   -- Continued.

65.   H.L. Van Trees, *Detection, Estimation, and Modulation Theory*, Part III, Wiley, 1968.

66.   R. Price and P.E. Green, "A Communication Technique for Multipath Channels," *Proc IRE*, Vol 46, pp. 555-570, March 1958.

67.   H.P. Hartmann, "Degradation of Signal-to-Noise Ratio Due to IF Filtering" *IEEE Trans. on Aerospace and Elect. Systems*, Vol AES-5, pp. 22-32; January 1969.

68.   J.J. Jones, "Filter Distortion and Intersymbol Interference Effects on PSK Signals", *IEEE Trans. on Comm. Tech.*, Vol. COM-19, pp. 120-132; April 1971.

69.   J. Jenny and P. Shaft "Performance of a Coherent PPM Detector" ESL Report GL 716, Electromagnetic Systems Laboratories, Sunnyvale, Calif. 15 July 1972.

70.   T. Hatley, "A Real Time Adaptive Digital Filter for Signal Processing" ESL-IR43; Electromagnetic Systems Laboratories, Sunnyvale, Calif; 3 February 1970.

71.   J.K. Omura, "Statistical Analysis of LF/VLF Communication Modems "Stanford Research Institute Special Technical Report 1, Project 7045; Menlo Park, Calif; August 1969.

6. _____ -- Continued.

72.   P.D. Shaft, "VLF Modem Performance in Atmospheric
        Noise" Stanford Research Institute Special Technical
        Report 1, Project 8078; Menlo Park, Calif. July 1970.

73.   C.E. Clutts, R.N. Kennedy and J.M. Trecker, "Results of
        Bandwidth Tests on the 185-Mile Florida-Cuba
        Tropospheric Scatter Radio System", _IRE Transaction on
        Communications Systems_, Vol. CS-9, pp. 434-438, Dec.
        1961.

74.   M.J. Di Toro, "Communication in Time-Frequency Spread
        Media Using Adaptive Equalization" _Proc. IEEE_, Vol. 56,
        pp. 1653-1679; October 1968.

75.   P. Monsen, "Feedback Equalization for Fading Dispersive
        Channels" _IEEE Trans. on Information Theory_, Vol. IT-16,
        pp. 56-64; January 1971.

76.   M.M. Goutmann, "Intersymbol Interference as a Natural
        Code" _IEEE Trans. on Comm._ Vol. COM-20, pp. 1033-1037;
        October 1972.

APPENDIX C - THE AMPLITUDE PROBABILITY DISTRIBUTION (APD) DETECTOR

1. INTRODUCTION

A prototype APD measurement instrument has been developed as part of the ILIR program at USAEPG. This instrument is intended to measure the APD of impulsive noise. The APD instrument, shown in figure 5, is presently in acceptance testing. The following paragraphs present a brief functional description of the APD instrument and its use in the field.

2. PROBABILISTIC DESCRIPTION OF NOISE

As indicated in paragraph 2.2 of this report, parameters which deal with the envelope, $v(t)$, of the noise voltage are used to describe the noise process. These parameters can then be used as input variables to the various communication system performance models identified in table IV. For digital communications systems, the following noise parameters (see table IV) are required as inputs:

    a. Noise Factor, F_a

    b. Amplitude Probability Distribution (APD)

The noise factor, F_a, can be related to the type of noise test receiver, the rms voltage reading (V_{rms}) of $v(t)$, and the various losses which are incurred through the antenna-noise test receiver combination. As shown in table II, APD is given by the following relation:

$$D(v) = \text{Prob}\ [v \geq v_i] = 1 - \text{Prob}\ [v < v_i] = 1 - \int_0^{v_i} p(v)dv$$

or

$$p(v) = -\frac{dD(v)}{dv}$$

where $p(v)$ is the probability density function for the noise. For a Gaussian noise environment, $D(v)$ is a straight line when plotted on Rayleigh paper which has coordinates of noise envelope voltage in dBμV/MHz versus Rayleigh probability (ref 3, app D). As the noise environment becomes more impulsive, the slope of the Gaussian straight line increases.

3. MEASURED APD AND COMMUNICATION SYSTEM PERFORMANCE

As indicated in table IV, all the digital communication system performance models require F_a and APD--$D(v)$ to reliably predict communication system degradation. At the present time, there are no statistical measures of F_a and $D(v)$ for the tactical vehicular noise environment. Direct measurement of these quantities would provide a realistic description of the noise which surrounds the communication system.
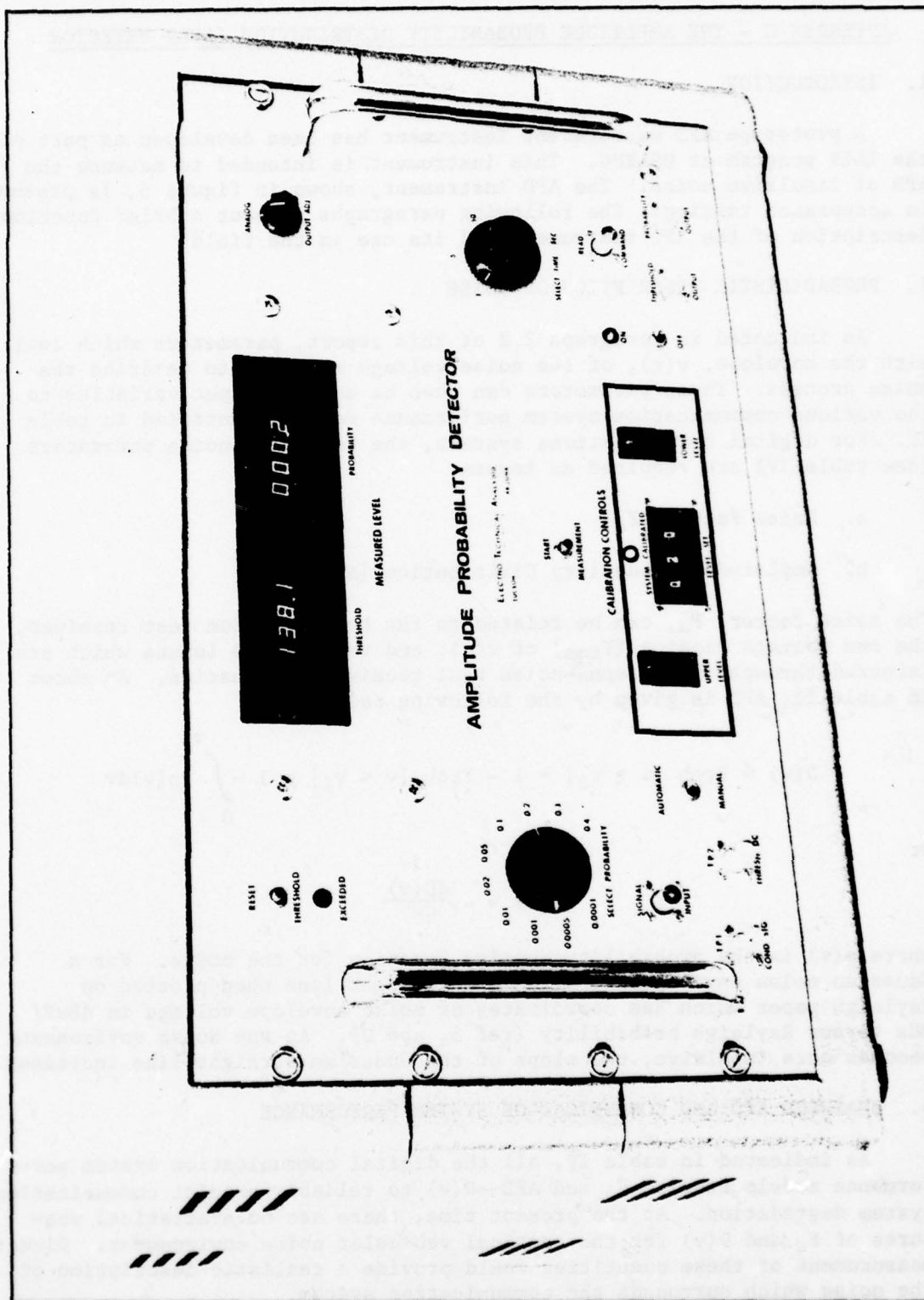
Figure 5. Amplitude Probability Detector, overall view.

4. APD MEASUREMENT INSTRUMENT

The APD detector evaluates the amplitude levels which the input signal exceeds with a selected probability during a selectable test time. The probability levels which can be preselected manually or automatically are: 0.0001, 0.0005, 0.001, 0.01, 0.02, 0.05, 0.1, 0.2, 0.3, and 0.4. Measurement times which can be preselected from the front panel are 1, 5, and 50 seconds.

4.1 Manual Measurement Procedure

Once the system is calibrated, a manual measurement can be made as follows: First, the calibration signal must be removed, the signal to be measured supplied to the system, and the MANUAL-AUTOMATIC toggle switch set to MANUAL. Next, the probability level to be tested and the measurement time must be selected by the front panel SELECT PROBABILITY and SELECT TIME switches. Finally, the THRESHOLD RESET button should be pushed to make certain the initial threshold is at maximum.

With the above steps completed, the START MEASUREMENT switch may be depressed. The system will make a test at the selected threshold and will indicate it is measuring by blanking the threshold portion of the display. If the threshold is not exceeded with the selected probability, the system will so indicate by decrementing the threshold and showing this new threshold on the display. The START MEASUREMENT switch will cause this level to be tested, with the procedure repeated until the threshold is exceeded at the specified probability. When this action occurs, the system will respond by "blinking" the threshold display.

A test of another probability level can be made by selecting the new level and pushing the THRESHOLD RESET button. This mode of operation was designed mainly for calibration purposes.

It should be noted that various events can disturb the stationarity of the input being tested. System disturbances or noise resulting from the turning on or off of external devices are examples of such occurrences. The result of such an event may cause the threshold to be exceeded during a measurement in a manner not representative of the stationary process being tested. Fortunately, such occurrences are easily detected and eliminated simply by always pushing the START MEASUREMENT button one more time after the device indicates the threshold has been exceeded. If the level reached is, in fact, correct, the system will respond by blinking the threshold level. If, however, a false reading occurred, the system will step to the next level and the test can proceed to the correct level.

4.2 Automatic Testing

Once the system is calibrated, an automatic measurement can be accomplished as follows: Set the toggle selector to AUTOMATIC, remove the calibration signal, and supply the signal to be measured to the system.

Next, the probability level to be tested and the measurement time must be selected by the front panel switches. Finally, the THRESHOLD RESET button should be pushed to make certain the initial threshold is at maximum.

With the above steps accomplished, an automatic measurement cycle is initiated by pushing the START MEASUREMENT button. The system will begin testing and will automatically decrement the threshold until the threshold is exceeded at the probability level specified. When this occurs, testing stops and the threshold level is blinked. The operator, by selecting another probability and pushing the START MEASUREMENT pushbutton, will cause the system to increment the threshold level until the signal exceeds the threshold of the preset probability.

For the same reasons discussed in the manual procedure, it is good practice to depress the START MEASUREMENT button one more time to assure the validity of the test.

In the event the system searches its entire range without the threshold being exceeded, the display will show "EEEE," indicating a measurement failure. This event may occur if no input is supplied to the instrument.

A fully automatic mode of operation is to be incorporated into the instrument which will increment both the threshold level and the preset probabilities. This mode, to be instituted by pushing the START MEASUREMENT pushbutton, will permit the measurement of the entire APD curve.

4.3 Recorder

Outputs have been provided on front panel BNC connectors to facilitate analog recording of the APD of the signal being analyzed. Two outputs to drive an X-Y type function and a READ COMMAND output to control pen lift are available.

4.4 Input Configuration

The instrument was designed with a replaceable input signal conditioning board. Boards designed to accommodate input signals from the HP 8552-B and Ailtech 727 spectrum analyzers are now available. Additional boards can be fabricated and inserted into the instrument to accommodate the output of other receivers.

4.5 Preselectors

A set of preselectors with a frequency range of 0.5-1000 MHz with a 2-MHz bandwidth at the 21.4-MHz IF output have been ordered to be used with either HP or Ailtech spectrum analyzers. The purpose of these preselectors is to reduce the impulsiveness of the input signal to minimize mixer overload and thus optimize the dynamic range of the APD measurement.

5. VEHICULAR NOISE TESTING

The APD detector can be used to provide APD noise data on a single vehicle as is illustrated in figure 6. The antenna may be moved around the vehicle to generate different APD plots, thereby defining the total noise environment which surrounds the vehicle. As shown in figure 6, the spectrum analyzer, in conjunction with the RF converter, controls and monitors the EM emission from the vehicle.

The spectrum analyzer, which is used in the time domain, provides a visual time display of the impulsive noise being measured and monitors the amplitude of this emission. The multibandwidth selection of the spectrum analyzer will permit APD measurements at these many bandwidths.

Specific vehicular data can be recorded on the sample data sheets as shown in figures 7 and 8. APD noise measurement data can then be plotted on the Rayleigh graph paper as shown in figure 9. When the APD detector is placed in the automatic mode, this plotting is done automatically on a plotter which is connected to the APD detector.

6. FUTURE APD DETECTOR CONSIDERATIONS

With the addition of another calculator chip, the APD detector can be made to calculate the mean (average) received noise power, P_N. This calculation would be a discrete summation based on the following continuous expression:

$$P_N = V_{rms}^2 = \frac{1}{T} \int_0^T v^2(t)dt = - \int_0^\infty v^2 dD(v)$$

where $V(t)$ is the envelope of the noise voltage, V_{rms} is the root mean square value of this voltage, T is the period of $V(t)$, and $D(v)$ is the amplitude probability distribution (see para 2 above). The value of P_N identified above would be the noise power dissipated in a 1-ohm load.

A circuit to measure the average crossing rate (ACR) will also be included. This feature can easily be incorporated, since the present circuitry includes gates which are activated by signals exceeding the threshold. An ACR measurement will be taken for each probability level.
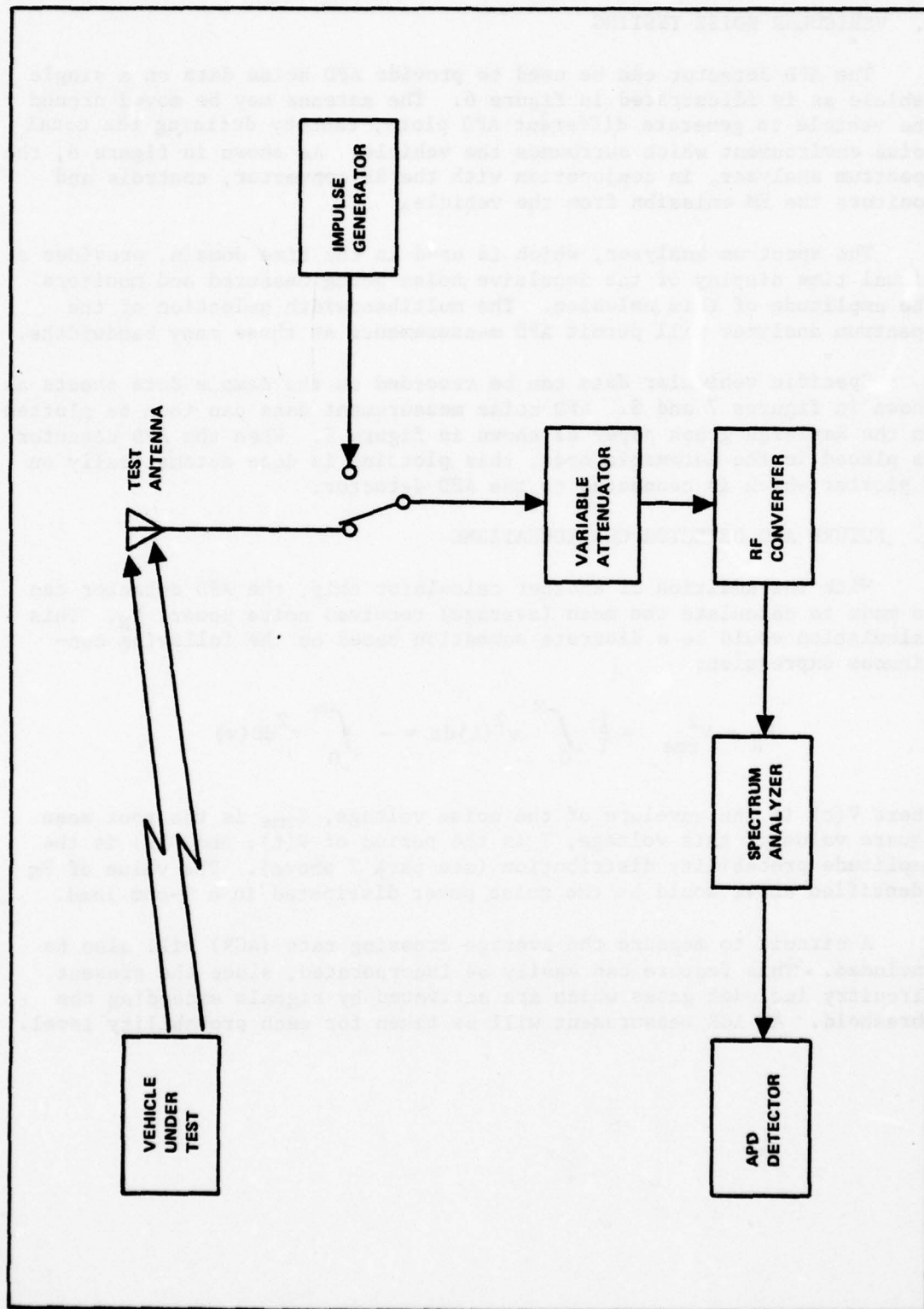
Figure 6. Measurement test setup utilizing an APD detector for vehicular noise.

DATA SHEET

VEHICULAR ELECTROMAGNETIC
NOISE MEASUREMENTS

NOISE AMPLITUDE PROBABILITY DISTRIBUTION (APD) METHOD

I. VEHICLE INFORMATION

a. Make:_____ b. Year:_____

c. Type:_____ d. No. Cylinders:_____

e. Mileage:_____ f. Serial No._____

g. Engine Speed (rpm):

   Normal_____ Measured_____

h. Specific Characteristics:_____

_____

_____

_____

_____

II. TEST EQUIPMENT:_____

_____

_____

_____

_____

III. TEST CRITERIA AND CONFIGURATION:_____

_____

_____

_____

_____

Figure 7. Data sheet, vehicular EM noise measurements (sheet 1 of 2).

IV. TEST INFORMATION

    a. Amplitude Probability Distribution Detector (APDD)

        Integration Time:_____seconds

    b. EMI Receiver

        (1) Tuned Frequency:_____MHz

        (2) Sensitivity:_____dBm

        (3) Bandwidth:_____kHz

        (4) Serial No:_____

    c. Point of Measurement:_____

_____

_____

_____

_____

Figure 7. Data sheet, vehicular EM noise measurements (sheet 2 of 2).

AMPLITUDE PROBABILITY DISTRIBUTION MEASUREMENTS

Test Item:_____ Date:_____

Preset Test Time:_____s Count Limit:_____

Rcvr Bandwidth:_____ Rcvr Tuned Freq:_____MHz

Antenna Factor (dB)	Transmission Line Factor-Loss (dB)	APDD Preset Probability Threshold Level	No. Times (Counts) Threshold Exceeded

Figure 8. APD measurement data sheet.

LINEAR BY -1/2 LOG (-1np)

FIELD STRENGTH (dB/μ V/MHz/m)

98 92 86 80 74 68 62 56 50 44 38 32 26 20

0.0001 0.01 0.1 1 5 10 20 40 60 80 90 95 98 99

PERCENT OF TIME ORDINATE IS EXCEEDED

NO. OF VEHICLES _____ BANDWIDTH 300 kHz _____ DATE _____

VEHICLE CODE _____ 100 kHz _____ REMARKS _____

SCAN TIME _____ /cm 30 kHz _____ _____

SCAN WIDTH_____ /cm 10 kHz_____ _____

INPUT LEVEL_____ dBμ V/MHz 3 kHz_____ _____

FREQUENCY _____ MHz FIELD STRENGTH_____dBμ V/MHz/m

Figure 9. Single vehicle APD data sheet.
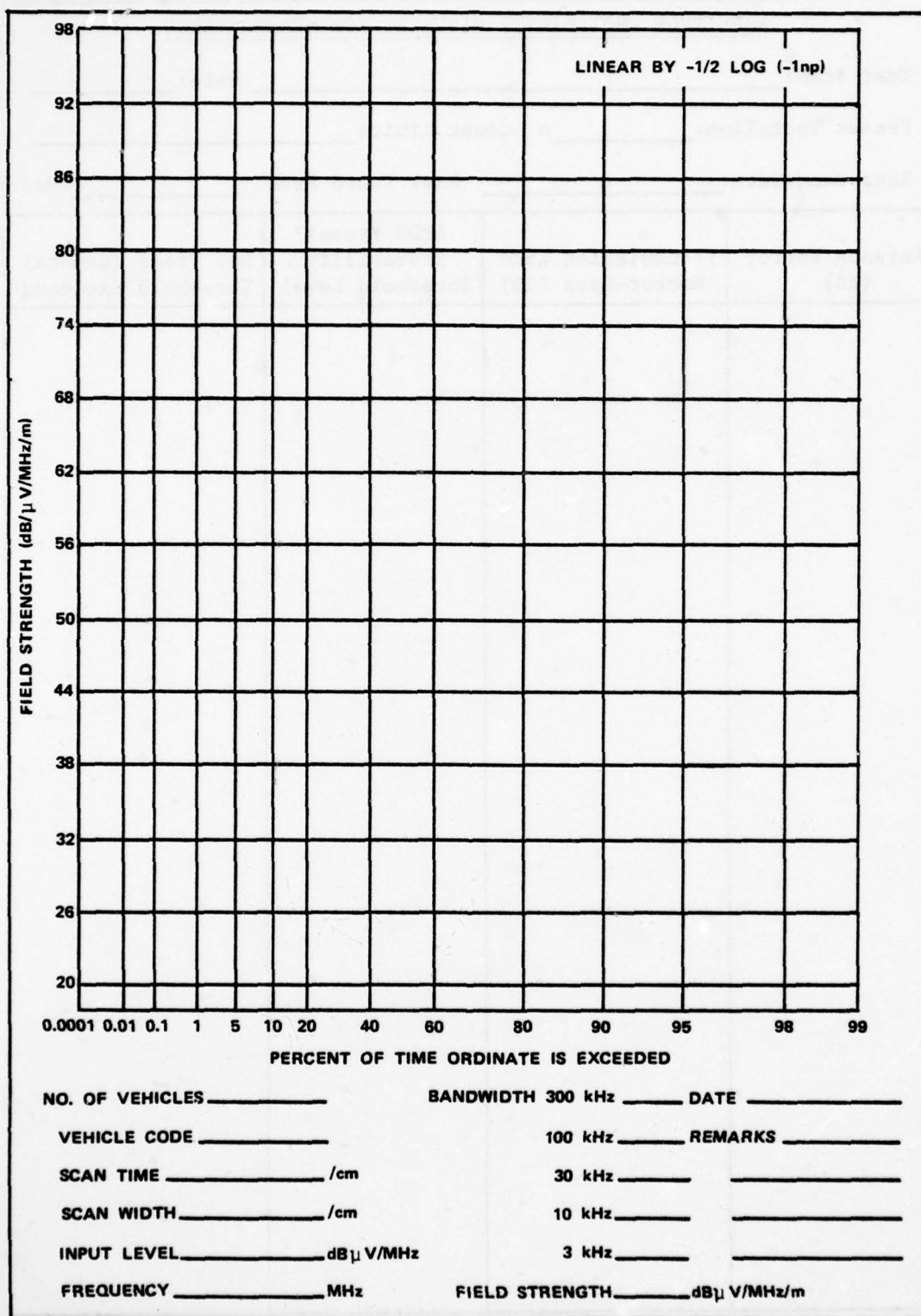
APPENDIX D - REFERENCES

1. Department of Defense (DoD), MIL-STD-461A, Military Standard, "Electromagnetic Interference Characteristics, Requirements for Equipment," 1 August 1978, Notice 1, 7 February 1969; Notice 2, 20 March 1969; Notice 3, May 1970; Notice 4, 9 February 1971; Notice 5, 6 March 1973.

2. The Wheels Study, "Vehicle EMI Suppression Measurements," Data Packet, U. S. Army Electronic Proving Ground (USAEPG), Fort Huachuca, AZ, May 1975. (Prepared by Lockheed Electronics Co., Tucson, AZ.)

3. A. D. Spaulding, "Man-Made Noise: The Problem and Recommended Steps Toward Solution," OT Report 76-85, Office of Telecommunications, U. S. Dept. of Commerce, April 1976.

4. G. H. Hagn and R. A. Shepherd, "Man-Made Electromagnetic Radio Noise from Unintentional Radiators: A Summary," NATO Advisory Group on Aerospace Research and Development (AGARD) Conference Proceedings No. 159, pp. 3-1 to 3-24, 1974. (Available from NTIS, Springfield, VA, as AD-A-018-980.)

5. H. N. Shaver, V. E. Hatfield, and G. H. Hagn, "Man-Made Noise Parameter Identification Task," Final Report, Contract N00039-71-A-0223, Stanford Research Institute, Menlo Park, CA, May 1972. (Available from NTIS, Springfield, VA, as AD-904405.)

6. "The Impact of the Application of SAE Standard J551 Requirements to XM861 Series 1 1/4 Ton Truck," U. S. Army Electronics Command, Fort Monmouth, NJ, 2 June 1975.

7. M. A. Merkel, "EMI Effects of Commercial Trucks on Army Tactical Receivers," Letter Report, CCC-EMEO-ECD, U. S. Army, CEEIA, Fort Huachuca, AZ, 16 February 1977.

8. R. A. Shepherd, J. C. Gaddie, V. E. Hatfield, and G. H. Hagn, "Measurements of Automobile Ignition Noise at HF," Final Report, SRI Project 2051, Contract N00039-71-A-0223, Delivery Order 0003, Stanford Research Institute, Menlo Park, CA, February 1973.

9. R. A. Shepherd, "Measurements of Amplitude Probability Distributions and Power of Automobile Ignition Noise at HF," IEEE Transactions on Vehicular Technology, Vol. VT-23, No. 3, pp. 72-83, August 1974.

10. A. D. Spaulding and R. T. Disney, "Man-Made Radio Noise, Part I: Estimates for Business, Residential and Rural Areas," OT Report 74-38, Office of Telecommunications, Institute for Telecommunication Sciences, Boulder, CO 80302, June 1974.

11. R. A. Shepherd, J. C. Gaddie, and D. L. Nielson, "Variability in Measurement Procedures for Ignition Noise," Final Report, Motor Vehicle Mfgs. Assn. (MVMA), Agreement No. SRI-7404-C2.10, Stanford Research Institute, Menlo Park, CA, October 1974. (Available from NTIS, Springfield, VA, as PB 244 538.)

12. R. A. Shepherd, J. C. Gaddie, and A. Shohara, "Measurement Parameters for Automobile Ignition Noise," Final Report, MVMA Agreement No. SRI 7502-C2.10, Stanford Research Institute, Menlo Park, CA, June 1975. (Available from NTIS, Springfield, VA, as PB 247-766.)

13. A. J. Rosa, "HF and VHF Automobile Ignition Measurements," IEEE Regional Electromagnetic Compatibility Symposium Record, IEEE Catalog No. 70C64-REGEMC, October 1970.

14. R. B. Schulz and R. A. Southwick, "APD Measurements of V-8 Ignition Emanations," IEEE Transactions on EMC, Vol. EMC-16, No. 2, pp. 63-70, May 1974.

15. R. A. Shepherd, J. W. Engles, and G. H. Hagn, "Automobile Ignition Noise and the Supernoisy Vehicle," Symposium Record, IEEE International Symposium on EMC, IEEE Catalog No. 76-CH-1104-9EMC, pp. 403-412, July 1976.

16. D. E. Baran, "Prediction of Relative Available Noise Power for Vehicular Ignition Noise," Final Report No. ESD-TR-76-007, Contract F-19628-76-C-0017, Electromagnetic Compatibility Analysis Center, Annapolis, MD 21402, October 1976.

17. R. A. Shepherd, J. C. Gaddie, and P. J. Bell, "Electromagnetic Radiation Statistics at 50 MHz and 153 MHz of the United States Vehicle Population," Final Report, MVMA Agreement No. SRI 7706-C2.10, SRI International, Menlo Park, CA, August 1977.

18. J. Deitz, F. Lucia, and M. Liebman, "Degradation of Mobile Radio Reception at UHF and VHF," Report No. R-7302, Federal Communications Commission, Washington, D. C., 17 August 1973.

19. J. Deitz, F. Lucia, and M. Liebman, "Degradation of Base Station Radio Reception at UHF and VHF," Report No. FCC/OCE RS75-OJ, Federal Communications Commission, Washington, D. C., June 1975.

20. F. Lucia, M. Liebman, and D. Desrosiers, "Motor Vehicle Ignition Radiation with Respect to the SAE Standard J551c," Report No. FCC/OCE 76-03, Federal Communications Commission, Washington, D. C., April 1976.

21. A. W. Anderson, Army Radio Frequency Manager, Telecommunications and Command and Control Directorate, Deputy Chief of Staff for Operations and Plans, Private Communications, Department of Army Headquarters, Washington, D. C., January 1978.

22. Society of Automotive Engineers, Inc., SAE J551e, "Limits and Methods of Measurement of Radio Interference Characteristics of Vehicles and Devices (20-1000 MHz)," June 1977.

23. Federal Communications Commission (FCC), "Notice of Inquiry on Interference from Spark-Type Ignition Systems in Motor Vehicles," Docket 20654, Federal Communications Commission, Washington, D. C., 16 December 1975.

24. R. A. Shepherd, J. C. Gaddie, and D. L. Nielson, "Improved Suppression of Radiation for Automobiles Used by the General Public," Final Report, SRI Project 2763, Contract FCC-0072, Stanford Research Institute, Menlo Park, CA, 1975. (Available from NTIS, Springfield, VA, as PB 239-471.) See also "New Techniques for Suppression of Automobile Ignition Noise," IEEE Transactions on Vehicular Technology, Vol. VT-25, No. 1, February 1976, by the same authors.

25. Bell Technical Operations, "Annotated Bibliography on Single and Multiple Vehicle Electromagnetic Noise Emanations and Their Resultant Effects and Degradation on Typical Communication Systems," Bell Report No. BTO 77-09-005, Contract DAEA18-76-C-0002, Bell Technical Operations, Tucson, AZ, 1978.

26. Department of Defense (DoD), MIL-STD-188C, Military Standards, Military Communication System, Technical Standards, 24 November 1969.

27. International Telecommunication Union (ITU), CCIR Report No. 413, "Improved Efficiency in the Use of the Radio-Frequency Spectrum," Oslo, Norway, 1966.

28. A. D. Whalen, Detection of Signals in Noise, Academic Press, New York, NY, 1971.

29. W. B. Davenport and W. L. Root, Random Signals and Noise, McGraw-Hill Book Co., Inc., New York, NY, 1958.

30. David Middleton, "Statistical-Physical Models of Electromagnetic Interference," IEEE Transactions on EMC, Vol. EMC-19, No. 3, pp. 106-127, August 1977.

31. A. D. Spaulding, "The Determination of Received Noise Levels from Vehicular Traffic Statistics," IEEE 1972 National Telecommunications Conference Record, 72CHO 601-5-NTC, 1972.

32. D. B. Geselowitz, "Response of Ideal Radio Noise Meter to Continuous Sine Wave, Recurrent Impulses and Random Noise," IRE Transactions on Radio Frequency Interference, May 1961.

33. W. Q. Crichlow, C. J. Robique, A. D. Spaulding, and W. M. Beery, "Determination of the Amplitude-Probability Distribution of Atmospheric Radio Noise from Statistical Moments," J. Research NBS 64D (Radio Prop.) No. 1, 49, 1960.

34. International Telecommunication Union (ITU), CCIR Report No. 322, "World Distribution and Characteristics of Atmospheric Radio Noise," Geneva, Switzerland, 1964.

35. Office of Telecommunications Policy (OTP), "Basic Parameter for Measurement of Radio Noise," Manual of Regulations and Procedures for Radio Frequency Management, Chapter 4, pp. 5-35, Sec. 5.8, Office of Telecommunications Policy, Executive Office of the President, 1970.

36. H. Hall, "A New Model for 'Impulsive' Phenomena: Application to Atmospheric-Noise Communication Channels," Ph.D. Thesis, Technical Report 7050-7, Stanford Electronics Laboratories, Stanford, CA, August 1966.

37. J. K. Omura, "Statistical Analysis of LF/VLF Communication Modems," Special Technical Report 1, SRI Project 7045, SRI International, Menlo Park, CA 94025, August 1969.

38. Aki Shohara, "Modeling Quasi Impulsive Noise as Modulated Gaussian Processes," 2nd Symposium on Electromagnetic Compatibility, Montreux, 77CH1224-5EMC, pp. 363-367, June 1977.

39. E. C. Field, and M. Lewinstein, "Amplitude-Probability Distribution for VLF/ELF Atmospheric Noise," IEEE Transactions on Communications Technology, Vol. Com-26, No. 1, pp. 83-87, January 1978.

40. D. J. Cohen, "A Statistical Ignition Noise Model," ECAC-PR-72-041, Electromagnetic Compatibility Analysis Center, North Severn, Annapolis, MD, October 1972.

41. G. H. Hagn, R. A. Shepherd, and J. C. Gaddie, "Measured Degradation Effects of Powerline Noise and Ignition Noise on an HF Non-Coherent FSK Digital Communication System," presented at 2nd International Symposium on Electromagnetic Compatibility, Montreux, Switzerland, 28-30 June 1977.

42. International Special Committee on Radio Interference (C.I.S.P.R.), CISPR Publication 12, "Limits and Methods of Measurement of Radio Interference characteristics of Ignition Systems of Motor Vehicles and Other Devices," 1975.

43. H. P. Hsu, "Quasi-Peak and Peak Ignition Noise Measurements and Degradation Effects of Ignition Noise on Communication Systems," 1st Symposium and Technical Exhibition on Electromagnetic Compatibility, Montreaux, Switzerland, IEEE 75CH1012-4 MONT, pp. 171-181, May 1975.

44. H. H. Cook, "Quasi-Peak to RMS Voltage Conversion," presented at 2nd International Symposium on Electromagnetic Compatibility, Montreaux, Switzerland, 77CH1224-5EMC, 28-30 June 1970.

45. G. H. Hagn, "Units for Electromagnetic Noise Measurements," IEEE Transactions on Electromagnetic Compatibility, 1978.

46. G. H. Hagn, "Definitions and Fundamentals of Electromagnetic Noise Interference and Compatibility," NATO AGARD Conference Proceedings 159, pp. 1-1 to 1-24, November 1975. (Available from NTIS, Springfield, VA, as AD-A-018980.)

47. E. Arthurs and H. Dym, "On the Optimum Detection of Digital Signals in the Presence of White Gaussian Noise--A Geometric Interpretation and a Study of Three Basic Data Transmission Systems," IRE Transactions Communication Systems, pp. 336-372, December 1962.

48. C. C. Watterson and C. M. Minister, "HF Channel-Simulator Measurements and Performance Analysis on the USC10, ACQ6, and MX190 PSK Modems," Office of Telecommunications Report 75-56, 1976.

49. Bell Technical Operations Textron, "Description of the Improved Voice Scoring Facility of the EMETF, BTO 77-07-002 (unpublished).

50. B. C. Tupper and G. H. Hagn, "Nap-of-the-Earth (NOE) Communications for U. S. Army Helicopters," Final Report, SRI Project 4979, Contract DAAB07-76-C-0868, SRI International, Menlo Park, CA 94025, 1978.

51. N. H. Shepherd, "Noise Measurements and Degradation of Land-Mobile Receiver Performance," an analysis of data from MVMA's 1971 Test Program, Motor Vehicle Manufacturers Association, Detroit, MI, 21 September 1971.

52. H. S. Oranc, "Ignition Noise Measurements in the VHF/UHF Bands," IEEE Transactions on Electromagnetic Compatibility, Vol. EMC-17, No. 2, pp. 54-64, May 1975.

53. N. H. Shepherd, "Standand Methods of Measurement for Impulse Radio Noise," U. S. National Committee (USNC), International Union of Radio Science (URSI), 1975 annual meeting, Program and Abstracts, p. 90, 1977.

54. R. W. Hubbard and W. J. Hartman, "Objective Measurement Techniques for Evaluating Voice Communication Channels," U. S. Dept. of Transportation, FAA, Report No. FAA-RD-74-77, July 1974. (Available from NTIS, Springfield, VA, as AD-786667/6GI.)

55. K. J. Gamauf and W. J. Hartman, "Objective Measurement of Voice Channel Intelligibility," U. S. Dept. of Transportation, FAA, Report No. FAA-RD-77-153, October 1977.

56. H. Akima and A. D. Spaulding, "A Simulation Model for Analyzing Performance of Some Simple Communication Systems on a Digital Computer," U. S. Department of Transportation, Federal Aviation Administration, Report No. FAA-RD-76-181, November 1976. (Available from NTIS, Springfield, VA, as AD-A036437/2GI.)

57. G. F. Montgomery, "Comparison of Amplitude and Angle Modulation for Narrowband Communications of Binary Coded Messages in Fluctuation Noise," Proceedings IRE, 42, pp. 447-454, 1954.

58. A. D. Spaulding and D. Middleton, "Optimum Reception in an Impulsive Interference Environment," Office of Telecommunications Report OT 75-67, 1975.

59. J. H. Halton and A. D. Spaulding, "Error Rates in Differentially Coherent Phase Systems in Non-Gaussian Noise," IEEE Transactions on Communications Technology, COM-14, No. 5, pp. 594-601, 1966.

60. J. K. Omura and P. D. Shaft, "Modem Performance in VLF Atmospheric Noise," IEEE Transactions on Communications Technology, Vol. COM-19, pp. 659-688, 1971.

61. J. T. Gamble, "An Analysis and Linear and Non-Linear Coherent Detection in Atmospheric Noise at Very Low Frequency," Rome Air Development Center Technical Report, TR-74-289, 1974.

62. W. J. Hartman, "Multipath in Air Traffic Control Frequency Bands," Vol. 1--"Classification of Multipath, Effects of Multipath on Systems, and Causes of Multipath," and Vol. II--Chapters CIII through VIV, "General Bibliography," FAA Report No. FAA-74-75, I and II, July 1974. (Available from NTIS, Springfield, VA as Vol. 1 AD-A006-267 and Vol. 2 AD-A006-268.)

63. J. S. Bendat and A. G. Piersol, Random Data: Analysis and Measurement Procedures, Wiley-Interscience, New York, 1971.

64. D. Middleton, "Acoustic Modeling, Simulation, and Analysis of Complex Underwater Targets; II. Statistical Evaluation of Experimental Data," Report No. ARL-TR-69-22, Contract N00024-69-C-1129, Project Serial No. SF 1010316, Task 8212, Applied Research Laboratories, The University of Texas at Austin, Austin, TX, 26 June 1969.

65. E. L. Crow and M. J. Miles, "Confidence Limits for Digital Error Rates from Dependent Transmissions," OT Report 77-118, Office of Telecommunications, U. S. Dept. of Commerce, March 1977.

66. A. D. Spaulding and G. H. Hagn, "On the Definition and Estimation of Spectrum Occupancy," IEEE Transactions EMC, Vol. EMC-19, No. 3, pp. 269-280, August 1977.

67. A. B. Bowker and G. J. Lieberman, Engineering Statistics, 2nd Edition, Prentice Hall, Englewood Cliffs, NJ, 1972.

68. M. Hollander and D. A. Wolfe, Nonparametric Statistical Methods, John Wiley & Sons, New York, 1973.

69. K. E. Gillilland and T. A. Brewer, "Experimental Verification of Ignition Noise APD Model and Digital-Receiver Bit-Error Probability Model," Technical Report ESD-TR-73-036, ECAC, North Severn, Annapolis, MD, January 1974.

70. H. P. Hsu, R. M. Storwick, D. C. Schlick, and G. L. Maxam, "Measured Amplitude Distribution of Automotive Ignition Noise," IEEE Transactions on EMC, Vol. EMC-16, No. 2, pp. 57-63, May 1974.

71. G. L. Maxam, H. P. Hsu, D. C. Schlick, and R. M. Storwick, "Measured Pulse Height Distributions of Individual Engine Cylinder Noise," Research Laboratories (G. M. Corp.), GMR-1424, 25 July 1973.

72. Department of the Navy, Bureau of Ships, NAVSHIPS 94180, "The Radio Frequency Interference Meter," Washington, D. C., July 1962.

73. International Special Committee on Radio Interference (C.I.S.P.R.), CISPR Publication 16, 1978.

74. Richard A. Shepherd, James C. Gaddie, and Paula J. Bell, "Electromagnetic Radiation Statistics at 50 MHz and 153 MHz of the United States Vehicle Population," Final Report, SRI Project 5959, SRI International, Menlo Park, CA 94025, August 1977.

75. Athansios Popoulis, _Probability, Random Variables, and Stochastic Processes_, McGraw Hill Book Co., 1965.

76. P. C. Minor and L. E. Wood, "A New State of the Art in EMC Field Measurement Instrumentations," _IEEE Transactions on Electromagnetic Compatibility_, Vol. EMC-19, No. 3, pp. 230-236, August 1977.

77. Robert J. Matheson, "A Radio Spectrum Measurement System for Frequency Management Data," _IEEE Transactions on Electromagnetic Compatibility_, Vol. EMC-19, No. 3, pp. 225-230, August 1977.

78. "SCORES Europe I - Sequence 4 Test Bed (U)," Volume 1-4, U. S. Army Management Systems Support Agency (USAMSSA), 30 June 1966, Secret.

79. "Standard Scenario for Combat Developments (U) Europe I - Sequence 2A," Volumes 1-5, Draft, U. S. Army Combined Arms Center, August 1975, Secret.

APPENDIX E - ANNOTATED BIBLIOGRAPHY

1. INTRODUCTION

This appendix presents an annotated bibliography of the current literature which describes recent advancements in vehicular noise emissions and the resultant effects on various communication systems. The purpose of this bibliography is to establish a readily available documentation data base on vehicular noise statistics, test methodologies, procedures, and bit error rate (BER) versus signal-to-noise ratio (S/N) for different communication systems.

The bibliography includes published reports and articles from the Office of Telecommunication (OT), Southwest Research Institute, SRI International, General Motors Corporation (GMC), Electromagnetic Compatibility Analysis Center (ECAC), Institute of Electrical and Electronic Engineers (IEEE), and various other agencies. The bibliography has been grouped into two major sections as follows:

    a. Abridged bibliographic reference guide

    b. Annotated bibliographic reference guide

The abridged guide has been further subdivided by subject headings to facilitate reporting. In some cases the same document is listed under subject headings thereby providing some degree of cross referencing.

The annotated guide presents an extended listing of all documents in alphabetical order according to the first author's last name.

Included with each document is a synopsis which identifies key points contained in the document.

2. ABRIDGED BIBLIOGRAPHIC REFERENCE GUIDE

2.1 Performance Measurements

Author	Document Date	Page No.	Item No.
Beerling, C. W.	Jan 1971	E-10	8
Cron, E. L.	Nov 1974	E-14	22
Dietz, J. et al.	Aug 1974	E-15	23
Dietz, J. et al.	Jun 1975	E-15	24
Hartman, W. J.	Jun 1977	E-17	34
Hawthorne, G. B. et al.	Jun 1959	E-18	35
Lucia, F. et al.	Apr 1976	E-20	44
Maruvada, P. S. and Trinh, N. G.	Sep/Oct 1975	E-21	46
Shepherd, R. A. et al.	Feb 1973	E-24	59
Shepherd, R. A. and Gaddie, J. C.	Apr 1976	E-26	64
Spaulding, A. D.	Apr 1976	E-31	82

2.2 Performance Models - Analog

Author	Document Date	Page No.	Item No.
Akima, H. et al.	Aug 1969	E-9	2
Akima, H. and Spaulding, A. D.	Aug 1977	E-9	4
Schwartz, M. et al.	1966	E-24	57
Shepherd, R. A. et al.	Jun 1975	E-25	62

2.3 Performance Models - Digital

Author	Document Date	Page No.	Item No.
Akima, H. et al.	Aug 1969	E-9	2
Akima, H. and Spaulding, A. D.	Aug 1977	E-9	4
Arthurs, E. and Dym, H.	Dec 1962	E-10	6
Bello, P. A.	Sep 1965	E-11	9

Brayer, K.	Oct 1971	E-12	12
Churchill, R. B.	Oct 1975	E-12	14
Churchill, R. B.	Sep 1977	E-13	16
Gillilland, K. E. and Brewer, T. A.	Jan 1974	E-16	29
Gillilland, K. E.	Dec 1972	E-16	30
Gillilland, K. E.	Apr 1975	E-17	31
Halton, J. H. and Spaulding, A. D.	Oct 1966	E-17	32
Hartley, H. F.	Oct 1967	E-17	33
Omura, J. K.	Aug 1969	E-22	51
Schwartz, M. et al.	1966	E-24	57
Shaver, H. N. et al.	May 1972	E-24	58
Southwick, R. A. and Schultz, R. B.	1974 ICC	E-28	72
Spaulding, A. D.	Jul 1969	E-29	77
Systems Technology Associates	Mar 1975	E-32	85
Wilson, K. E.	Nov 1974	E-33	90

2.4 Noise Source Characteristics - Measurements

Author	Document Date	Page No.	Item No.
Bronaugh, E. L. and Kerns, D. R.	Jul 1976	E-12	13
Crichlow, W. Q. et al.	1960 b	E-14	19
Disney, R. T. and Spaulding, A. D.	1970	E-15	25
Electromagnetic Compatibility Analysis Center (ECAC)	Jun 1977	E-15	27
Hsu, H. P. et al.	May 1974	E-18	36
Lauber, W. R. and Bertrand, J. M.	Jun 1977	E-19	43

| Yamamoto, S. et al. | Aug 1977 | E-33 | 92 |

2.5 Noise Source Characteristics - Models

Author	Document Date	Page No.	Item No.
Akima, H.	Mar 1972	E-9	3
Baran, D. E.	Oct 1976	E-10	7
Churchill, R. B.	Oct 1975	E-12	14
Churchill, R. B.	Jul 1976	E-13	15
Churchill, R. B.	Sep 1977	E-13	16
Cohen, D. J.	Oct 1972	E-13	17
Cook, J. H.	Jun 1977	E-13	18
Crichlow, W. Q. et al.	1960 a	E-14	20
Disney, R. T. and Spaulding, A. D.	Feb 1970	E-15	25
Gillilland, K. E. and Brewer, T. A.	Jan 1974	E-16	29
Gillilland, K. E.	Apr 1975	E-17	31
International Telecommunication Union (ITU) - CCIR 322		E-19	41
Middleton, D.	Apr 1974	E-22	48
Middleton, D.	Apr 1976	E-22	49
Shaver, H. N. et al.	May 1972	E-24	58
Shohara, A.	Jun 1977	E-27	67
Southwick, R. A. and Schultz, R. B.	1974 ICC	E-28	72
Spaulding, A. D. et al.	Dec 1962	E-29	76
Spaulding, A. D.	Jul 1972	E-29	78
Spaulding, A. D. and Disney, R. T.	Jun 1974	E-30	79

Spaulding, A. D. and Middleton, D.	Jun 1975	E-30	81
Waterson, C. C. et al.	Dec 1970	E-32	87
Wilson, K. E.	Nov 1974	E-33	90

2.6 Noise Source Characteristics – Simulation

Author	Document Date	Page No.	Item No.
Bolton, E. C.	Aug 1972	E-11	10
Bolton, E. C.	Aug 1974	E-11	11
Watterson, C. C. et al.	Dec 1970	E-32	87

2.7 Propagation Models

Author	Document Date	Page No.	Item No.
Churchill, R. B.	Sep 1977	E-13	16
Shepherd, R. A. et al.	Jul 1976	E-27	65
Spaulding, A. D.	Jul 1972	E-29	78

2.8 Antennas or Coupling

Author	Document Date	Page No.	Item No.
Bronaugh, E. L. and Kerns, D. R.	1976	E-12	13
Lauber, W. R. and Bertrand, J. M.	1977	E-19	43

2.9 Protection Methods

Author	Document Date	Page No.	Item No.
Crippen, L. J. et al.	Nov 1970	E-14	21
Shepherd, R. A. et al.	Feb 1976	E-26	63
Shepherd, R. A. et al.	Aug 1977	E-27	66
Spaulding, A. D.	Apr 1976	E-31	82

2.10 Instrumentation

Author	Document Date	Page No.	Item No.
American Electronic Laboratories, TR 1020-2	--	E-10	5
Cook, J. H.	Jun 1977	E-13	18
Fairchild, Electro-Metric Corp. EMC-25		E-16	28
Kerns, D. R. et al.	Oct 1975	E-19	42
Matheson, R. J.	Nov 1970	E-20	45
Oliver, W.	Sep 1964	E-22	50
Richard Brancker Research Ltd, V_{rms} and V_d Converter Model 895		E-23	54
Singer Instrumentation, Model NM-25T		E-28	68
Singer Instrumentation, Model NM-37/57		E-28	69
Singer Instrumentation, Model NM-17/27		E-28	70
Southwick, R. A.	Jun 1974	E-28	73
Southwick, R. A.	May 1975	E-29	74
Southwick, R. A.	May 1976	E-29	75
Stoddart Electro-Systems NM-30A		E-31	83
Stoddart Electro-Systems, NM-52A		E-32	84
Wood, P.	Jul 1973	E-33	91

2.11 Standards and Specifications

Author	Document Date	Page No.	Item No.
Institute for Electrical and Electronic Engineers (IEEE)	Oct 1966	E-18	37

International Special Committee on Radio Interference (C.I.S.P.R.) Publication 9	1966	E-19	40
International Special Committee on Radio Interference (C.I.S.P.R.) Publication 1	1961	E-18	38
International Special Committee on Radio Interference (C.I.S.P.R.) Publication 1a	1966	E-19	39
Lucia, F. et al.	Apr 1976	E-20	44
Maruvada, P. S. and Trinh, N. G.	Sep/Oct 1975	E-21	46
Pearlson, C. B.	Apr 1967	E-23	53
Shepherd, R. A. et al.	Oct 1974	E-25	61
Shepherd, R. A. et al.	Jul 1976	E-27	65
Shepherd, R. A. et al.	Aug 1977	E-27	66
Society of Automotive Engineers (SAE)	Feb 1974	E-28	71

2.12 Bibliographies and Miscellaneous

Author	Document Date	Page No.	Item No.
Adams, J. W. et al.	Aug 1977	E-9	1
Disney, R. T. et al.	Nov 1971	E-15	26
Gillilland, K. E.	Apr 1975	E-17	31
Schwartz, M. et al.	1966	E-24	57
Spaulding, A. D. et al.	May 1975	E-30	80
Systems Technology Associates	Mar 1975	E-32	85
Weibull, W.	Sep 1951	E-32	88
Whalen, A. D.	1971	E-33	89

3. ANNOTATED BIBLIOGRAPHIC REFERENCE GUIDE

1. Adams, J. W., M. Kanda, J. Shafer, and Y. Wu, August 2-4, 1977, Near-Field Electric Field Strength Levels of EM Environments Applicable to Automotive Systems, IEEE International Symposium on Electromagnetic Compatibility, Seattle, Washington.

This paper presents the results of electric field strength measurements for the near-field inside and outside a passenger vehicle and a tractor-trailer vehicle. These measurements were made with all common combinations of mobile transmitters and antennas. The RF transmitting sources used the maximum legal output power (110 watts) at 40, 162, and 416 MHz, and nominal 100-watt power levels in the HF band (3-30 MHz). Data are presented for fields of vehicles on normally conducting surfaces, such as concrete and asphalt as well as on metal ground screens. The results of the electric field strength measurements in the near-field regions of fixed, high-power transmitters are also reported in this paper. These sites include AM, FM, TV broadcast stations, and high-power military and FAA fixed transmitters.

2. Akima, H., et. al., August 1969, Required Signal-to-Noise Ratios for HF Communication Systems, August 1969, ESSA Technical Report ERL 1 31-ITS 92.

This report identifies the estimated required signal-to-noise ratios (S/N) for the following HF communication systems: amplitude modulation (AM) voice communication systems, noncoherent frequency shift keying (NCFSK) radio teletypewriter systems, composite voice and teletypewriter systems, aural-reception radio telegraphy, and phototelegraphy. The S/N for these systems were derived for nonfading conditions, fading conditions without diversity, and fading conditions with diversity.

3. Akima, Hiroshi, March 1972, A Method of Numerical Representation for the Amplitude Probability Distribution of Atmospheric Radio Noise, Telecommunication Research and Engineering Report 27, U. S. Department of Commerce, Office of Telecommunication.

This report presents a method for numerically representing the APD function of atmospheric radio noise for a specified V_d value. It presents two computer subprograms that implement this method.

4. Akima, H. and A. D. Spaulding, August 1977, Development of a Computer Simulation Model for Analyzing Performance of Communication Systems, 1977 IEEE International Symposium on Electromagnetic Compatibility, 77CH 1231-0 EMC, pp. 47-52.

A digital-computer simulation model for analyzing performances of some communication systems has been developed for the purpose of studying the effects of interfering signals, noise and/or distortions on various communication systems. Development of the model is largely based on the analogy with the laboratory tests of communication system performances.

The model consists of computer subprograms, each of which either simulates a basic component of communication systems or calculates characteristics of a component. An introductory explanation of computer simulation, guidelines for developing a simulation model, and an outline of the model are presented.

5. American Electronic Laboratories, Amplitude Distribution Measurement Instrument, Technical Report 1020-2, P. O. Box 552, Lansdale, Pa. 19446.

This report describes an amplitude distribution (AD) measurement instrument. Also included in the report are examples showing the AD instrument's implementation.

6. Arthurs, E., and H. Dym, December 1962, On the Optimum Detection of Digital Signals in the Presence of White Gaussian Noise - A Geometric Interpretation and a Study of Three Basic Transmission Systems, IRE Transactions on Communications Systems, Vol CS-10, No. 4, pp 336-372.

This paper considers the problem of optimally detecting digital waveforms in the presence of additive white Gaussian noise. A technique for representing the transmitted signals and the additive noise leading to a geometric interpretation of the detection problem is presented on a tutorial level. Subsequently, this technique is used to derive the optimum detector for each of the three basic data transmission systems: M-level phase-shift keying (PSK), M-level amplitude-shift keying (ASK), and M-level frequency-shift keying (FSK). Corresponding probability of error curves are derived, compared, and discussed with reasonable detail.

7. Baran, Daniel E., October 1976, Prediction of Relative Available Noise Power for Vehicular Ignition Noise, Electromagnetic Compatibility Analysis Center, ESD-TR-76-007, Final Report.

This report describes a high frequency radio noise model which was developed for predicting average received electromagnetic noise (EMN) levels from a number of vehicles traveling on a roadway. This model is an extension of a model previously developed by A. D. Spaulding of the Department of Commerce. Measurements of the EMN level variations with respect to the vehicular make, distance, frequency, orientation of the vehicle, number of cylinders, and engine RPM were made on a number of individual vehicles, and these measurements were supplemented with measured ignition noise data from similar published studies. This information was used for assessing and determining relationships for the model developments.

8. Beerling, C. W., Ignition Noise Effects on Land Mobile Communications Receivers, January 1971, Paper 710029, presented at SAE Automotive Engineering Congress, Detroit, Michigan.

Autobile ignition noise effects on land mobile communications receivers are a function of engine rpm, the antenna position relative to the vehicle, and the type of spark plugs and wires used in the ignition system. The purpose of this paper is to summarize measurements made on the degradation to receiver sensitivity by ignition noise and to discuss the use of electronic noise suppression. The data presented are restricted to the effects upon a Motorola receiver used in the test. The receiver was tuned to 36 MHz. The data is restricted to a receiver operating at this frequency because the degradation effects are the most severe at that frequency compared to effects on receivers tuned to 150 MHz or 450 MHz. The receiver sensitivity test referred to in this paper is the 20 dB quieting method. This test is a measure of the signal strength required at the receiver antenna input to reduce the noise at the receiver audio output by 20 dB.

9. Bello, Phillip A., September 1965, Error Probabilities Due to Atmospheric Noise and Flat Fading in HF Ionospheric Communication Systems, IEEE Transactions on Communication Technology, Vol COM-13, No. 3, pp 266-279.

This paper presents analytical expressions for the binary error rate for FSK and PSK communications systems in atmospheric noise and fading environments. It is demonstrated that the error rate depends on the atmospheric noise in the various diversity receivers only through a single composite noise variable equal to the sum of the detected noise powers of the outputs of identical diversity receiver filters. At large S/N and L^{th} order diversity the error rate is shown to be proportional to the reciprocal of the S/N raised to the Lth power. This paper also presents simple expressions showing the system degradation resulting from the presence of atmospheric rather than Gaussian noise.

10. Bolton, E. C., August 1972, Simulating LF Atmospheric Radio Noise and Comparative Characteristics of Man-Made Atmospheric Radio Noise at 60, 76, and 200 kHz, Office of Telecommunication Technical Memorandum 97, U. S. Department of Commerce, Office of Telecommunication.

This report provides a comparative analysis of atmospheric radio noise and man-made radio noise. Additionally, the report describes the detailed circuitry incorporated in the construction of an atmospheric radio noise digital simulator in the 60, 76, and 200 kHz range.

11. Bolton, Earl C., August 1974, Simulating Atmospheric Radio Noise at 60 kHz, 200 kHz, and 5 MHz, Office of Telecommunication Technical Memorandum 74-177, U. S. Department of Commerce, Office of Telecommunication.

This report describes in detail the methodology and associated hardware to simulate atmospheric radio noise at 60 kHz, 200 kHz, and 5 MHz. Magnetic tape recordings were made of atmospheric radio noise from low frequency through high frequency. The recordings were computer analyzed

and were used as a model for the design of the atmospheric noise simulator. Schematics showing the functional digital networks of the simulator are included.

12. Brayer, Kenneth, October 1971, Error Correction Code Performance on HF, Troposcatter, and Satellite Channels, IEEE Transactions on Communication Technology, Vol CS-10, No. 4, pp 781-789.

This paper presents four forward error correction techniques and their performance compared on several real channels. Techniques of both adaptive and nonadaptive black and convolutional coding are examined. The Golay code is considered in a random error correcting mode and in an adaptive burst random mode. The codes are evaluated and compared on three channels: a transcontinental HF 4800 bit per second (b/s) channel between San Diego, California, and Bedford, Massachusetts; a mixed wireline microwave troposcatter 2400 b/s channel dominated by a 583-mile troposcatter hop; and a 2400 b/s satellite communications circuit from Ascension Island to Andover, Maine, with wireline transmission from Andover, Maine, to Greenbelt, Maryland.

13. Bronaugh, Edward L., and Donald R. Kerns, July 13, 14, 15, 1976, Characterization of Single Vehicle Ignition Noise at 4 GHz and Related Susceptibility Analysis of a Satellite Receiving System, IEEE International Symposium on Electromagnetic Compatibility Symposium Record, Shoreham Americana Hotel, Washington, D. C.

This paper describes the methodology and results of measurements performed to characterize the radiated emissions from a modern automobile V-8 ignition system. The overall radiated pulse shape and frequency distribution are described. Sample calculations are performed to determine the effect of these emissions on a 500-MHz communications channel in the frequency band 3.7-4.2 GHz. The overall pulse shape can be best described by a decaying exponential. For frequencies greater than 1 kHz, the pulse produced a continuous monotonically decreasing frequency distribution which has a slope of 6 dB per octave. The resultant spectral amplitude distribution in the 500-MHz band between 3.7-4.2 GHz is nearly flat. The time domain representation of the signal present in the 500-MHz bandwidth between 3.7-4.2 GHz is a critically damped exponential pulse with a rise time of 0.37 nanosecond and a fall time on the order of 2.1 nanoseconds. Measurements to determine the coupling effects of ignition emissions to a satellite earth station 42-foot full performance antenna are described. The results of these measurements show that the antenna, in its near field, has a very small effective area.

14. Churchill, Robert Bruce, October 1975, Modeling the Relative Amplitude Probability Distribution of Power Line Noise, Electromagnetic Compatibility Analysis Center, ESD-TR-75-019.

This report describes the APD analytical method for predicting the effects of interference from power lines on the combination R-1051 receiver and AN/VRA-17 modem. Empirical verification of this model for the case of a high frequency (HF) digital receiver system operating in presence of powerline noise is provided.

15. Churchill, R. Bruce, July 1976, Prediction of Relative Available Noise Power for Power-Line Radio Noise, Electromagnetic Compatibility Analysis Center, ESD-TR-76-006, Final Report.

This report describes models that can be used to predict the available noise power $(Fa)_{std}$, relative to receiver thermal noise, that would be received by a standard lossless measurement antenna in the presence of an isolated power-line noise source. Separate models are presented for extremely high voltage, high voltage, and low voltage power lines. Model predictions are compared with measured data.

16. Churchill, R. B., September 1977, Naval Shore Electronics Criteria: Man Made Noise, Second Edition, Final Report, ESD-TR-77-004, Contract F-19628-76-C-0017, Electromagnetic Compatibility Analysis Center, North Severn, Annapolis, Maryland 21402.

This is a handbook documenting step-by-step procedures to predict the degradation effect on a representative HF digital receiver system composed of the R-1051/URR receiver and AN/URA-17 modem operating in environments of power line and auto ignition noise. This report is a revised edition of an earlier handbook; it includes new information on receiver system environments of composite, atmospheric, and galactic noise. A discussion of the handbook capabilities and applications is also presented.

17. Cohen, Dr. David J., October 1972, A Statistical Ignition Noise Model, Electromagnetic Compatibility Analysis Center, ECAC-PR-72-041, Project Report.

This report presents a model for the APD of ignition noise as a function of a specific road geometry. Two types of ignition noise models are identified: (1) equal source model and (2) the variable amplitude model. The APD for both models is for a long time period when samples are made on a number of vehicles.

18. Cook, J. H., June 1977, Quasi-Peak to RMS Voltage Conversion, 2nd EMC Symposium on Electromagnetic Compatibility, Montreux, 77CH1224-5EMC, pp. 407-412.

A technique is presented by which the conversion between quasi-peak and rms voltage levels may be made for any noise process for which the relative amplitude probability distribution is known. The technique is not exact, since it requires that the time waveform of the quasi-peak voltage be constant. The resulting error seems to be small for many

cases, however. Several examples of the technique are given and compared with measurements. An analysis is also presented of the effect of the constant quasi-peak voltage requirement on the error.

19. Crichlow, W. Q., A. D. Spaulding, C. J. Roubique, and R. T. Disney, 1960b, Amplitude Probability Distributions for Atmospheric Radio Noise, National Bureau of Standards Monograph 23.

     This paper identifies the APD for atmospheric radio noise. The APD curves were developed from recorded noise envelope data taken at different points around the world.

20. Crichlow, W. Q., C. J. Roubique, A. D. Spaulding, and W. M. Beery, 1960a, Determination of the Amplitude Probability Distribution of Atmospheric Radio Noise from Statistical Moments, J. Research NBS 64D (Radio Propagation) No. 1, 49.

     This paper identifies and describes an empirically derived graphical method of obtaining the amplitude probability distribution of atmospheric noise from the measured statistical moments of this noise-average power, average voltage, and average logarithm of voltage. Possible errors in and the magnitudes of these moments are discussed.

21. Crippen, L. J., D. D. Stewart, and J. W. Engles, November 1970, Program for Controlling the Effects of Radio Noise and Improving Telecommunication System Effectiveness, Proposal for the Department of the Navy.

     This program proposal discusses the specific circumstances requiring radio noise measurements and the factors that determine the usefulness of the noise measurements in solving telecommunication problems. A description of the interference environment is presented as background material. Deficiencies in existing criteria are explained. This proposal presents suggested approaches for improving radio systems' operational effectiveness, protecting the Navy's investment in real estate and equipment, and reducing operating costs. Applications of this proposal are discussed.

22. Cron, Edwin L., November 1974, Confidence Limits for Digital Error Rates, Office of Telecommunication Report 74-51, U. S. Department of Commerce, Office of Telecommunication.

     In this report, confidence limits for error rates (probabilities of an error) of digital communication systems are derived and implemented under the assumptions that the error rate is constant and the trials are independent. Four types of samples are considered: prescribed sample size (binomial sampling), prescribed number of errors (inverse binomial sampling), both sample size and number of errors bounded (truncated binomial sampling), and truncated binomial sampling with sample size also bounded below. Both exact confidence limits and good approximations for

them in the communications situation of very small error rates are presented. Point as well as interval estimates are presented. The planning of the experiment is discussed.

23. Deitz, J., F. Lucia, and M. Liebman, August 1974, Degradation of Mobile Radio Reception at UHF and VHF, Due to the Effects of Automobile Ignition Systems and Multipath Propagation, FCC, PB-234 216.

This report presents data showing the degrading effects of man-made noise and multipath path in VHF and UHF communication systems. Specifically, this report is concerned with the degradation effects in a mobile vehicle for communications equipment operating at 37.5 MHz, 153.185 MHz, and 459.4 MHz.

24. Deitz, J., F. Lucia, and M. Liebman, June 1975, Degradation of Base Station Radio Reception at UHF and VHF Due to the Effects of Automobile Ignition Systems and Multipath Propagation, Report No. RS75-05, Federal Communications Commission, Washington D. C.

This report presents the results of measurements of degradation caused to base station land mobile radio systems by ignition noise and by multipath. Several frequencies were used from 37 MHz to 950 MHz. The authors discuss supernoisy vehicles and attempt to identify the supernoisy vehicles by type.

25. Disney, R. T., and A. D. Spaulding, February 1970, Amplitude and Time Statistics of Atmospheric and Man-Made Radio Noise, ESSA Technical Report ERL 150-ITS 98.

This report presents man-made noise data given in the form of tables and plots of APD, pulse duration distributions, pulse spacing distributions, and average crossing rates. The amplitude variations within 200-millisecond noise samples are shown and discussed. Measured noise levels in rural areas are compared with the curves prepared for JTAC (1968) and CCIR (1964). Information is presented on the mathematical modeling of the noise process.

26. Disney, R. T., R. J. Matheson, and A. D. Spaulding, November 1971, Radio Noise Measuring and Analysis Facility, U. S. Department of Commerce, Office of Telecommunication, Institute for Telecommunication Sciences.

This report provides a general overview of the radio noise measuring and analysis facility located at the Institute for Telecommunication Sciences, Boulder, Colorado. This report identifies the facility's capabilities in the areas of measurement, analysis, and data base compilation.

27. Electromagnetic Compatibility Analysis Center, June 1977, An Improved Approach to Man-Made Noise Measurement Techniques, Technical Note, ECAC-TN-77-013.

This technical note presents a brief description of measurements conducted on various noise sources for different receiver bandwidths. Data are presented in graphical and tabular form and the results showed the level differences of peak, rms, and average receiver noise voltage as a function of receiver bandwidth. The term "knee bandwidth" is defined for reference.

28. Fairchild, Electro-Metric Corporation, Interference Analyzer Model EMC-25, Mark II Version, 14 kHz-1 GHz.

This technical bulletin presents a description of the Model EMC-25 Interference Analyzer which is used in the 14 kHz to 1 GHz frequency range. Some of the electrical characteristics identified in the bulletin are dynamic range and bandwidth ratio.

29. Gillilland, Kitt E., and Thomas A. Brewer, January 1974, Experimental Verification of Ignition Noise APD Model and Digital Receiver Bit Error Probability Model, Electromagnetic Compatibility Analysis Center, ESD-TR-73-006, Final Report.

This report describes the experiment which was used to verify the computer model that predicts the relative APD of ignition noise for cases of vehicles moving along a straight road and for stationary vehicles. A digital receiver system performance model, designed to predict bit error probability for the binary FSK receiver system with frequency detection and post detection integration, is also verified. An R-1051/URR receiver with an AN/URA-17 model is subjected to automobile ignition noise to obtain the measurements for these verifications.

30. Gillilland, Kitt E., December 1972, Models of Nondiversity Digital Receiver Performance in General Noise, Electromagnetic Compatibility Analysis Center, ESD-TR-72-295, Technical Report.

This report documents theoretical nondiversity degradation models which predict bit error probability for five types of digital receivers. The five types of digital receivers included are coherent phase-shift keying, coherent on-off keying, coherent frequency-shift keying, noncoherent frequency-shift keying, and binary frequency-shift keying with frequency-detection and post-detection integration. These models were formulated as part of an Electromagnetic Compatibility Analysis Center (ECAC) project on man-made noise. The required inputs to each model are (1) a statistical description of the noise output from the receiver predetection filter, (2) the available noise power, measured with respect to available thermal noise power in the bandwidth of the receiver predetection filter, (3) the available signal power, and (4) receiver parameters available from manufacturers' specifications. The first input could, if necessary, be obtained from measurement but usually would be obtained from a statistical noise model of the noise source of concern. Depending upon the application, the second input would be obtained either from an available noise power model which operates from a data base library file of noise source electrical characteristics or from measurement. The third input could be obtained from standard propagation computations.

31. Gillilland, Kitt E., April 1975, The Navelex Man-Made Radio Noise
        Program, Electromagnetic Compatibility Analysis Center, ESD-TR-
        75-007 Final Report.

    This report provides a brief description of the overall man-made
radio noise program at the Naval Electronics Systems Command. The dis-
cussion includes the types of models which are used in the description
of noise, the receiver, and associated antenna. A flow diagram showing
the relationships of these models for predicting the performance of com-
munications systems is provided.

32. Halton, J. H., and A. D. Spaulding, October 1966, Error Rates in
        Differentially Coherent Phase System in Non-Gaussian Noise,
        IEEE Transactions on Communication Technology, Vol COM-14,
        No. 5, pp 594-601.

    This paper presents a theoretical analysis of the DCPSK system acting
under a wide range of noise and signal conditions. In addition to the ele-
mental error rate, the paper includes error rates for sequences of errors.
Examples of BER curves are given for Gaussian noise and the characteristic
sample of atmospheric noise. Results for constant and slow flat Rayleigh
fading signal for the two- and four-phase systems are given, and compari-
sons of experimental results with the theoretical error rates are made.

33. Hartley, Harry F., 30 October 1967, Analysis of the Performance of
        CPSK and CSK in Atmospheric Noise, DECO Communications Depart-
        ment, Defense and Space Center, Westinghouse Electric Corpora-
        tion.

    This report presents an analysis of the performance of CPSK and CSK
in the presence of impulsive atmospheric noise.

34. Hartman, W. J., June 1977, Objective Performance Measures for Voice
        Systems, 2nd EMC Symposium on Electromagnetic Compatibility,
        Montreux, 77CH1224-5EMC, pp. 521-524.

    This paper presents a discussion of two studies on the use of linear
predictive coding (LPC) techniques for deriving an objective measure of
intelligibility over voice communications channels. The first study is a
feasibility study, and the second study an extension of this. The tech-
niques used in the two are similar, but the detailed differences are sig-
nificant. The results of the feasibility study support the suitability
of LPC techniques for the objective measurement of intelligibility.

    Because of the time and expense involved in making subjective mea-
surements over voice channels, an objective measurement technique is
desired. Such a technique should relate to the subjective scoring. This
study has examined the feasibility of using an analysis of the same data
used for subjective scoring. The results given here, although hampered
by a small data base with some inherent inaccuracies, indicate that the

objective measure developed here can be used as a predictor of subjective scores. New studies also support this conclusion.

Methods for eliminating the major problems encountered with the data have been tested and found adequate.

35. Hawthorne Jr., G. B., W. B. Jones Jr., and W. W. Wright, 1 June 1959, Performance of Communication Systems in the Presence of Interference, Engineering Experiment Station of the Georgia Institute of Technology, Final Report-Vol I, Project No. A-345, Contract No. AF30(602)-1789, Rome Air Development Center AD No. 227176.

This report contains data resulting from laboratory experiments performed at Georgia Tech, and a brief statistical summary of similar data obtained by other agencies. Data pertaining to both voice and digital systems are included. More attention is given to voice systems, since the art of predicting the amount of (interference produced) degradation in performance for these systems is less well developed than for digital systems. In addition, the report contains some general comments on the interference problem and recommendations for future work.

36. Hsu, H. P., R. M. Storwick, D. C. Schlick, and G. L. Maxam, May 1974, Measured Amplitude Distribution of Automotive Ignition Noise, IEEE Transactions on Electromagnetic Compatibility, Vol EMC-16, No. 2, pp 57-63.

This paper describes a series of tests conducted to statistically characterize the amplitude distribution of automotive ignition noise and determine whether such test results can be reproduced. Some tests show the amplitude distribution to be Weibull and others indicated a log normal distribution. However, under controlled conditions the results obtained from an individual vehicle were quite repeatable.

37. IEEE Trans. Veh. Commun., October 1966, Measurement of Radio Noise, Generated by Motor Vehicles, and Affecting Mobile Communications Receivers in the Frequency Range 25 to 1000 Mc/s, IEEE Standard 263, Vol. VC-15, pp. 67-72.

The purpose of the standard is to provide a uniform method of measurement of radio noise generated by a motor vehicle, which may affect the performance of mobile communications receivers in the vehicle. The standard describes specifications for a particular antenna type and for a peak detector.

38. International Special Committee on Radio Interference (C.I.S.P.R.), 1961, Publication 1, Specification for C.I.S.P.R. Radio Interference Measuring Apparatus for the Frequency Range 0.15 Mc/s to 30 Mc/s.

This specification presents the requirements for designing a quasi-peak type of voltmeter which can be used to measure radio interference

for the frequency range 0.15 Mc/s to 30 Mc/s. Some of the fundamental electrical characteristics identified in this specification are bandwidth, electrical charge and discharge time constraints and overload factor.

39. International Special Committee on Radio Interference (C.I.S.P.R.), 1966, Publication 1a, First Supplement to C.I.S.P.R. Publication 1 (1961), Specification for C.I.S.P.R. Radio Interference Measuring Apparatus for the Frequency Range 0.15 MHz to 30 MHz.

This supplement presents the special requirements that have to be met in the measurement of terminal noise voltages and field generated by industrial, scientific, and medical equipment and high voltage transmission lines and associated plant equipments. Some of the electrical characteristics identified in this supplement are frequency range, background noise level and measuring impedance.

40. International Special Committee on Radio Interference (C.I.S.P.R.), 1966, Publication 9, C.I.S.P.R. Limits of Radio Interference and Report of National Limits.

This publication presents the C.I.S.P.R. limits of radio interference and the national limits of radio interference for various countries. Limits are stated in microvolts (μV) as a function of frequency in megahertz (MHz).

41. International Telecommunication Union, World Distribution and Characteristics of Atmospheric Radio Noise, C.C.I.R. Report 322, Geneva, Switzerland.

This report identifies and presents values of atmospheric noise power and of other noise parameters which are used to evaluate the probable performance of a radio link. Noise data are given in terms of 3-month intervals for selected stations in the northern and southern hemispheres. This report includes examples which facilitate its use and understanding.

42. Kerns, Donald R., Edwin L. Bronaugh, and Roger A. Southwick, October 1975, An Amplitude Probability Distribution Detector System, IEEE 1975 Electromagnetic Compatibility Symposium Record, pp 6BIc1-6BIc4.

This paper describes an amplitude probability distribution detector that is used in conjunction with an electromagnetic interference (EMI) receiver. The detector is easy to use, small in size, reasonable in cost, and compatible with most standard EMI measurement equipment that employs a logarithmic intermediate frequency (IF) system.

43. Lauber, W. R. and J. M. Bertrand, June 1977, Preliminary Urban VHF/ UHF Radio Noise Intensity Measurements in Ottawa, Canada, 2nd EMC Symposium on Electromagnetic Compatibility, Montreaux, 77CH1224-5EMC, pp. 357-362.

Measurements of the VHF/UHF radio environment were carried out over a 17 day period in November 1976 at four sites in downtown Ottawa. The radio noise parameters, F_a (the available noise power spectral density) and V_d (the voltage deviation) which both relate directly to the performance of communication systems, were measured. The measurements tested the feasibility of using commercially available equipment to make such measurements. The F_a values were computed for a discone antenna which is different from the short vertical monopole usually used in measurements of the radio environment. The results compare favorably with those published in the literature. The dominant noise source for frequencies between 160 and 500 MHz is automobile ignition noise.

44. Lucia, F., M. Liebman, D. Desrosiers, April 1976, Motor Vehicle Ignition Radiation with Respect to the SAE Radiation Standard J551c, Report FCC/OCE RS 7603, Federal Communications Commission, Washington, D. C. 20554.

Previous reports (FCC/OCE RS 75-05 and R-7302) which were based on subjective testing under common, real-life traffic conditions, have shown that degradation to reception exists in the land mobile radio services due to the radiation from ignition systems of motor vehicles. The purpose of this report was to determine on an individiual basis the percentage of vehicles in a large sample size that exceeded the SAE J551(c) standard, and which vehicles caused degradation to land mobile reception.

Ten thousand vehicles were measured at each test frequency, 50 MHz and 153 MHz, as each vehicle passed the measurement site located on a single-lane ramp connecting two interstate highways. Data were obtained to answer the following questions about each vehicle.

1. Was the vehicle's radiation above the industry's voluntary limit?

2. Was the signal quality degraded by the vehicle's radiation?

3. How long was the degradation present?

4. What was the make and type of the vehicle?

The percentage of vehicles exceeding the SAE radiation limit was 3.6% at 50 MHz and 2.6% at 153 MHz. All of these vehicles caused degradation of at least one quality grade to land mobile reception based on our subjective grading scale. Additionally, 16.3% of the vehicles at 50 MHz and 8.0% of the vehicles at 153 MHz caused degradation of one quality grade or more even though their radiation was below the SAE limit.

45. Matheson, Robert J., November 1970, Instrumentation Problems Encountered Making Man-Made Electromagnetic Noise Measurements for Predicting Communication System Performance, IEEE Transactions on Electromagnetic Compatibility, Vol EMC-12, No. 4, pp 151-158.

This paper describes the inadequacies of commercially available RFI field intensity meters for the measurement of noise as applied to communication system performance. The author recommends that the noise root-mean-square (rms) voltage be measured simultaneously with average voltage and average logarithm of the voltage. These parameters can be used to derive the APD of noise which is the required statistic for predicting communication system performance. An appendix describing hardware solutions to the measurement problems is included.

46. Maruvada, P. S., and N. G. Trinh, Sept./Oct. 1975, A Basis for Setting Limits to Radio Interference from High Voltage Transmission Lines, IEEE Trans. on Power Apparatus and Systems, Vol. PAS-94, No. 5.

Radio interference generated due to corona on transmission line conductors and hardware causes a deterioration in the quality of radio reception in the vicinity of the line, especially in the AM broadcast frequency band. It is therefore necessary, from the point of view of an acceptable line design, to define allowable limits to the RI. From a study of the characteristics of RI from transmission lines and of the factors influencing the quality of AM radio reception, a number of parameters which would best describe the influence of RI on radio reception are identified. On the basis of this study, an approach is suggested in the paper for defining tolerable limits for RI from high voltage transmission lines.

The approach suggested in the paper for defining tolerable limits for RI from high voltage transmission lines may be summarized as:

a. On the basis of local medial signal strength, three regions are defined as high, medium, and low signal level regions;

b. The fair weather RI level of a transmission line should not exceed a value RI_o at a distance D_m from the outer phase of the line, in such a way that class C radio reception is guaranteed at the edge of the right of way of the line;

c. The RI level of the line should be below the value defined above for at least a specified percentage time during a year.

47. Maxam, G. L., H. P. Hsu, D. C. Schlick, and R. M. Storwick, July 25, 1973, Measured Pulse Height Distributions of Individual Engine Cylinder Ignition Noise, Research Laboratories (G. M. Corp.), GMR-1424.

This report describes the measurement of ignition noise pulse height distributions caused by individual cylinders of an automotive ignition system. These distributions are measured by enabling the pulse height analyzer to accept an input only at those times that a particular cylinder is ready to fire. This report presents statistics, in graphical form, of individual cylinder noise.

48. Middleton, D., April 1974, Statistical-Physical Models of Man-Made Radio Noise, Part I: First-Order Probability Models of the Instantaneous Amplitude, Office of Telecommunication Report 74-36, U. S. Department of Commerce, Office of Telecommunication.

This report presents the development of analytically tractable, experimentally verifiable, and statistical physical models for non-Gaussian man-made and natural electromagnetic interference. The interference is described with first-order probability models of the instantaneous amplitude of the noise voltage.

49. Middleton, D., April 1976, Statistical-Physical Models of Man-Made and Natural Radio Noise, Part II: First-Order Probability Models of the Envelope and Phase, Office of Telecommunication Report 76-86, U. S. Department of Commerce, Office of Telecommunication.

This report presents the development of analytical tractable, experimentally verifiable, statistical physical models for non-Gaussian, man-made, and natural electromagnetic interference. Three classes of noise are discussed: Class A (narrowband), Class B (broadband), and Class C (Class A + Class B). First-order statistical models, including the APD and associated probability densities of the noise envelope, were constructed for Class A and Class B. Excellent agreement between theory and experiment is demonstrated for many types of electromagnetic noise, man-made and natural, as shown by a broad spectrum of examples.

50. Oliver, W., September 1964, White Noise Loading of Multichannel Communication Systems, Marconi Instruments, 100 Stonehurst Ct., Northvale, N. J.

This report is a general introduction to the principles of noise and its measurement. Several methods of noise measurement techniques, including noise power ratio (NPR) and crosstalk, are described. Allied measurement techniques, such as out-of-band testing, are also described.

51. Omura, J. K., August 1969, Statistical Analysis of LF/VLF Communication Modems, Special Report 1, DASA-2324, SRI.

This report presents a statistical analysis of typical LF/VLF modems. The report includes basic bit error rate (BER) and S/N relations for these modems.

52. Oranc, H. S., May 1975, Ignition Noise Measurements in the VHF/UHF Bands, IEEE Transactions on Electromagnetic Compatibility, Vol EMC-17, No. 2, pp 54-64.

This paper presents data on noise amplitude distribution measurements which were conducted on ignition systems in the VHF and UHF bands.

The information derived from the noise amplitude distribution is the peak amplitude distribution of the impulses; in addition, the average repetition frequency of the impulses is provided.

53. Pearlson, Jr., C. B., April 1967, Historical Analysis of Electromagnetic Interference Limits, Air Force Report No. SSD-TR-67-127, Contract No. AF 04-(695)-1001.

This paper examines the development of interference and susceptibility limits in various military specifications indicating the technique by which the limits were derived, the rationale for such derivation, and the changes in various limits with time since their original formulation. It discusses certain inconsistencies within and among the limits of the various specifications.

54. Richard Brancker Research Ltd, V_{rms} and V_d Converter Model 895, Richard Brancker Research Ltd, 27 Monk Street, Ottawa, Canada K1S3Y7.

This brochure presents a description of the Model 895 V_{rms} and V_d converter measurement instrument. Some of the electrical characteristics identified in the brochure are crest factor, V_{rms} range and V_d range.

55. Rosa, A. J., October 1970, HF and VHF Automobile Ignition Measurements, 1970 IEEE Regional Electromagnetic Compatibility Symposium Record, 70C64-REGEMC.

Experiments conducted in San Antonio, Texas, using United States Air Force (USAF) equipments, showed that approximately one vehicle in five, of the over 3,000 measured, radiated with sufficient signal strength to cause interference to sensitive receiving equipment located nearby. Most important, the frequency response of automobile ignition in HF was found to peak at about 20 MHz and alternate sharply below about 18 MHz whereas there was a gradual reduction in field strength with increasing frequency above the peak frequency.

Conclusions state that auto ignition radiation is a source of interference to receiving systems above about 10 to 15 MHz depending on system sensitivity, proximity, and shielding to vehicular thoroughfares. Below about 20 MHz, powerlines become the major interference problem and should be treated in a similar fashion. It would be unwarranted to remote a facility to avoid automobile ignition interference beyond the point where the minimum expected atmospheric noise equals the ignition noise. Hence, in siting a facility all aspects of man-made and natural interference should be considered prior to site selection.

56. Schulz, R. B., and R. A. Southwick, May 1974, APD Measurements of V-8 Ignition Emanations, IEEE Transactions on Electromagnetic Compatibility, Vol EMC-16, No. 2, pp 63-70.

This paper presents APD data for ignition emanations from V-8 engines of used motor vehicles. Data for both single and multiple engines running at 1500 rpm are recorded on Weibull distribution sheets. Measurements were conducted with an omnidirectional antenna from approximately 20 MHz to 1 GHz. APD distributions are given for various received bandwidths between 1 and 300 kHz on each Weibull sheet.

57. Schwartz, Mischa, William R. Bennett, and Seymour Stein, 1966, Communication Systems and Techniques, McGraw Hill Book Company.

This textbook presents a basic introduction to narrowband noise processes and its effect on various analog and digital communications systems. This textbook discusses methodologies to increase system performance by use of different signal detection techniques.

58. Shaver, H. N., V. E. Hatfield, and G. H. Hagn, May 1972, Man-Made Radio Noise Parameter Identification Task, Final Report, Stanford Research Institute, Contract N00039-71-A-0223.

This report is the final report on the parameter identification task of the NAVELEX man-made noise program. This report includes an analysis and modeling of three modems. System performance calculations were made for these modems with a Markov regime model of man-made noise. The noise parameters necessary for evaluating the system performance were identified. It was observed that quadratic forms of the complex noise envelope could be used to simplify the evaluation and identify the important parameters. The parameters F_a and V_d were required for each modem but were insufficient for evaluating system performance. Needed also were probabilistic measures of the noise and depending upon the modem, frequency- or time-correlation measures of the noise.

59. Shepherd, R. A., J. C. Gaddie, V. E. Hatfield, and G. H. Hagn, February 1973, Measurements of Automobile Ignition Noise of HF, Final Report SRI Project 2051, Contract N00039-71-A-0223, Delivery Order 0003, Stanford Research Institute, Menlo Park, Calif. 94025.

SRI made measurements of automobile ignition noise in direct support of the Electromagnetic Compatibility Analysis Center (ECAC). Tests were conducted at nominal frequencies of 24 and 30 MHz in mid-December 1972 at a quiet field site and at two distances from busy Interstate 280 near Palo Alto, California. At the quiet location, a solitary, stationary, noisy pickup was operated at engine speeds corresponding to idle and cruise, while the ignition noise was used to degrade the performance of a binary FSK modem (AN/URA-17C). Simultaneously, the amplitude probability distribution (APD) of the noise envelope was measured for three bandwidths by using specially developed instrumentation and software. This measurement system consisted of phase-stable receivers with coherent quadrature detectors whose outputs were digitized in real time and recorded on magnetic tape for computer processing. Noise amplitude and phase information was

made available for processing. The measured binary error rates and the APD's were to be used later by ECAC to check an error-rate model. Measurements of the noise power available at the antenna terminals (related by a constant to the noise parameter F_a) and the noise parameter V_d, made by using the SRI sampling system, were compared with those made with a modified Stoddart NM-25T receiver. At the freeway location, the antenna was placed at distances of 52 ft and 137 ft from the nearest traffic lane, and ignition noise measurements (using the SRI noise measurement system) were made to produce the APD of ignition noise near a highway for light traffic (approximately 20 cars per minute) and for heavy traffic (approximately 45 cars per minute). Counts were also made of automobiles passing the site and of ignition noise pulses. It was observed that only about 10% of the cars could be considered noisy in the sense that they caused a significant increase in the ambient noise level.

60. Shepherd, Richard A., August 1974, Measurements of Amplitude Probability Distributions and Power of Automobile Ignition Noise at HF, IEEE Transactions on Vehicular Technology, Vol VT-23, No. 3, pp 72-83.

    This paper describes measurements which were conducted to determine the APD of the envelope of automobile ignition noise between 24-30 MHz. The measurements were conducted at a quiet site where several single stationary vehicles were operated at engine speeds corresponding to idle and cruise. Measurements were also made at two distances near a freeway, for light traffic (approximately 20 vehicles per minute) and for heavy traffic (approximately 45 vehicles per minute). The report presents computer plotted APD's on Rayleigh paper in dB relative to thermal noise for these measurements.

61. Shepherd, R. A., J. C. Gaddie, and D. L. Nielson, October 1974, Variability in Measurement Procedures for Ignition Noise, Final Report, Stanford Research Institute, Motor Vehicle Manufacturers Association Agreement Number SRI-7404-C2.10 (available from NTIS, PB244533).

    This report presents a study of the SAE Standard J551c, Measurement of Electromagnetic Radiation from a Motor Vehicle or Other Internal-Combustion-Powered Device (Excluding Aircraft) (20-1000 MHz). This study was performed to determine whether portions of this standard are open to misinterpretation or may be imprecise enough that allowable differences in measurement setups or procedures could lead to variability in the results. In addition to a section-by-section critique of the measurement standard, this report details a number of experiments and analyses to determine what variability might be obtained through various usages of the antenna and configurations of the test site allowable under the standard.

62. Shepherd, Richard A., James C. Gaddie, and Aki Shohara, June 1975, Measurement Parameters for Automobile Ignition Noise, Stanford Research Institute, MVMA Agreement Number SRI 7502-C2.10, Final Report (available from NTIS, FB247766).

This report presents the results of literature survey and study to determine whether three of the more common methods for measuring man-made radio noise actually provide information useful for estimating the degradation to the more important communication services. The advantages and disadvantages of peak, quasi-peak and noise amplitude distribution (NAD) measurements are discussed in detail. Ideal and practical modeling methods are discussed for determining the effect of ignition noise upon communication systems, with emphasis on voice communications.

63. Shepherd, R. A., J. C. Gaddie, and D. L. Nielson, February 1976, New Techniques for Suppression of Automobile Ignition Noise, IEEE Transactions on Vehicular Technology, VT-25, No. 1 (The paper was based on a report to the FCC, by the same authors, Improved Suppression of Radiation from Automobiles Used by the General Public, Contract FCC-0072, available from NTIS, Springfield, Va. 22161, Accession Number PB 239-471.)

This paper presents new techniques for the suppression of automobile ignition noise. The intent of the work was to take an individual vehicle, already suppressed by the techniques used in mass production at the time in the United States, and to improve the suppression by at least 10 dB over the frequency range 30-500 MHz.

64. Shepherd, Richard A. and James C. Gaddie, April 1976, Measurements of the APD and the Degradation Caused by Power Line Noise at HF, Stanford Research Institute, Contract N00039-74-0077, Final Report.

The report presents the results of measurements of electromagnetic noise from power lines which were made by Stanford Research Institute (SRI) in direct support of the Electromagnetic Compatibility Analysis Center (ECAC) in their work in the Naval Electronic System Command (NAVELEX) man-made radio noise program. Tests were conducted at 3 MHz in the late spring of 1975 in the vicinity of three power transmission lines (two at 230-kV and one at 115-kV) expected to be sources of corona noise and three low-voltage power distribution lines expected to be sources of gap noise. The power-line noise was used to degrade the performance of a binary FSK modem (AN/URA-17). Simultaneously, the amplitude probability distribution (APD) of the noise envelope was measured in three bandwidths, and in the unused channel of the URA-17, using specially developed instrumentation and software. This instrumentation samples and digitizes the noise envelope from each receiver at a rate of 200 samples per second and records these samples on magnetic tape. A computer processes the noise samples to calculate the rms noise voltage (V_{rms}), (which is convertible to the effective antenna noise factor F_a), the parameter V_d, and the APD. The V_{rms} and V_d measurements were compared with those from a Singer NM-26T receiver. Photographs of both gap and corona noise envelope voltage were made in several bandwidths. Corona noise measurements were made in weather conditions ranging from no rain to heavy rain.

65.   Shepherd, Richard A., James W. Engles, and George H. Hagn, July 1976, Automobile Ignition Noise and the Supernoisy Vehicle, IEEE International Symposium on Electromagnetic Compatibility, 76-CH-1104-9 EMC, pp 403-412.

This paper presents measured data on vehicular noise at different frequencies and on different vehicles. Data were taken with a modified Singer NM-25T noise meter. This paper provides a graphical comparison of measured data on vehicular noise and attempts to define the term "supernoisy" vehicle.

66.   Shepherd, R. A., J. C. Gaddie, and P. J. Bell, August 1977, Electromagnetic Radiation Statistics at 50 MHz and 153 MHz of the United States Vehicle Population, Final Report for Motor Vehicle Manufacturers Association, MVMA Agreement Number SRI-7706-C2.10, SRI International, Menlo Park, California 94025.

In mid-1977 the electromagnetic noise from the ignition systems of more than 11,000 individual vehicles in service in four states in the United States was measured at 50 MHz and at 153 MHz simultaneously. The measurement technique (the choice of antenna distances and heights, and so on) was meant to yield, as closely as possible, the results that would have been obtained for stationary-vehicle measurements according to the measurement standard SAE J551c. Nationwide, about 7.1% and 7.9% of the vehicles in service exceed the recommended limit of SAE J551c at 50 MHz and 153 MHz, respectively. The median noise level is about 15 dB below the SAE-recommended limit.

Approximately 100 vehicles with noise exceeding that limit at 50 MHz were examined. Of the domestic vehicles in this group, 70% had had noticeable changes to their ignition systems, and half of those had had suppressive components removed.

Twelve noisy vehicles were chosen to have their ignition noise suppression components restored to their original condition. When owner-removed suppressive components had been restored, the ignition noise of these 12 vehicles dropped by 10 to 20 dB throughout SAE J551c's frequency range (20-1000 MHz).

67.   Shohara, A., June 1977, Modeling Quasi-Impulsive Noise as Modulated Gaussian Processes, 2nd EMC Symposium on Electromagnetic Compatibility, Montreux, 77CH1224-5EMC, pp. 363-367.

A new model of quasi-impulsive noise having the form of a modulated Gaussian random process is presented. The impulsive modulation of the model is a modified lognormal random process. This model is appropriate for impulsive noise having an envelope probability distribution whose tail is approximately lognormally distributed. A comparison of the model with measured VLF atmospheric noise data is presented.

68. Singer Instrumentation, Data Bulletin RFI-100, Radio Interference and
        Field Intensity Analyzer, Model NM-25T, 150 kHz-32 MHz.

        This technical bulletin presents a description of the Model NM-25T
Radio Interference and Field Intensity Analyzer which is used in the 150
kHz to 32 MHz frequency range. Some of the electrical characteristics
identified in this bulletin are voltage measurement range (dynamic range),
undesired response rejection, RF input VSWR and RF input impedance.

69. Singer Instrumentation, Data Bulletin RFI-103B, EMI/Field Intensity
        Meter, Model NM-37/57, 30 MHz-1 GHz.

        This technical bulletin presents descriptions of the Model NM-37/57
EMI/Field Intensity Meters which are used for the 30 MHz-1 GHz frequency
range. Some of the electrical characteristics identified in this bulletin
are voltage measurement range (dynamic range), undesired response rejec-
tion, RF input VSWR, and RF input impedance.

70. Singer Instrumentation, Data Bulletin RFI-104B, EMI/Field Intensity
        Meter, Model NM-17/27, 10 kHz-32 MHz.

        This technical bulletin presents descriptions of the model NM-17/27
EMI/Field Intensity Meters which are used for the 10 kHz to 32 MHz fre-
quency range. Some of the electrical characteristics identified in the
bulletin are voltage measurement range (dynamic range), undesired response
rejection, RF input VSWR and RF input impedance.

71. Society of Automotive Engineers, Inc., February 1974, Measurement of
        Electromagnetic Radiation From a Motor Vehicle or Other Inter-
        nal-Combustion-Powered Device (Excluding Aircraft), (20-1000
        MHz), SAE J551c, 2 Pennsylvania Plaza, New York, N. Y. 10001.

        This standard identifies uniform test procedures and recommended lim-
its to assist engineers in the measurement of electromagnetic radiation
from a motor vehicle or internal-combustion-powered device (excluding air-
craft) to insure spurious radiation does not seriously interfere with
radio frequency (RF) communications and other electronic devices outside
the vehicle.

72. Southwick, Roger A. and Richard B. Schultz, A Method to Evaluate the
        Degradation Effects of Impulsive Interference, Paper, Presented
        at the 1974 International Conference on Communications.

        This paper considers the use of measurements of the APD of random
impulsive signals generated by vehicle ignition systems. The post de-
tected signal is defined in terms of the Weibull distribution parameters
m and k. The prediction of communication degradation effects with the
Weibull distribution parameters is also considered.

73. Southwick, Roger, June 1974, An Investigation of Impulsive Noise
        Signal Measurements.

This paper presents the various aspects of impulsive and radio noise signals and directs attention to the feasibility of simple measurement techniques which could provide a more relevant approach to EMC/RFI measurements.

74. Southwick, Roger A., May 20-22, 1975, An Investigation of Impulsive and Noise Radio Signal Measurements, IEEE 1st Symposium and Technical Exhibition on Electromagnetic Compatibility, Montreux, pp 235-238.

This paper identifies the characteristics of impulsive and Gaussian radio noise signals. This paper also includes examples of simple measurement techniques which can provide a more relevant approach to the definition of noise and its applicability to electromagnetic compatibility (EMC) and radio frequency interference (RFI).

75. Southwick, Roger A., Inventor, 19 May 1976, Amplitude Probability Detector, Patent Description of Invention, Patent Pending.

This patent application provides a system level description of an improved amplitude probability distribution detector to measure radiated electromagnetic noise signals. A block diagram of the detector is included.

76. Spaulding, A. D., C. J. Roubique, and W. Q. Crichlow, November - December 1962, Conversion of the Amplitude Probability Distribution for Atmospheric Radio Noise from One Bandwidth to Another, J. Research NBS 66D (Radio Propagation) No. 6.

This paper presents a method for predicting the APD function of atmospheric radio noise for any specified receiver noise bandwidth. The APD function is interpolated from the movements of the noise measured at a particular bandwidth.

77. Spaulding, A. D., July 1969, System Required Signal-to-Noise Ratios, Lecture No. 29, CU/ESSA Summer Course on HF Ionospheric Radio Propagation, Prediction Methods and Applications, Boulder, Colorado.

This lecture identifies the required S/N for different types of communication systems including differentially coherent phase-shift keying (DCPSK), noncoherent frequency-shift keying (NCFSK), and coherent phase-shift keying (CPSK). These S/N were derived for nonfading conditions, fading conditions without diversity, and fading conditions with diversity.

78. Spaulding, A. D., July 1972, The Determination of Received Noise Levels from Vehicular Traffic Statistics, IEEE 1972 NTC Record, 72CHO 601-5-NTC.

A simple method of determining the received noise power levels from distributions of vehicles is presented. The method takes into account

the statistics of the noise power radiated from individual vehicles and propagation. The statistics of the received noise power are given for arbitrary receiver locations. Comparisons of the calculated received power with measurements are presented also.

79. Spaulding, A. D. and R. T. Disney, June 1974, Man-Made Noise, Part I: Estimates for Business, Residential, and Rural Areas, OT Report 74-38, U. S. Department of Commerce, Office of Telecommunications.

This paper describes an analysis which was performed on a data base of man-made radio noise measurements in the frequency range 250 kHz-250 MHz taken in a number of geographical areas. The analysis of this data base provided estimates of the expected characteristics of man-made radio noise in business, residential, and rural areas. The parameters used are the average available power spectral density, the ratio of the rms to the average voltage of the noise envelope, and the ratio of the rms to the average logarithm of the envelope voltage. The variations of these parameters as a function of frequency, location, and time are shown and discussed. Examples of amplitude and time statistics of the received man-made radio noise process are also shown and discussed.

80. Spaulding, A. D., R. T. Disney, and A. G. Hubbard, May 1975, Man-Made Radio Noise, Part II: Bibliography of Measurement Data, Applications, and Measurement Methods, Office of Telecommunication Report 75-63, U. S. Department of Commerce, Office of Telecommunication.

This report is a compilation of references on man-made radio noise and is divided into five sections: section I, Measurements and Data; section II, Applications to Systems and Mathematical Modeling; section III, Measurement Experiments and Methods; section IV, General; and section V, Atmospheric Radio Noise.

81. Spaulding, A. D. and David Middleton, June 1975, Optimum Reception in an Impulsive Interference Environment, Office of Telecommunications Report 75-67, U. S. Department of Commerce, Office of Telecommunications.

This paper presents David Middleton's recently developed physical-statistical model of impulsive interference as applied to real world communications channels.

The main impulsive interference models that have been proposed to date are summarized and Middleton's model is specified in some detail, giving the statistics required for the solution of signal detection problems. Excellent agreement of these statistics with corresponding measured statistics is shown.

Middleton's model for narrow-band impulsive interference (a subset of the overall model) is applied to a class of optimal signal detection

problems. Optimum detection algorithms are given for coherent and noncoherent binary detection. The three basic digital signaling waveforms are considered; i.e., antipodal, orthogonal, and ON-OFF keying. Performance bounds are obtained for these signaling situations. Since it is known that in order to gain significant improvement over current receivers, the number of independent samples of the received interference waveform must be large, the performance results are given parametrically in the number of samples, or equivalently, the time-bandwidth product. Performance of the current suboptimum receivers is obtained and compared to the optimum performance. It is shown that substantial savings in signal power and/or spectrum space can be achieved.

Since physical realization of the completely optimum detection algorithms cannot, in general, be economically obtained, the corresponding locally optimum or threshold receivers are derived and their performance given. These threshold receiver structures are canonical in nature in that their structure is independent of the form of the interference. They are also adaptive in that they must be able to adjust to the changing interference environment. Locally optimum structures are given here for coherent and noncoherent detection with constant signal levels and various kinds of fading. The case in which phase estimation is used (partially coherent reception) is also considered.

82. Spaulding, A. D., April 1976, Man-Made Noise: The Problem and Recommended Steps Toward Solution, U. S. Department of Commerce, Office of Telecommunication, Office of Telecommunication Report 76-85.

This report concentrates on man-made noise resulting from incidental radiation devices and makes recommendations as to required abatement measures for these devices. General and specific examples of degradation to systems by man-made noise are given. It is shown that both technically and economically, further suppression of automotive ignition noise at the manufacturing level is required. Means of achieving this required suppression are given. Other devices (for example, power transmission lines) are discussed. Programs for noise measurement, analysis, and model development are summarized, and recommendations for the attaining of required additional information on the noise environments are given. In addition, the role that better information on the noise environment should play in the proper management of the spectrum resource is covered.

83. Stoddart Electro Systems, October 1967, Division of Tamar Electronics, Inc., Catalog, the NM-30A, 20 MHz-400 MHz.

This section of the Stoddart catalog presents a discussion on the NM-30A microvoltmeter and special purpose receiver in the 20 MHz to 400 MHz frequency range. Some of the electrical characteristics identified in the bulletin are voltage measurement range (dynamic range), sensitivity, RF input impedance, and spurious response rejection.

84. Stoddart Electro Systems, Division of Tamar Electronics, Inc.,
         Catalog, the NM-52A, 375 MHz-1000 MHz.

    This section of the Stoddart catalog presents a discussion on the
NM-52A microvoltmeter and special purpose receiver in the 375 MHz to 1000
MHz frequency range. Some of the electrical characteristics identified
in the bulletin are voltage measurement range (dynamic range), sensitiv-
ity, RF input impedance, and spurious response rejection.

85. Systems Technology Associates, March 1975, Signal-to-Noise Study for
         HF Data Communication Systems, Contract DAEA18-74-0-0321.

    This report presents the results of a literature survey concerning
data communications in the HF spectrum. This report incorporates suc-
cinct descriptions on the treatment of noise, system reliability, BER ver-
sus S/N, modulation and detection processes, S/N enhancement techniques
and system capacity, bandwidth, and information rate tradeoffs. The re-
port concentrates on the classical ASK, FSK, and PSK modulation processes.

86. U. S. Army Electronic Proving Ground, February 1977, Support to
         Project Wheels, Final Report (Letter Report), TECOM Project No.
         6-CO-242-ESS-102, BAC-77-02-009.

    This report presents EMC automotive ignition noise test data for vari-
ous commercial vehicles. Test data were recorded at the Arizona Highway
Inspection Station on Interstate 10 several miles east of San Simon, Ari-
zona. Measurements were made in compliance with SAE Standard J551c at
25.1 MHz, 32 MHz, and 138 MHz.

87. Waterson, C. C., J. R. Juroshek, and W. O. Bensema, December 1970,
         Experimental Confirmation of an HF Channel Model, IEEE Trans-
         actions on Communication Technology, Vol COM-18, No. 6, pp 792-
         803.

    This paper presents an analog model which is used to simulate an HF
path. In the model the input (transmitted) signal feeds an ideal delay
line and is delivered at several taps with adjustable delays, one for
each resolvable ionospheric model component. Each delayed signal is mod-
ulated in amplitude and phase by a baseband tap-gain function, and the de-
layed and modulated signals are summed (with additive noise) to form the
output (received) signal.

88. Weibull, Waloddi, September 1951, A Statistical Distribution Function
         of Wide Applicability, Journal Applied Mechanics, Vol 18, pp
         293-297.

    This paper discusses the applicability of the Weibull distribution
to different types of problems. Examples are provided showing the rela-
tionship of the distribution to the various parameters of a specific
problem.

89. Whalen, Anthony D., 1971, Detection of Signals in Noise, Academic Press, New York.

This textbook presents a basic description of statistical noise processes. Additive and multiplicative noise are considered and examples of different modulation processes are given.

90. Wilson, Kenneth E., November 1974, Analysis of the Crichlow Graphical Model of Atmospheric Radio Noise at Very Low Frequencies, AD-A008 679.

This report presents an analysis of the Crichlow graphical model for the APD of atmospheric radio noise. The performance of the binary and M-ary coherent phase shift keyed communication systems is predicted based upon the density of the graphical model and the less precise log normal model. Additionally, the statistics and probability density of the narrowband atmospheric radio noise process are found numerically for bandwidths other than the 200 Hz bandwidth of the graphical model.

91. Wood, Paul, July 24, 1973, A Synchronous Gate Pulse Generator for Use in Automotive Ignition Systems Radio Frequency Interference Studies, Research Laboratories (G. M. Corp.), GMR-1433.

This report describes an electronic device which is used to search for ways of understanding and reducing RFI generated by spark ignition engines. Electronic circuitry which, when used in conjunction with present-day RFI instrumentation, provides for the observation and documentation of RFI generated by any specific cylinder of an automobile engine.

92. Yamamoto, S., M. Furuhashi, T. Yamanaka, and H. Kondo, August 2-4, 1977, Electrical Environmental Characteristics for Automotive Electronic Systems, IEEE International Symposium on Electromagnetic Compatibility, Seattle, Washington.

This paper presents the results of studies and measurements conducted to determine the characteristics of transients and high-frequency noise generated in automotive electrical components. The high-frequency noise data were obtained. It has been found that the most important transient for automotive electronic systems is alternator load dump transient caused by battery disconnection and the most influential high-frequency noise is caused by contact breaking. The high-frequency noise characteristics can be expressed in amplitude-frequency relation in the frequency range 100 kHz-80 MHz.

APPENDIX F - LIST OF ABBREVIATIONS

α	an empirical impulsiveness parameter
A_α	effective impulsive index
A_B	impulsive index
ACR	average crossing rate
AI	articulation index
AL	loss in antenna
AM	amplitude modulation
APD	amplitude probability distribution
AS	articulation score
ASK	amplitude shift keying
b	noise power bandwidth
BER	bit error rate
BPSK	biphase shift keying
BW_r	bandwidth of receiving system
CDF	cumulative distribution function
CER	character error rate
CF	crest factor
CFSK	coherent frequency shift keying
CNR	carrier-to-noise ratio
CVSD	continuous variable slope delta
DQPSK	differential quadriphase shift keying
EMC	electromagnetic compatibility
EMI	electromagnetic interference
E_p	peak field intensity
E_{qp}	quasi-peak field intensity
ϵ_B	empirically determined "bend-over" point of the APD
f	frequency
F_a	external antenna noise figure
f_c	center tuned frequency
FIM	field intensity meter
FM	frequency modulation
Γ_B	ratio of intensity of Gaussian to impulsive noise
γ^2	a measure of ratio of impulsive to Gaussian noise
HF	high frequency
IF	intermediate frequency
L_d	average-logarithmic voltage deviation
lim	limit
LOS	line-of-sight
LPC	linear predictive coding
m	number of degrees of freedom of the regime process
MF	medium frequency
ML	mismatch loss
MSK	minimal shift keying
MUX	multiplex
MVMA	Motor Vehicle Manufacturers Association
NAD	noise amplitude distribution
NCFSK	noncoherent frequency shift keying

N(t)	additive noise
N_I	scaling factor
Ω_{2B}	intensity of impulsive noise
PCM	pulse code modulation
PDD	pulse duration distribution
PSD	pulse spacing distribution
$\phi(t)$	random process describing instantaneous phase of noise
P_N	noise power
Prob	probability
Ψ	ratio of total noise power to Gaussian background noise power
PSK	phase shift keying
Q_d	quasi-peak voltage deviation
QPSK	quadriphase shift keying
RATT	radioteletypewriter
RF	radio frequency
rms	root mean square
R_r	antenna input resistance
r(t)	received signal-plus-noise waveform
$R(\tau)$	autocorrelation function
SCIM	speech communication intelligibility measure
S(f)	power spectral density
S/N	signal-to-noise ratio
SSB	single sideband
s(t)	desired signal at receiver
s*(t)	distortion of original transmitted signal
σ^2	variance of noise process
T	time interval
T_a	external noise temperature
τ_i	time limit
TL	antenna-to-receiver transmission line insertion loss
UHF	ultrahigh frequency
V_{av}	average voltage
V_d	average voltage deviation
VHF	very high frequency
V_{log}	average voltage logarithm
V_p	peak voltage
V_{qp}	quasi-peak voltage
V_{rms}	root mean square voltage
v(t)	random process describing instantaneous envelope of noise